Appendix II

Selected publications

Publication list by the author related to this Ph. D. Thesis.

Publications

1. Vázquez, J. L.; Montero, M. T.; Merino, S.; **Domènech, Ò.**; Berlanga, M.; Viñas, M.; Hernández-Borrell, J., Location and Nature of the Surface Membrane Binding Site of Ciprofloxacin: A Fluorescence Study. *Langmuir* **2001,** 17, 1009-1014.

2. Vázquez, J. L.; Berlanga, M.; Merino, S.; **Domènech, Ò.**; Viñas, M.; Montero, M. T.; Hernández-Borrell, J., Determination by Fluorimetric Titration of the Ionization Constants of Ciprofloxacin in Solution and in Presence of Liposomes. *Photochemistry and Photobiology* **2001,** 73, (1), 14-19.

3. Vázquez, J. L.; Merino, S.; **Domènech, Ò.**; Berlanga, M.; Viñas, M.; Montero, M. T.; Hernández-Borrell, J., Determination of the partition coefficients of a homologous series of ciprofloxacin: influence of the N-4 piperazinyl alkylation on the antimicrobial activity. *Internationa Journal of Pharmaceutics* **2001,** 220, 53-62.

4. Merino, S.; Vázquez, J. L.; **Domènech, Ò.**; Berlanga, M.; Viñas, M.; Montero, M. T.; Hernández-Borrell, J., Fluoroquinolone-Biomembrane Interaction at the DPPC/PG Lipid Bilayer Interface. *Langmuir* **2002,** 18, 3288-3292.

5. Grancelli, A.; Morros, A.; Cabañas, M.; **Domènech, Ò.**; Merino, S.; Vázquez, J. L.; Merino, S.; Viñas, M.; Hernández-Borrell, J., Interaction of 6-Fluoroquinolones with Dipalmitoylphosphatidylcholine Monolayers and Liposomes. *Langmuir* **2002,** 18, 9177-9182.

6. Merino, S.; **Domènech, Ò.**; Díez, I.; Sanz, F.; Montero, M. T.; Hernández-Borrell, J., Effects of Ciprofloxacin on *Escherichia coli* Lipid Bilayers: An Atomic Force Microscopy Study. *Langmuir* **2003,** 19, 6922-6927.

7. Ruiz, N.; Merino, S.; Viñas, M.; **Domènech, Ò.**; Montero, M. T.; Hernández-Borrell, J., Preliminary studies of the 2D crystallization of Omp1 of *Serratia marcescens*: observation by atomic force microscopy in native membranes environment and reconstituted in proteolipid sheets. *Biophysical Chemistry* **2004,** 111, 1-7.

8. Merino, S.; **Domènech, Ò.**; Montero, M. T.; Hernández-Borrell, J., Atomic force microscopy study of Escherichia coli lactose permease proteolipid sheets. *Biosensors and Bioelectronics* **2005,** 20, 1843-1846.

9. Domènech, Ò.; Torent-Burgués, J.; Merino, S.; Sanz, F.; Montero, M. T.; Hernández-Borrell, J., Surface thermodynamics study of monolayers formed with heteroacid phospholipids of biological interest. *Colloids and Surfaces B: Biointerfaces* **2005,** 41, 233-238.

10. Merino, S.; **Domènech, Ò.**; Viñas, M.; Montero, M. T.; Hernández-Borrell, J., Effects of Lactose Permease on the Phospholipid Environment in Which It Is Reconsituted A Fluorescence and Atomic Force Microscopy Study. *Langmuir* **2005,** 21, 4642-4647.

11. Merino, S.; **Domènech, Ò.**; Díez-Pérez, I.; Sanz, F.; Montero, M. T.; Hernández-Borrell, J., Surface thermodynamic properties of monolayers versus reconstitution of a membrane in solid-supported bilayers. *Colloids and Surfaces B: Biointerfaces* **2005,** 44, 93-98.

12. Merino-Montero, S.; **Domènech, Ò.**; Montero, M. T.; Hernández-Borrell, J., Preliminary atomic force microscopy study of two-dimensional crystals of lactose permease from *Escherichia coli*. *Biophysical Chemistry* **2006,** 119, 78-83.

13. Domènech, Ò.; Merino-Montero, S., Surface planar bilayers of phospholipids used in protein membrane reconstitution: An atomic force microscopy study. *Colloids and Surfaces B: Biointerfaces* **2006,** 47, 102-106.

14. Domènech, Ò.; Sanz, F.; Montero, M. T.; Hernández-Borrell, J., Thermodynamic and structural study of the main phospholipid components comprising the mitochondrial inner membrane. *Biochimica et Biophysica Acta: Biomembranes* **2006,** 1758, 213-221.

15. Domènech, Ò.; Sanz, F.; Montero, M. T.; Hernández-Borrell, J., Supported planar bilayers from hexagonal phases. *Biochimica et Biophysica Acta: Biomembranes* **2007**, 1768, 100-106.

16. Domènech, Ò.; Morros, A.; Cabañas, M.; Montero, M. T.; Sanz, F.; Hernández-Borrell, J., Thermal response of domains in cardiolipin content bilayers. *Ultramicroscopy* **2006,** *Accepted 2007/01/26*.

17. Garcia-Manyes, S.; **Domènech, Ò.**; Sanz, F.; Montero, M. T.; Hernández-Borrell, J., Atomic force microcopy and force spectroscopy of Langmuir-Blodgett films formed by heteroacid phospholipids of biological interest. *Biochimica et Biophysica Acta: Biomembranes* **2006,** *sumitted*.

18. Domènech, Ò.; Redondo, L.; Montero, M. T.; Hernández-Borrell, J., Specific adsorption of cytochrome *c* on cardiolipin-glycerophospolipid monolayers and bilayers. *Langmuir* **2006,** *submitted*.

Oral and poster presentations in meetings

1. Domènech, Ò.; Merino, S.; Montero, M.T. "Interaction Protein-Membrane Models: an AFM Study". *III Congreso Español de Microscopía de Fuerzas y Efecto Túnel Sociedad Española de Microscopía*. Zamora (2002).

2. Domènech, Ò.; Merino, S.; Hernández-Borrell, J.; Montero, M.T. "Surface thermodynamics of monolayers formed with heteroacid phospholipids of biological interest". *3rd Portuguese-Spanish Biophysics Congress*. Lisbon (2004).

3. Merino, S; **Domènech, Ò.**; Montero, M.T.; Hernández-Borrell, J. "Lactose permease affects the phospholipid environment in which it is reconstituted: an atomic force microscopy study". *3rd Portuguese-Spanish Biophysics Congress*. Lisbon (2004).

4. Merino, S; **Domènech, Ò.**; Viñas, M.; Montero, M.T.; Hernández-Borrell, J. "In the search of 2D crystals of lactose permease using the atomic force microscope". *VIth European Symposium of the Protein Society*. Barcelona (2005).

5. Doménech, Ò.; Morros, A.; Cabañes, M.E.; Montero, M.T.; Hernández-Borrell, J. "Interaction of cytochrome *c* on liposomes and supported planar bilayers of cardiolipin and phosphatidylethanolamine" *COST ACTION D-22. Workshop on Lipid-Protein Interactions*. Murcia (2006).

6. Domènech, Ò.; Montero, M. T.; Hernández-Borrell, J. "Algunes aplicacions de la Microscòpia de Força Atòmica (AFM) a la biologia: de les proteïnes als bacteris". *RECAM,* Barcelona (2006).

7. Domènech, Ò.; Sanz, F., Morros, A., Montero, M.T., Hernández-Borrell, J. "Supported planar bilayers from hexagonal phases: interaction of cytochrome *c*". *Scanning Probe Microscopy, Sensors, and Nanostructures*. Montpellier (2006).

Available online at www.sciencedirect.com
SCIENCE DIRECT®
Colloids and Surfaces B: Biointerfaces 41 (2005) 233–238
COLLOIDS AND SURFACES B
www.elsevier.com/locate/colsurfb

Surface thermodynamics study of monolayers formed with heteroacid phospholipids of biological interest

Òscar Domènech [a, c], Juan Torrent-Burgués [c, 1], Sandra Merino [b, c], Fausto Sanz [a, c], M. Teresa Montero [b, c], Jordi Hernández-Borrell [b, c, *]

[a] *Departament de Química Física, Universitat de Barcelona, E-08028 Barcelona, Spain*
[b] *Departament de Fisicoquímica, Universitat de Barcelona, E-08028 Barcelona, Spain*
[c] *Centre de Bioelectrònica i Nanobiociència (CBEN), Parc Científic de Barcelona, Josep Samitier 1-5, E-08028 Barcelona, Spain*

Received 17 August 2004; accepted 20 December 2004

Abstract

The interaction of 1-palmitoy-2-oleoyl-*sn*-glycero-3-phosphocoline (POPC) and 1-palmitoy-2-oleoyl-*sn*-glycero-3-phosphoethanolamine (POPE), two of the major components in biological membranes, were investigated using the monolayer technique at the air–water interface. The pressure–area isotherms indicate that both phospholipids are miscible through all range of compositions. POPE–POPC form stable mixtures, with a minimum for the Gibbs energy of mixing at $X_{POPC} = 0.4$. A virial equation of state was fitted to the experimental values. Positive values found for the second virial coefficient indicate repulsion between POPC and POPE. The interaction parameter was evaluated which indicated that a corresponding decrease in the repulsion occurs when POPC molar fraction is low. This effect suggests the existence of hydrogen bonds between POPE and the water beneath the interface.

Keywords: Monolayer; Surface pressure isotherms; Phospholipids; Equation state; Thermodynamic analysis

1. Introduction

Phospholipids are the most abundant lipids in biological membranes, where they act as a matrix in which proteins are embedded or adsorbed. They are believed to play an important role not only as the structural units of the bilayer but also in the integration and function of membrane proteins [1].

Currently, there is renewed interest in the investigation of the phospholipid systems found in biological membranes [2], including the phospholipid compositions required to reconstitute a particular membrane function [3,4]. These compositions generally include phospholipids with mixed acyl chains, one saturated (at the *sn-1* position) and the other unsaturated (at the *sn-2* position), linked to the glycerol backbone, as in the case of 1-palmitoyl-2-oleoyl-*sn*-glycero-3-phosphoethanolamine (POPE) and 1-palmitoyl-2-oleoyl-*sn*-glycero-3-phosphocholine (POPC).

Both native lipids of natural origin and synthetic lipids are commonly used in the reconstitution of membrane proteins in proteoliposomes [5], as well as in the two-dimensional crystallization of protein membranes [6]. The use of a particular phospholipid composition is usually determined by practical constraints, often associated with large screening studies [7,8]. Thus, POPC is a phospholipid with a low transition temperature and reasonable chemical stability that is commonly used as a model lipid [9]. However, in many cases, such as the lactose permease of *Escherichia coli*, the presence

* Corresponding author. Tel.: +34 934035986; fax: +34 934035987.
E-mail address: jordihernandezborrell@ub.edu (J. Hernández-Borrell).
[1] Permanent address: Departament d'Engenyeria Quimica, UPC 08222 Terrassa, Spain.

0927-7765/$ – see front matter © 2005 Elsevier B.V. All rights reserved.
doi:10.1016/j.colsurfb.2004.12.012

of the phosphatidylethanolamine headgroup is required for correct protein membrane insertion [10] and folding [11]. There are also many examples of cytoplasmic proteins, e.g. protein kinase C, whose regulation appears to be affected by the presence of POPE [12,13]. Therefore, research on the mixing properties of POPE and POPC in monolayers is of interest.

Here we present a thermodynamic study of the mixing properties of POPE and POPC in which we examine the interactions between the phospholipids using the equation of state of the film.

A study of the same phospholipid system has been started by using spectroscopic techniques and atomic force microscopy on Langmuir–Blodgett films (LBs) to gain insight into their structural characteristics [14].

2. Theory

2.1. Experimental

1-Palmitoyl-2-oleoyl-*sn*-glycero-3-phosphoethanolamine (POPE) and 1-palmitoyl-2-oleoyl-*sn*-glycero-3-phosphocholine (POPC), specified as 99% pure, were purchased from Avanti Polar Lipids (Alabaster, AL, USA) and used without further purification. The subphase buffer for preparing the Langmuir films was a 50 mM Tris–HCl buffer (pH 7.4) containing 150 mM NaCl, prepared in Ultrapure water (Milli Q® reverse osmosis system, 18.3 MΩ cm resistivity). Chloroform and methanol, HPLC grade, were purchased from SIGMA (St. Louis, MO, USA).

The lipids were dissolved in chloroform–methanol (3:1, v/v) to a final concentration of 1 mg mL^{-1}. The monolayers of POPE, POPC and their mixtures were prepared in a 312 DMC Langmuir-Blodgett trough manufactured by NIMA Technology Ltd. (Coventry, England). The trough was placed on a vibration-isolated table (Newport, Irvine, CA, USA) and enclosed in an environmental chamber. The subphase was filtered with a Kitasato system (450 nm pore diameter) before use. The resolution of surface pressure measurement was ±0.1 mN m^{-1}. In all experiments, the temperature was controlled at 24.0 ± 0.2 °C by an external circulating water bath. Before each experiment, the trough was washed with chloroform and rinsed thoroughly with purified water. The cleanliness of the trough and subphase was ensured before each run by cycling the full range of the trough area and aspirating the air–water surface, while at the minimal surface area, to zero surface pressure.

The corresponding aliquot of lipid was spread on the surface of the subphase solution with a Hamilton microsyringe. A period of 15 min was required to allow the solvent to evaporate before the experiment was started. The compression rate was 5 cm^2 min^{-1}. Every π–A isotherm was repeated at least three times and the isotherms showed satisfactory reproducibility.

2.2. Surface thermodynamic analysis

The area per molecule for an ideal mixed monolayer with two components A^{id} can be calculated from:

$$A^{id} = \chi_1 A_1 + \chi_2 A_2 \quad (1)$$

where χ_1 and χ_2 are the mole fractions of the components, and A_1 and A_2 are the area per molecule of the pure components at the same surface pressure.

The excess area, A^E, for a binary monolayer can be expressed as:

$$A^E = A_{12} - (\chi_1 A_1 + \chi_2 A_2) \quad (2)$$

where A_{12} is the average area per molecule of the mixed monolayer. A_{12}, A_1 and A_2 can be obtained from the corresponding π–A isotherms.

The interaction between two phospholipid components in a mixed monolayer, at a constant surface pressure π and temperature, can be evaluated from the calculation of the excess Gibbs energy (G^E), which is given by:

$$G^E = \int_0^{\pi} [A_{12} - (\chi_1 A_1 + \chi_2 A_2)]\, d\pi \quad (3)$$

The Gibbs energy of mixing is given by:

$$\Delta_{mix} G = \Delta_{mix} G^{id} + G^E \quad (4)$$

where the first term, the ideal Gibbs energy of mixing ($\Delta_{mix} G^{id}$), can be calculated from the equation:

$$\Delta_{mix} G^{id} = RT(\chi_1 \mathrm{Ln}\, \chi_1 + \chi_2 \mathrm{Ln}\, \chi_2) \quad (5)$$

where R is the universal gas constant and T is the temperature.

2.3. Equation of state analysis

For a two-dimensional ideal gas we may write:

$$\pi A = kT \quad (6)$$

where k is the Boltzmann constant and T the temperature.

If it is assumed that the phospholipid molecules cannot be compressed to a zero area, the equation of state can be expressed [15] as:

$$\pi (A - A_0) = \alpha kT \quad (7)$$

or in its linear form:

$$\frac{\pi A}{kT} = \alpha + \frac{\pi A_0}{kT} \quad (8)$$

where α is a factor related to the aggregation between molecules in the monolayer and A_0 is the minimum area per molecule occupied by the monolayer molecules. A value of $\alpha = 1$ is attributed to the ideal gas monolayer behaviour.

The surface pressure, area and temperature behaviour for non-ideal phospholipid monolayers have been more accurately represented using other equations of state [16–18].

Thus, the two-dimensional virial equation of state can be written as:

$$\frac{\pi A}{kT} = b_0 + b_1\pi + b_2\pi^2 \quad (9)$$

where b_0, b_1 and b_2 are the virial coefficients. The value of b_0 is attributed to the aggregation state of the film-forming molecules. When π tends towards zero, the πA product would tend towards the kT value, or a fraction of kT for aggregate systems [19]. On the other hand, the value of b_1 provides information about the exclusion volumes and the interaction between the molecules in the film. Negative or positive values indicate attractive or repulsive interactions between the molecules, respectively. The rest of the virial coefficients are not significant.

3. Results and discussion

The surface pressure area (π–A) isotherms of POPE:POPC mixed monolayers are shown in Fig. 1, at 24.0 ± 0.2 °C for both pure phospholipids and their mixtures. The monolayer of POPE exhibited a LC–LC′ transition at 36.0 mN m^{-1} due to a different ordering of the molecules within the same physical state. Apparently, the POPE monolayer collapsed at 50.7 mN m^{-1}. These features are in agreement with previously published data [20,21]. Interestingly, a discontinuity was observed at a surface pressure of 45.5 mN m^{-1}. Typically, the monolayer of pure POPC was always in the LE phase, showing a collapse pressure of 46 mN m^{-1}, also in agreement with data from other studies [22]. The LC–LC′ transition of POPE gradually disappeared when POPC was incorporated in the monolayer, and vanished for the mixture of $\chi_{POPC} = 0.6$.

The values of excess area (A^E) obtained by using Eq. (2) versus composition at various surface pressures are shown in Fig. 2. The maximum and minimum absolute values were found at 5 mN m^{-1} and $\chi_{POPC} = 0.2$ and 40 mN m^{-1} and $\chi_{POPC} = 0.8$, respectively. Negative values were found, however, in most of the compositions and surface pressures.

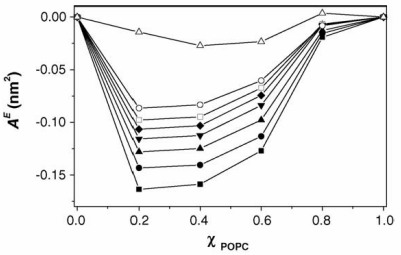

Fig. 2. Excess area per molecule as a function of composition for pure and mixed POPE:POPC monolayers at various surface pressures: (■) 5, (●) 10, (▲) 15, (▼) 20, (♦) 25, (□) 30, (○) 35 and (Δ) 40 mN m^{-1}.

Table 1
Excess of Gibbs energy of mixing, G^E, of POPE:POPC mixtures at different surface pressures

π (mN m^{-1})	G^E/n (kJ mol^{-1})			
	χ_{POPC}			
	0.2	0.4	0.6	0.8
40	−2.74	−2.75	−2.08	−0.23
35	−2.61	−2.60	−1.97	−0.22
30	−2.31	−2.32	−1.76	−0.19
25	−2.02	−2.04	−1.56	−0.17
20	−1.69	−1.71	−1.32	−0.15
15	−1.31	−1.35	−1.04	−0.13
10	−0.90	−0.96	−0.73	−0.08
5	−0.44	−0.50	−0.36	−0.02

The values of G^E at different pressures calculated according to Eq. (3) are listed in Table 1. The highest absolute values of G^E appeared at the highest surface pressures (40 mN m^{-1}). The values of $\Delta_{mix}G$ calculated from data in Table 1 using Eqs. (4) and (5), associated with changes in χ_{POPC}, are shown in Fig. 3. Values of $\Delta_{mix}G$ were all negative, suggesting that no phase separation occurs

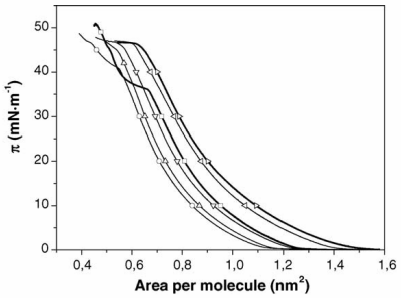

Fig. 1. Surface pressure versus area per molecule isotherms of POPE (□), $\chi_{POPC} = 0.2$ (○), $\chi_{POPC} = 0.4$ (Δ), $\chi_{POPC} = 0.6$ (▽), $\chi_{POPC} = 0.8$ (◁) and POPC (▷).

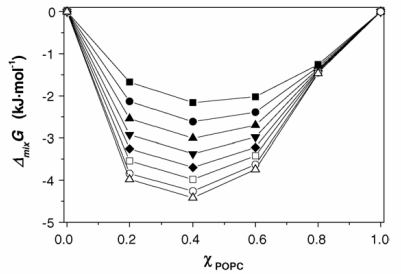

Fig. 3. Variation of the Gibbs energy of mixing with the mole fraction of POPC at different surface pressures: (■) 5, (●) 10, (▲) 15, (▼) 20, (♦) 25, (□) 30, (○) 35 and (Δ) 40 mN m^{-1}.

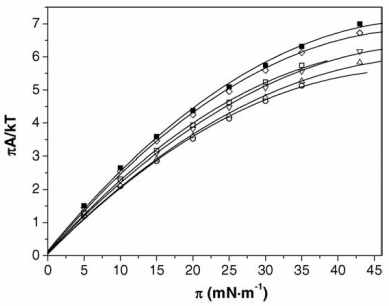

Fig. 4. Variation of $\pi A/kT$ values with surface pressure at different mole fractions, POPE (□), $\chi_{POPC} = 0.2$ (○), $\chi_{POPC} = 0.4$ (Δ), $\chi_{POPC} = 0.6$ (▽), $\chi_{POPC} = 0.8$ (◊) and POPC (■).

in the mixed monolayers. A minimum value of $\Delta_{mix}G$ was found at $\chi_{POPC} = 0.4$ for all surface pressures studied (5–40 mN m^{-1}). As can be observed, the absolute values of $\Delta_{mix}G$ increase as surface pressure increases. This can be explained by the shorter intermolecular distances associated with high surface pressures [23].

This thermodynamic analysis indicates that the interaction between POPE and POPC is energetically favourable, showing the greatest stability across a range of surface pressures for monolayers with $\chi_{POPC} = 0.2$–0.6. Remarkably, many biological membranes [2] and compositions used in the reconstitution of transmembrane proteins in proteoliposomes contain a high proportion of POPE [24–26].

A plot of $\pi A/kT$ versus π at 24.0 ± 0.2 °C is shown in Fig. 4. This plot indicates that neither Eq. (6) nor Eq. (8) are fulfilled even when $\pi \to 0$. Alternatively, the well-known virial equation of state was used (Eq. (9)). The virial coefficients (b_0, b_1, b_2) and correlation coefficients obtained are listed in Table 2. Since the values of the first virial coefficient (b_0) are lower than 1, two-dimensional phospholipid aggregates could exist at low surface pressures. Thus, in agreement with the literature [17,19], their aggregation number ($1/b_0$) can be estimated within the order of tens. This could be related, at least indirectly, to the existence of laterally structured lipids (microdomains), also shown in POPE:POPC liposomes using fluorescence techniques [27].

The values of the second virial coefficient, b_1, were all positive (Table 2), indicating that the predominant interactions present in the monolayer were repulsive. This is in agreement with the earlier work of Stigter and Dill [28]. These interactions, however, are slightly more repulsive for POPC than POPE. This observation can be understood taking in consideration: (i) that the van der Waals forces between the acyl chains should be higher for POPE than for POPC because the PE headgroup is smaller than PC [29]; and (ii) that the ethanolamine group is less hydrophobic than the choline group which results in a different orientation of each headgroup [30]. Also, the ions and water molecules beneath the monolayer may reduce the electrostatic repulsion [31], and particularly the ability of POPE to form hydrogen bonds. Thus, while POPE could form hydrogen bonds with water and other molecules, POPC cannot [30,32].

The values of b_1 for POPE and POPC (Table 2) are higher than those reported for DSPE and DSPC, 0.127 and 0.158, respectively [17] and, similarly to what we reported here, are related with negative values of G^E [33]. DSPE and DSPC are homophospholipids with 18C saturated chains and higher enthalpies and transition temperatures than POPE and POPC [9,34]. Possibly, the electrostatic repulsion between the headgroups may be more efficiently counterbalanced by the attractive hydrophobic interactions of the stearoyl chains [35].

For an evaluation of the nature of the interaction between two molecules in a mixed monolayer the following equation can be used [36]:

$$(b_1)_m = (b_1)_1\chi_1^2 + (b_1)_2\chi_2^2 + 2(b_1)_{12}\chi_1\chi_2 \quad (10)$$

where $(b_1)_1$ and $(b_1)_2$ are the second virial coefficients of the pure components 1 (POPE) and 2 (POPC), respectively, and $(b_1)_{12}$ is the second virial coefficient due to interactions between both components. The obtained values of $(b_1)_{12}$, shown in Table 2, are positive, confirming the existence of repulsive interactions between POPC and POPE. Nevertheless, these values are lower than the mean value of the individual second virial coefficients [36], that is $[(b_1)_1 + (b_2)_2)]/2 = 0.254$, indicating a less repulsive interaction between molecules of POPE and POPC in the mixture than between molecules in the pure components. The fact that a unique value of $(b_1)_{12}$ is not obtained indicates that other interactions are present, probably involving the subphase. The zwitterionic nature of the phospholipids and the ability of PE to form hydrogen bonds [32] suggest that interactions exist between the phospholipids at the interface and the water molecules and ions

Table 2
Virial coefficients and correlation coefficient from the fitting of the values shown in Fig. 4

	χ_{POPC}					
	0	0.2	0.4	0.6	0.8	1
b_0	0.093	0.089	0.093	0.112	0.141	0.168
b_1 (m mN^{-1})	0.243	0.210	0.215	0.228	0.259	0.265
b_2 (m^2 mN^{-2})	−0.0024	−0.0019	−0.0019	−0.0020	−0.0025	−0.0025
r	0.9996	0.9996	0.9995	0.9995	0.9995	0.9992
$(b_1)_{12}$ (m mN^{-1})	–	0.137	0.177	0.195	0.249	–

of the subphase [28,32]. This would explain the increased contribution of the subphase at lower χ_{POPC}.

Water can form hydrogen bonds with PE and with itself, leading to some sort of bi-dimensional network around the PE heads [37]. Since PC does not form hydrogen bonds, the introduction of PC into the film interferes with the hydrogen-bonding network [3] and permits a more favourable interaction between the tails of the molecules. The breakdown of the hydrogen bonding leads to an effective decrease in the mean area per molecule, as can be observed in the isotherms (see Fig. 1). The dynamics of hydrogen bonds between water molecules and micelles, lipid vesicles, bilayers or proteins [38] is slower; that is, the lifetime of the hydrogen bond between the polar groups of the molecules of these systems and a water molecule is much longer than that between two water molecules. This implies that the molecules of PE in the film are more static than those of PC, and consequently the attractive interactions between hydrocarbon chains could be less favourable. These observations are in agreement with the differences between PC and PE headgroups reported elsewhere [30].

The network breakdown described above leads to an increase in entropy, which contributes to a decrease in the excess of Gibbs energy (Table 1). It should be pointed out that the described behaviour occurs when PE and PC are in the low condensed state. At high surface pressures, when PE is in the more condensed state, the behaviour is different, as can be seen in Fig. 2 for a surface pressure of 40 mN m^{-1}.

If the value $(b_1)_{12} = [(b_1)_1 + (b_2)_2)]/2$ is introduced in Eq. (10), the following expression for $(b_1)_m$, that we represent as $(b_1)_m^{id}$ by similarity with Eq. (1), can be obtained:

$$(b_1)_m^{id} = (b_1)_1\chi_1 + (b_1)_2\chi_2 \quad (11)$$

We can predict that ideal behaviour will be observed in the case of either an ideal mixture or when the components are immiscible. Also, by similarity with Eq. (2), we can define:

$$(b_1)^E = (b_1)_m - (b_1)_1\chi_1 - (b_1)_2\chi_2 \quad (12)$$

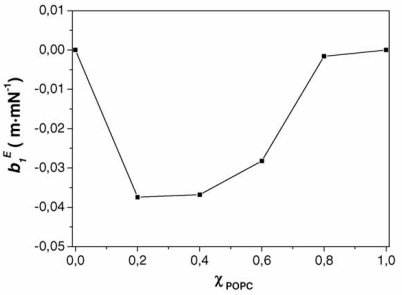

Fig. 5. Values of the parameter b_1^E as a function of composition.

The values of $(b_1)^E$, which are negative, are shown in Fig. 5, and indicate that less repulsive interactions are present in the mixture (this behaviour can be also infered by inspection of Fig. 2). In contrast, at high χ_{POPC} ($\geq$0.8) the mixture shows a $(b_1)^E$ value of practically zero, indicating either that the mixture tends to an ideal behaviour or that the components are practically immiscible or seggregated [27]. This behaviour is in agreement with the results shown in Fig. 2 and Table 1.

4. Conclusions

The most stable composition for the mixed monolayers, minimum values of G^E and $\Delta_{mix}G$, was found at $\chi_{POPC} = 0.4$. Therefore, the POPE:POPC (0.6:0.4, mol/mol) monolayer would be one of the most appropriate phospholipid matrix for use in the analysis of biological membranes, in particular for membrane protein insertion [8,39].

The fitting of a virial equation of state to the experimental values shows positive values for the second virial coefficient, b_1, and indicating repulsive interactions. Additionally, the $(b_1)_{12}$ coefficient indicates less repulsive interactions in the mixture than in the pure components, especially for low POPC compositions. The properties of the mixtures may be explained by the ability of PE to form hydrogen bonds with the water beneath the monolayer, and the possibility that PC could break them.

5. Future directions

Taking the collapse pressures of the single monolayers as 50.7 and 46 mN m^{-1} for the POPE and the POPC monolayer, respectively, the mixed monolayers will be miscible at $\chi_{POPC} = 0.2$ and 0.4 (different collapse pressure) and immiscible at $\chi_{POPC} = 0.6$ and 0.8 (similar collapse pressure). Contrarily, taking the collapse pressure of POPE as 45.5 mN m^{-1}, all mixed monolayers would become immiscible.

The nature of the discontinuity at 45.5 mN m^{-1} for the POPE monolyer requires further investigation. Atomic force microcopy of Langmuir–Blodgett monolayers could provide detailed information on the nanostructure of this monlayer (work in progress).

Acknowledgements

Ò.D. and S.M. are recipients of 'Recerca i Docència' fellowships from the University of Barcelona. J.T.B. gratefully acknowledges the Polytechnic University of Catalonia for facilitating his sabbatical year. This work was supported by Grant TIC-2002-04280-C03-01 from the Ministerio de Ciencia y Tecnología (MCYT) of Spain.

References

[1] A.G. Lee, Biochim. Biophys. Acta 1612 (2003) 1.
[2] D. Marsh, FEBS Lett. 268 (1990) 371.
[3] J.M. Wrigglesworth, in: G.C. Brown, C.E. Cooper (Eds.), Bioenergetics: A Practical Approach, IRL Press, Oxford, 1995 (Chapter 4).
[4] W. Dowhan, Ann. Rev. Biochem. 66 (1997) 199.
[5] P. Viitanen, M.J. Newman, D.L. Foster, T.H. Wilson, H.R. Kaback, Methods Enzymol. 125 (1986) 429.
[6] J.L. Rigaud, G. Mosser, J.J. Lacapere, A. Olofsson, D. Levy, J.L. Ranck, J. Struct. Biol. 118 (1997) 226.
[7] J. Zhuang, G.G. Privé, G.E. Werner, P. Ringler, H.R. Kaback, A. Engel, J. Struct. Biol. 125 (1999) 63.
[8] N. Ruiz, S. Merino, M. Viñas, Ò. Domènech, M.T. Montero, J. Hernández-Borrell, Biophys. Chem. 111 (2004) 1.
[9] J. Hernández-Borrell, K.M.W. Keough, Biochim. Biophys. Acta 1153 (1993) 277.
[10] M. Bogdanov, W. Dowhan, J. Biol. Chem. 270 (1995) 732.
[11] M. Bogdanov, W. Dowhan, EMBO J. 17 (1998) 5255.
[12] R.M. Epand, R. Bottega, Biochim. Biophys. Acta 944 (1988) 144.
[13] M.D. Bazzi, A. Youakim, G.L. Nelsestuen, Biochemistry 31 (1992) 1125.
[14] J.M. Soletti, M. Botrean, F. Sommer, W.L. Brunat, S. Kasas, T.M. Duc, M.R. Celio, Langmuir 12 (1996) 5379.
[15] A.W. Adamson, A.P. Gast, Physical Chemistry of Surfaces, sixth ed., Wiley, New York, 1997 (Chapter 3).
[16] D. Marsh, Biophys. J. 81 (2001) 2154.
[17] J. Sánchez-González, M.A. Cabrerizo-Vílchez, M.J. Gálvez-Ruiz, Colloids Surf. B: Biointerf. 12 (1999) 123.
[18] S.J. Pogorzelski, A.D. Kogut, J. Sea Res. 49 (2003) 347.
[19] K.S. Birdi, V.S. Gevod, Colloid Polym. Sci. 265 (1987) 257.
[20] N.K. Mizuno, J.M. Smaby, B.A. Cunningham, M.M. Monnsen, H.L. Brockman, Langmuir 19 (2003) 1802.
[21] H.L. Brockman, K.R. Applegate, M.M. Momsen, W.C. King, J.A. Glomset, Biophys. J. 85 (2003) 2384.
[22] J. Miñones Jr, P. Dynarowicz-Latka, O. Conde, J. Miñones, E. Iribarnegaray, M. Casas, Colloids Surf. B: Biointerf. 29 (2003) 197.
[23] K. Gong, S.S. Feng, M. Go, P.H. Soew, Colloids Surf. A 207 (2002) 113.
[24] J.L. Vazquez-Ibar, A.B. Weinglass, H.R. Kaback, Proc. Natl. Acad. Sci. 99 (2002) 3487.
[25] J. Le Coutre, L.R. Narasimhan, C.K.N. Patel, H.R. Kaback, Proc. Natl. Acad. Sci. 94 (1997) 10167.
[26] S. Morein, A.S. Anderson, L. Rilfors, G. Lindblond, J. Biol. Chem. 12 (1996) 6801.
[27] T. Ahn, C.H. Yun, Arch. Biochem. Biophys. 15 (1999) 288.
[28] D. Stigter, K.A. Dill, Langmuir 4 (1988) 200.
[29] M. Langner, K. Kubica, Chem. Phys. Lipids 101 (1999) 3.
[30] K.A. Dill, D. Stigter, Biochemistry 27 (1988) 3446.
[31] J.F. Tocanne, J. Teissie, Biochim. Biophys. Acta 1031 (1990) 111.
[32] H. Hauser, I. Pascher, R.H. Pearson, S. Sundell, Biochim. Biophys. Acta 650 (1981) 21.
[33] J. Sánchez-González, M.A. Cabrerizo-Vílchez, M.J. Gálvez-Ruiz, Colloid Polym. Sci. 276 (1998) 239.
[34] K.M.W. Keough, P.J. Davis, Biochemistry 18 (1979) 1453.
[35] J. Israelachvili, Intermolecular and Surface Forces, second ed., Academic Press, London, 1992.
[36] I.N. Levine, Physical Chemistry, fifth ed., McGraw-Hill Companies Inc., USA, 2002 (Chapter 5).
[37] D.B. Kell, Biochim. Biophys. Acta 549 (1979) 55.
[38] S. Balasubramanian, S. Pal, B. Bagchi, Phys. Rev. Lett. 89 (2002) 115505.
[39] S. Merino, Ò. Domènech, M.T. Montero, J. Hernández-Borrell, Biosens. Biolectron., in press (available on line since July 2004).

Available online at www.sciencedirect.com
SCIENCE DIRECT
Biochimica et Biophysica Acta 1758 (2006) 213–221
BIOCHIMICA ET BIOPHYSICA ACTA BBA
http://www.elsevier.com/locate/bba

Thermodynamic and structural study of the main phospholipid components comprising the mitochondrial inner membrane

Òscar Domènech [a,c], Fausto Sanz [a,c], M. Teresa Montero [b,c], Jordi Hernández-Borrell [b,c,*]

[a] *Departament de Química Física, U.B. 08028-Barcelona, Spain*
[b] *Departament de Fisicoquímica, U.B. 08028-Barcelona, Spain*
[c] *Centre de Bioelectrònica i Nanobiociència (CBEN), Parc Científic de Barcelona, Josep Samitier 1-5/08028 Barcelona, Spain*

Received 24 November 2005; received in revised form 24 January 2006; accepted 7 February 2006
Available online 3 March 2006

Abstract

Cardiolipin (CL) is a phospholipid found in the energy-transducing membranes of bacteria and mitochondria and it is thought to be involved in relevant biological processes as apoptosis. In this work, the mixing properties of CL and 1-palmitoyl-2-oleoyl-*sn*-glycero-3-phosphocoline (POPC) and 1-palmitoyl-2-oleoyl-*sn*-glycero-3-phosphoethanolamine (POPE) at the air–water interface, have been examined using the thermodynamic framework analysis of compression isotherms. Accordingly, the values of the Gibbs energy of mixing, the more stable monolayers assayed were: POPC:CL (0.6:0.4, mol:mol) and POPE:CL (0.8:0.2, mol:mol). The results reflect that attractive forces are the greatest contributors to the total interaction in these compositions. Supported planar bilayers (SPBs) with such compositions were examined using atomic force microscopy (AFM) at different temperatures. With the POPC:CL mixture, rounded and featureless SPBs were obtained at 4 °C and 24 °C. In contrast, the extension of the POPE:CL mixture revealed the existence of different lipid domains at 24 °C and 37 °C. Three lipid domains coexisted which can be distinguished by measuring the step height difference between the uncovered mica and the bilayer. While the low and intermediate domains were temperature dependent, the high domain was composition dependent. When cytochrome *c* (cyt *c*) was injected into the fluid cell, the protein showed a preferential adsorption onto the high domain of the POPC:CL. These results suggest that the high domain is mainly formed by CL.

Keywords: Monolayers; Supported planar bilayers; Atomic force microscopy

1. Introduction

The three major components comprising the mitochondrial inner membrane of eukaryotic cells are phosphatidylcholine (PC, 40% in weight), phosphatidylethanolamine (PE, 40%), and cardiolipin (CL, 20%) [1]. Naturally occurring phospholipids include mixed acyl chains, one saturated (at the *sn*-1 position) and the other unsaturated (at the *sn*-2 position) linked to the glycerol backbone, which is normally in a fluid state under physiological conditions [2]. Such is the case with 1-palmitoyl-2-oleoyl-*sn*-glycero-3-phosphoethanolamine (POPE) and 1-palmitoyl-2-oleoyl-*sn*-glycero-3-phosphocholine (POPC), whose mixing properties at the interface have been previously reported [3]. Our interest in these particular species stems from our finding that transmembrane protein reconstitution in proteoliposomes was highly dependent upon the presence of phospholipids with low gel-to-liquid crystalline phase transition temperatures (T_m) [4,5]. Moreover, the physiological activity of many transmembrane proteins is dependent upon the ability of phospholipids, such as PE, to establish intermolecular hydrogen bonding [6,7]. While neutral phospholipid matrices (i.e., POPC) are widely used in biophysical studies [8,9], mixtures with POPE or anionic phospholipids [10] that establish hydrogen bonds at the protein–membrane interface should be used to mimic standard physiological conditions. For these purposes, one effective phospholipid is CL, which is a doubly negatively-charged four-tailed phospholipid, and the most unsaturated

* Corresponding author. Departament de Fisicoquímica, U.B. 08028-Barcelona, Spain.
E-mail address: jordihernandezborrell@ub.edu (J. Hernández-Borrell).

0005-2736/$ - see front matter © 2006 Elsevier B.V. All rights reserved.
doi:10.1016/j.bbamem.2006.02.008

lipid found not only in mitochondria [11], and in bacterial membranes, for which few studies on its interactions with other phospholipid species are available [12]. On the other hand, the proportion of CL in the inner membrane of mitochondria is quite variable, ranging from 3 to 9 mol%, depending on the evolution stage [13]. Significantly, CL is essential for fundamental processes that occur at the inner mitochondrial membranes, such as ATP synthesis, ADP/ATP translocation, or electron transport. Furthermore, many inner membrane proteins and transporters (i.e., cytochrome *c* (cyt *c*)), interact selectively with CL as their activity depends on its presence [14,15]. In particular, it has been reported that electron transport through cytochrome *c* oxidase requires at least 3 or 4 molecules of CL to be available within the neighboring phospholipid matrix [16].

The loss of CL from the inner membrane of mitochondria has been related to several pathologic conditions such as ischemia [17,18] and aging [19,20]. Moreover, it has been suggested that the release of cyt *c* from the inner mitochondrial membrane during apoptosis may be related to or dependent upon levels of CL [21]. Thus, although several studies [22,23] have established the crucial role of mitochondrial lipids during cell death, it remains unclear why CL appears to be so fundamental to the overall process. Hence, an investigation of the mixing properties of CL with other major components of the inner mitochondrial membrane (PE and PC) will peovide valuable information on the nature of their interactions and their possible implications for processes of biological interest.

Here, we examine the mixing properties of two binary systems, POPC:CL and POPE:CL, at the air–water interface using a thermodynamic framework analysis of compression isotherms. Moreover, we have studied the bilayer structure by atomic force microscopy (AFM), which is an effective technique for obtaining information on phospholipid domains [24,25] under biomimetic conditions. The occurrence of laterally segregated lipid regions is important, considering that lipid domains might play a role in the insertion of proteins [10,26]. Hence, to examine them in our own phospholipid matrices, we used AFM to characterize supported planar bilayers (SPBs) of those POPC:CL and POPE:CL compositions that were judged, based on a thermodynamic study, to be the most stable.

2. Materials and methods

2.1. Langmuir trough

2.1.1. Preparation of lipid monolayers

POPC (1-palmitoyl-2-oleoyl-*sn*-glycero-3-phosphocholine), POPE (1-palmitoyl-2-oleoyl-*sn*-glycero-3-phosphoethanolamine), and CL (Cardiolipin), specified as 99% pure, were purchased from Avanti Polar Lipids (Alabaster, AL, USA) and used without further purification. Horse heart cytochrome *c* was purchased from Sigma Chemical Co. (Madrid, Spain). The buffer beneath the monolayers was 50mM Tris–HCl buffer (pH 7.40) containing 150mM NaCl, prepared in Ultrapure water (Milli Q® reverse osmosis system, 18.3MΩ·cm resistivity) and filtered with a Kitasato system (450nm pore diameter) before use. The preparation of the monolayers was performed in a 312 DMC Langmuir-Blodgett trough manufactured by NIMA Technology Ltd. (Coventry, England). The trough (total area: 137cm^2) was placed on a vibration-isolated table (Newport, Irvine, CA, USA) and enclosed in an environmental chamber. The resolution of surface pressure measurement was ±0.1mN m^{-1}. In all experiments the temperature was maintained at 24.0±0.2 °C via an external circulating water bath. Before each experiment, the trough was washed with chloroform and rinsed thoroughly with purified water. The cleanliness of the trough and subphase was ensured before each run by cycling the full range of the

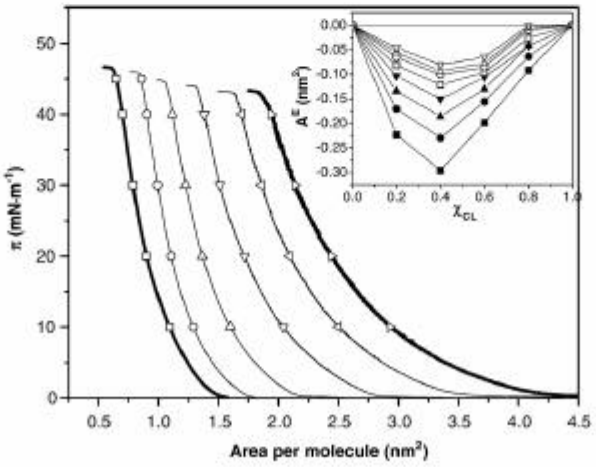

Fig. 1. Surface pressure versus area per molecule isotherms of (□) POPC, (○) χ_{CL}=0.2, (△) χ_{CL}=0.4, (▽) χ_{CL}=0.6, (◁) χ_{CL}=0.8, and (▷) CL. Inset: Excess area per molecule as a function of composition for POPC:CL mixed monolayers at various surfaces pressures: (■) 5, (●) 10, (▲) 15, (▼) 20, (□) 25, (○) 30, (△) 35, (▽) 40 mN m^{-1}.

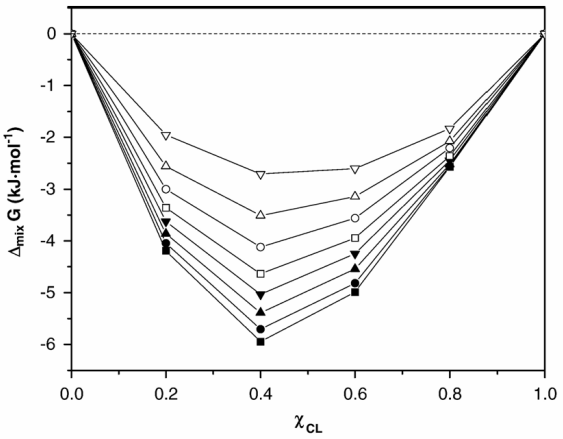

Fig. 2. Variation of the Gibbs energy of mixing for the POPC:Cl system with the mole fraction of CL at different surface pressures: (■) 5, (●) 10, (▲) 15, (▼) 20, (□) 25, (○) 30, (△) 35, (▽) 40 mN·m^{-1}.

trough area and aspirating the air–water surface, while at the minimal surface area, to zero surface pressure.

The lipids were dissolved in chloroform–methanol (3:1, v/v) to a final concentration of 1 mg·mL^{-1}. The corresponding aliquot of lipid was spread onto the surface of the subphase solution with a Hamilton microsyringe. A 15-min period was required to allow the solvent to evaporate before the experiment was begun. The compression barrier speed, calculated to the final surface pressure, was 5 cm^2·min^{-1}. Every π-A isotherm was repeated three times minimum, with the isotherms showing satisfactory reproducibility.

2.1.2. Isotherm analysis

The area per molecule of an ideal mixed monolayer of two components can be calculated as follows:

$$A^{id} = \chi_1 A_1 + \chi_2 A_2 \quad (1)$$

where A^{id} is the area per molecule of the mixed monolayer and χ_1, A_1 and χ_2, A_2 are the molar fractions and the area per molecule of the pure component 1 and 2, respectively.

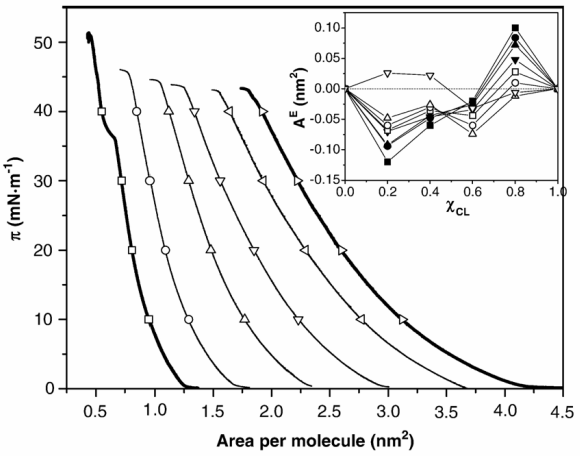

Fig. 3. Surface pressure versus area per molecule isotherms of (□) POPE, (○) χ_{CL}=0.2, (△) χ_{CL}=0.4, (▽) χ_{CL}=0.6, (◁) χ_{CL}=0.8, and (▷) CL. Inset: excess area per molecule as a function of composition for POPE:CL mixed monolayers at various surfaces pressures: (■) 5, (●) 10, (▲) 15, (▼) 20, (□) 25, (○) 30, (△) 35, (▽) 40 mN·m^{-1}.

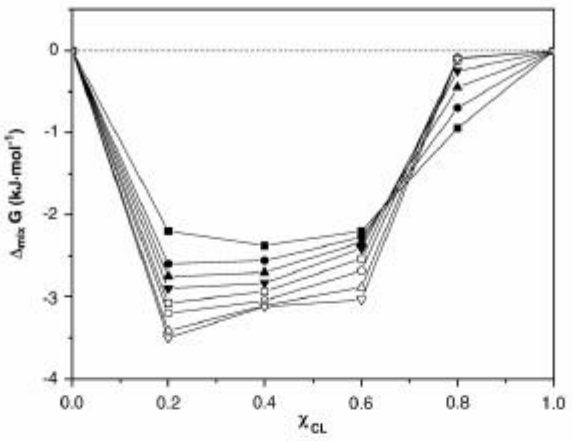

Fig. 4. Variation of the Gibbs energy of mixing for the POPE:CL system with the mole fraction of CL at different surface pressures: (■) 5, (●) 10, (▲) 15, (▼) 20, (□) 25, (○) 30, (△) 35, (▽) 40 mN·m^{-1}.

The excess area, A^E, for a binary monolayer can be expressed as follows:

$$A^E = A_{12} - (\chi_1 A_1 + \chi_2 A_2) \quad (2)$$

where A_{12} is the area per molecule of the mixed monolayer.

The interaction between two phospholipid components in a mixed monolayer, at a constant surface pressure π and temperature, can be evaluated from the calculation of the excess Gibbs energy (G^E), which is given by

$$G^E = \int_0^{\pi} [A_{12} - (\chi_1 A_1 + \chi_2 A_2)] d\pi \quad (3)$$

The Gibbs energy of mixing is given by

$$\Delta_{mix} G = \Delta_{mix} G^{id} + G^E \quad (4)$$

where the first term, the ideal Gibbs energy of mixing ($\Delta_{mix} G^{id}$), can be calculated from the equation

$$\Delta_{mix} G^{id} = RT(\chi_1 \mathrm{Ln}\chi_1 + \chi_2 \mathrm{Ln}\chi_2) \quad (5)$$

where R is the universal gas constant and T is the temperature.

2.2. Supported bilayer studies

2.2.1. Preparation of liposomes

The method for obtaining liposomes has been previously described [25]. Briefly, lipids were dissolved in chloroform:methanol (3:1, v/v) and mixed to obtain the desired composition in a conical tube. The solvent was evaporated under a stream of nitrogen. The lipid film was maintained under reduced pressure for at least 2 h. The resulting film was hydrated in 50 mM Tris–HCl, 150 mM NaCl, pH 7.40 to a final concentration of 250 μM. To obtain unilamellar vesicles, the hydrated lipids were extruded 10 times through two polycarbonate filters (400 nm pore size, Nucleopore, CA, USA) with an extruder device obtained from Lipex Biomembranes (Vancouver, BC, Canada). The size and polydispersity of each preparation were monitored systematically by quasi-elastic light scattering using an Autosizer IIc photon correlation spectrophotometer (Malvern Instruments, U.K.). A dominant peak was typically observed indicating the presence of ~400 nm sized particles.

2.2.2. Atomic force microscopy

Images were generated with a commercial AFM (Nanoscope IV, Digital Instruments, CA, USA) and Si_3N_4 cantilevers (Olympus, Tokyo, Japan) with a nominal spring constant of 0.08 N m^{-1}. The instrument was equipped with a "J" scanner (120 μm) and the Tapping mode fluid cell was extensively washed with ethanol and water before each experiment. Mica squares (0.4 cm^2, from Asheville-Schoonmaker Mica Co., VA, USA) were glued to a Teflon disc mounted on a steal disc. Subsequently, 50 μl of liposomes were spread on the mica. For in situ AFM measurements, cyt *c* was added into the fluid cell at a final concentration of 5 μM. The height difference between the heating element on the piezo-scanner and the surface of the sample is around 3–5 mm. It has been seen experimentally that the difference between the temperature of the heating element and the mica surface can reach up to a 25%, so the real temperature of the sample was measured with a thermocouple (Cole Palmer thermocouple thermometer EW-91100-20 DigiSense, Resolution: 0.1 °C, Accuracy: ±0.25% provided with Omega Precision Fine Wire Thermocouples). A dwell time of

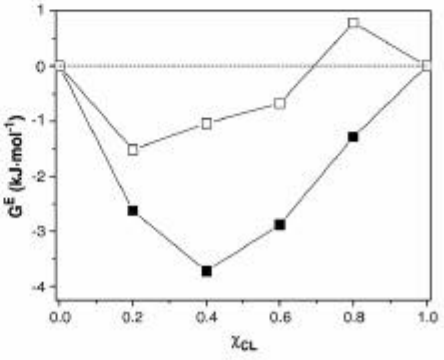

Fig. 5. Excess Gibbs energy of mixing versus composition for POPC:CL (■) and POPE:CL (□) monolayers at 30 mN·m^{-1}.

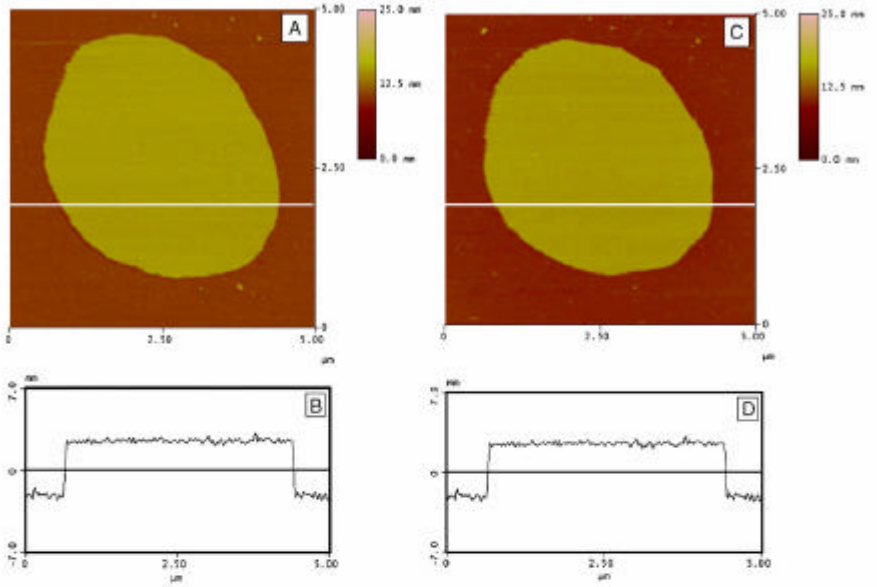

Fig. 6. (A, C) Topographic image of an SPB of POPC:CL (0.6:0.4, mol:mol) at 4 °C and 24 °C, respectively. Buffer (pH 7.40), 50 mM Tris–HCl and 150 mM NaCl. (B, D) Height profile analyses along the white line shown in A and C, respectively.

20 min is waited for the sample to reach thermal equilibrium with the heating element after increasing the temperature. Images were recorded in a constant-force mode and in liquid. The set point was continuously adjusted during the imaging to minimize the force applied. Prior to imaging the sample, the tip-sample pair was thermally stabilized. All the images were processed using Digital Instruments software.

3. Results and discussion

3.1. Langmuir trough

Lipid monolayers formed at the air–water interface constitute a versatile membrane model to investigate the interactions and physicochemical properties of their components. Thus, the mixing properties of CL with the two major phospholipids components of the inner mitochondrial membrane (POPC and POPE) may be related to, or influence the interaction and activity of, some relevant proteins (i.e., cyt *c*).

The surface pressure-area (π-A) isotherms of the pure phospholipids and POPC:CL mixed monolayers are shown in Fig. 1. At the temperature of these experiments (24.0 ± 0.2 °C), all monolayers exhibited a liquid-expanded (LE) phase.[1] Collapse pressure values (π_c) of the POPC:CL mixed monolayers fell within the values of the pure components, 46 mN m^{-1} and 43.1 mN m^{-1} for POPC and CL respectively, following a linear relationship. These results are consistent with those reported elsewhere [12] and can be interpreted according to the Gibbs phase rule as an indication of complete miscibility between POPC and CL at the air–water interface.

The miscibility of POPC and CL, however, can be further evaluated by using Eq. (1) and calculating the excess area per molecule (A^E). As can be seen in the inset of Fig. 1, the values of A^E were negative for all compositions and surface pressures. The minimum negative values were observed at χ_{CL} = 0.4. These results reflect the existence of attractive forces between POPC and CL, whose exact nature is difficult to ascertain based only on thermodynamic analysis. Indeed, if A^E is evaluated at high proportions of CL ($\chi_{CL} \geq 0.8$), its values approach zero. Thus, behavior, at this limit, would reflect the relative increase of the repulsive forces due to increasing encounters of CL molecules at the interface. However, proportions of POPC as low as 20% would reduce the frequency of such encounters, allowing the monolayer to become stable. For a more accurate interpretation, the values of $\Delta_{mix}G$, calculated according to Eq. (4) and associated with changes in χ_{CL}, are shown in Fig. 2. As can be seen, $\Delta_{mix}G$ values were all negative, suggesting that no phase separation occurs in the mixed monolayers. In concordance with the values given in the inset of Fig. 1, the minimum value occurred at χ_{CL} = 0.4 for all surface pressures studied. Hence, we can conclude that this monolayer is, in comparison with the others, the more stable. It is worth noting, however, that this molar ratio was higher in CL than the naturally occurring molar

[1] The features of the pure POPE and POPC monolayers and the interaction in mixed monolayers have been discussed in a previous paper [3].

ratio found in the mitochondria inner membrane ($\chi_{CL}=0.2$) [1]. Our results are similar to those found for the egg PC:CL system [12], which underlines the fact that neutral species have a definite influence on CL mixing properties, distribution, and ultimately on the potential formation of domains. Obviously, the presence of other phospholipids such as PE will result in substantial changes in the PC:CL molar ratio. To evaluate such an influence, the binary mixture of PE and CL was also investigated.

The surface pressure-area (π-A) isotherms of POPE:CL mixed monolayers are shown in Fig. 3 at 24±0.2 °C for both phospholipids and their mixtures. The features of the POPE monolayer, mainly its collapse at 50.7 mN m^{-1} and the nature of the typical LC–LC′ phase transition [27], have been previously discussed [3]. Of note, the POPE monolayer aside, surface collapse pressure values decreased gradually by increasing the molar fraction of CL. According to the Gibbs phase rule, this indicates that the mixed monolayers are miscible at $\chi_{CL}>0.2$. Beginning with this lowest proportion of CL, the LC–LC′ phase transition becomes abolished (Fig. 3).

The values of A^E versus the molar fraction of CL at different surface pressures are shown in the inset of Fig. 3. As can be seen at $\chi_{CL}\geq 0.8$, the values of A^E were positive and decreased when surface pressure increased. The excess areas were negative for $\chi_{CL}<0.8$ and up to $\pi=30$ mN m^{-1}, suggesting that attractive forces are the greatest contributor to the total interaction. Indeed, this is quite conceivable based on the tendency of POPE to form hydrogen bonds [28]. On the other hand, repulsive forces would predominate at high mole fractions of CL (>80%), as indicated by the positive values of A^E obtained. This behavior, also observed at low mole fractions of CL (30–40%) at 40 mN m^{-1}, most likely results from the negative charge carried by CL. It is worth noting that the surface charge density increases with increasing surface pressure, which results in increased repulsion between CL molecules. Remarkably, except for the values calculated at 40 mN m^{-1}, A^E displayed opposite behavioral tendencies. As can be inferred from the $dA^E/d\pi$ values, repulsive forces would predominate as the surface pressure increased, while attractive forces would predominate as surface pressures decreased.

Fig. 4 shows the Gibbs energy resulting from mixing the POPE:CL binary system at different surface pressures. As can be seen, at high CL molar fractions ($\chi_{CL}\geq 0.8$) the monolayers become less stable and repulsive forces arise. As discussed above for A^E values, this behavior would result from the negative electric charge carried by CL molecules. The more thermodynamically stable composition occurs at $\chi_{CL}=0.2$ over the range of surface pressures studied. At such a composition, the attractive forces in the system would be higher than in the other compositions. This POPE:CL molar ratio coincides with the proportion of those components found in the mitochondrial inner membrane.

For a quantitative justification of the interaction between PC, PE and CL, G^E values can be calculated from Eq. (4). Taking for instance the monolayer at 30 mN m^{-1} (Fig. 5), it becomes clear that the POPC:CL system is more stable than the POPE:CL system. It is also evident that the replacement of the PC by PE group changes the character of the interaction from attractive to repulsive at $\chi_{CL}\geq 0.8$.

Table 1
Height and roughness (R_a) at two temperatures of the SPBs of POPC:CL (0.6:0.4, mol:mol) presented in Fig. 5A and C

Lipid domain height	T=4 °C		T=24 °C	
	h (nm)	R_a (nm)	h (nm)	R_a (nm)
No lipid domains	5.60±0.18	0.15	4.52±0.16	0.17

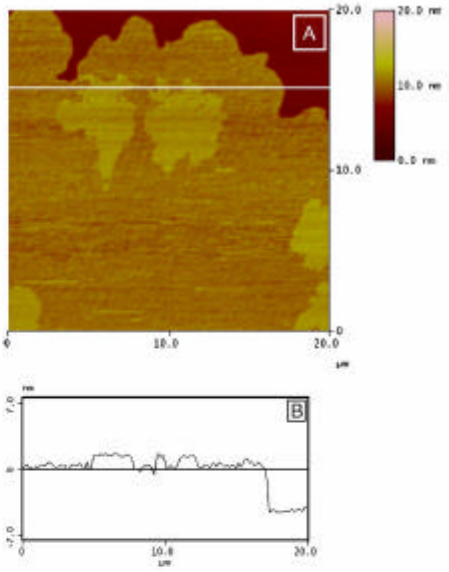

Fig. 7. (A) Topographic image of an SPB of POPE:CL (0.8:0.2, mol:mol) at 24 °C. Buffer (pH 7.40): 50 mM Tris–HCl and 150 mM NaCl. (B) Height profile analysis along the white line shown in panel A.

3.2. AFM study of supported planar bilayers (SPBs)

It is well known that the phospholipid composition of certain biological membranes, contain high proportions of PE and CL. SPBs, formed from simple extensions of liposomes onto

Table 2
Height and roughness (R_a) at the two temperatures of the lipid domains in the SPBs of POPE:CL (0.8:0.2, mol:mol) presented in Fig. 7A and B

Lipid domain height	T=24 °C		T=37 °C	
	h (nm)	R_a (nm)	h (nm)	R_a (nm)
Low	4.7±0.2	0.14	4.2±0.2	0.17
Intermediate	5.1±0.2	0.16	4.7±0.1	0.19
High	6.6±0.2	0.13	6.4±0.2	0.23

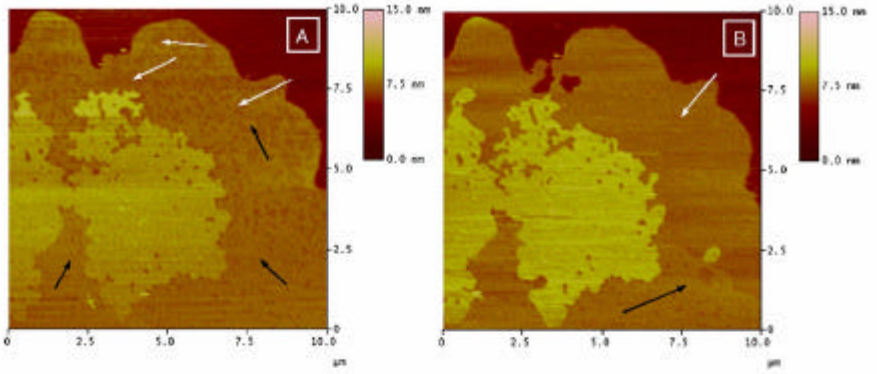

Fig. 8. Higher resolution topographic image of the same SPB presented in Fig. 6 at A 24 °C and B 37 °C. The white and black arrows correspond to the low and intermediate domains.

convenient surfaces [29] have been accepted as suitable models for studying the topographic characteristics of bilayers. Although comparisons of monolayers and bilayers can be contentious, it is accepted that the surface pressure of the biological membranes is about 30 mN m^{-1} [30]. Thus, the most stable monolayers at this pressure (Fig. 5) were taken to form SPBs with the same composition.

Characterization of the SPBs formed from POPC:CL liposomes was carried out at 4 °C and 24 °C, right and above the phase transition temperature (T_m) of the mixture in solution. On the other hand the characterization of the SPBs formed from POPE:CL liposomes was carried out at 24 °C and 37 °C, above the T_m.[2] Nevertheless, the use of T_m here is merely indicative, because it has been shown that the supporting material has a definite effect on the phase transition of each phospholipid mixture [31].

By spreading liposomes formed with the POPC:CL (0.6:0.4, mol:mol) phospholipid matrix onto mica, rounded and featureless SPBs were obtained, at 4 °C (Fig. 6A) and 24 °C (Fig. 6C). As suggested by the thermodynamic analysis performed above, lateral separations were not observed. The bilayers' thicknesses, calculated from cross-sectional analysis (Fig. 6B and D, respectively), decreased as the visualization temperature increased, while the roughness (R_a) values were very similar (Table 1).

A topographic image of an SPB formed with the POPE:CL (0.8:0.2, mol:mol) phospholipid matrix above the T_m of the mixture is shown in Fig. 7. The POPE:CL (0.8:0.2, mol:mol) system covers more substrate than the POPC:CL (0.6:0.4, mol:mol) for the same extension time. The differences in the spreading behavior between POPE:CL and POPC:CL preparations could be related with: (i) the propensity of POPE and CL to form non-lamellar phases [32]; and (ii) the different hydration degrees of PC and PE [33,34].

The thickness, obtained by measuring the step height in Fig. 7B between the uncovered mica (darkest region in Fig. 7A) and the layer, was established in 5.1 ± 0.2 nm (n = 50) with a mean R_a value of 0.16 nm (n = 50) (Table 2). Interestingly, lipid domains appeared, which can be distinguished by differences in the color scale. This observation is in concordance with CL domains revealed in natural membranes using fluorescent probes [35] and recent AFM observations [36]. From Fig. 7B, two lipid domains were visualized with a difference in height of 1.5 ± 0.2 nm (n = 50). Similar values have been reported for interdomain differences with other phospholipids systems [24,37]. Interestingly, close inspection of high-resolution images in the same area revealed the existence of two different lipid subdomains (Fig. 8A) in the lower domain of Fig. 7A. At this time, three lipid

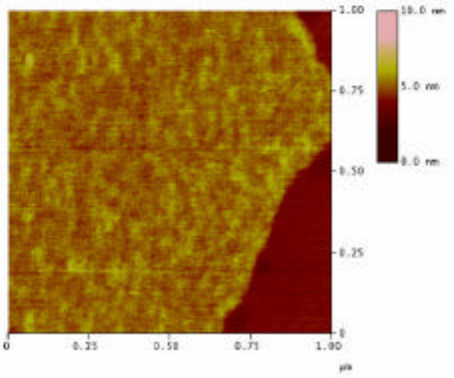

Fig. 9. Topographic image of an SPB of POPE:CL (0.8:0.2, mol:mol) at 24 °C. Buffer (pH 7.40): 50 mM Tris–HCl and 150 mM NaCl after in situ injection of cyt c (1 μM).

[2] T_ms for POPC, CL and POPE are −5 °C, 19 °C and 25.5 °C, respectively; the T_ms for the POPC:CL and POPE:CL mixtures used in the AFM experiments were established at 4 °C and 22 °C (unpublished TMA-DPH and DPH steady-state anisotropy experiments).

domains coexisted: low, intermediate and high (Table 2). Although the differences in height between the low and intermediate domains were small, they were always reproducible and much lower than the high domain. The differences between the low and the intermediate domains could result from a difference in tilt of the species, asymmetric distribution of the species, or alternatively, because of the formation of non-lamellar phases [38]. To investigate the nature of each lipid domain, the temperature of the sample was changed. AFM images taken at 37 °C (Fig. 8B) show that the low domain (white arrow) spreads, occupying a larger area than at 24 °C (Fig. 8A), while the intermediate domain (black arrow) is restricted to a minor area. Strikingly, while the low and intermediate domains were temperature-dependent the higher domain remained unaltered in height and extension when the observation temperature was increased. This behavior could result because of CL is present in just one leaflet in these regions, which could in turn be related with the uncoupling transition of top and distal monolayers of the SPBs [31].

These observations suggest that CL might be laterally segregated from POPE. At this point, we presume that the highest lipid domain could be mainly enriched in CL, based in the fact that its extension is 17% of the total area of the SPB and is consistent with the nominal composition of the liposomes used to form these SPBs. In agreement with this interpretation, we have observed (data not shown) that the area increases as the proportion of CL in the binary mixture increases. On the other hand, this behavior compares well with the domains observed in SPBs of POPE:POPG [10]. Caution, however, should be taken with this interpretation taking into account the impossibility of assigning these domains to a particular phospholipid species. On the other hand, thermodynamic analysis of POPE:CL monolayers suggests that some sort of miscibility exists between both phospholipids. Hence, it is possible that the low and intermediate domains could result from a different POPE enrichment in CL than in the high domain.

To explore the surface charge exposed by each domain, cyt *c* (positively charged at this pH) [39] was injected into the fluid cell where SPBs similar to that shown in Fig. 7A were previously formed. In agreement with other works [40], protein molecules were not topographically visible onto the SPBs interface (Fig. 9). Importantly, there was a remarkable increase, from 0.13 (Table 2) to 0.29, in the R_a value of the high domain while the low domain remain unaffected. These observations strongly suggest that the high domain is mainly formed by CL [12]. This observation is in agreement with results elsewhere published [41] where it has been shown that cyt *c* adsorbs preferentially at anionic bilayer-buffer interfaces.

It is well known that CL is functionally relevant for the energy transduction process based on evidence that it facilitates the binding of cyt *c* to cyt *c* oxidase. There are currently three proposed models to explain the effects of CL on cyt *c* oxidase [42]. One of these proposed models is based on the fact that CL may increase the surface concentration of cyt *c* close to the respiratory chain. Thus, the interaction of cyt *c* with the SPBs showed here will be of relevance for a fuller understanding of electron-transfer processes, as well as for greater insight into apoptosis when the matrix where the proteins are located is modified. Work is currently underway in our laboratory to demonstrate these points.

Acknowledgements

Ò.D. is the recipient of a "Recerca i Docència" fellowship from the University of Barcelona. This work has been supported by grants CTQ2004-08046-C02-01 and CTQ2005-07989 from the Ministerio de Ciencia y Tecnología (MCYT) and SGR00664 from DURSI (Generalitat de Catalunya) Spain.

References

[1] S. Fleischer, G. Rouser, B. Fleischer, A. Casu, G. Kritchevsky, Lipid composition of mitochondria from bovine heart, liver and kidney, J. Lipid Res. 8 (1967) 170–180.
[2] G. Daum, Lipids of mitochondria, Biochim. Biophys. Acta 684 (1985) 1–42.
[3] Ò. Domènech, J. Torrent-Burgués, S. Merino, F. Sanz, T. Montero, J. Hernández-Borrell, Surface thermodynamics study of monolayers formed with heteroacid phospholipids of biological interest, Colloids Surf., B Biointerfaces 41 (2005) 233–238.
[4] S. Merino, Ò. Domènech, I. Díez-Pérez, F. Sanz, T. Montero, J. Hernández-Borrell, Surface thermodynamic properties of monolayers versus reconstitution of a membrane protein in solid-supported bilayers, Colloids Surf., B Biointerfaces 44 (2005) 93–98.
[5] S. Merino-Montero, Ò. Domènech, T. Montero, J. Hernández-Borrell, Preliminary atomic force microscopy study of two-dimensional crystals of lactose permease from *Escherichia coli*, Biophys. Chemist. 118 (2005) 114–119.
[6] R.M. Ep, R. Bottega, Determination of the phase behaviour of phosphatidylethanolamine admixed with other lipids and the effects of calcium chloride: implications for protein kinase C regulation, Biochim. Biophys. Acta 944 (1988) 144–154.
[7] M.D. Bazzi, M.A. Youakim, G.L. Nelsestuen, Importance of phosphatidylethanolamine for association of protein kinase C and other cytoplasmic proteins with membranes, Biochemistry 31 (1992) 1125–1134.
[8] B. Hoff, E. Strandberg, A.S. Ulrich, D.P. Tieleman, C. Posten, 2H-NMR study and molecular dynamics simulation of the location, alignment, and mobility of pyrene in POPC bilayers, Biophys. J. 88 (2005) 1818–1827.
[9] H.N. Hunter, W. Jing, D.J. Schibli, T. Trinh, I.Y. Park, S.C. Kim, H.J. Vogel, The interactions of antimicrobial peptides derived from lysozyme with model membrane systems, Biochim. Biophys. Acta 1668 (2005) 175–189.
[10] S. Merino, Ò. Domènech, M. Viñas, M.T. Montero, J. Hernández-Borrell, Effects of lactose permease on the phospholipid environment in which it is reconstituted: a fluorescence and atomic force microscopy study, Langmuir 21 (2005) 4642–4647.
[11] M. Schlame, K. Beyer, M. Hayer-Hartl, Molecular species of cardiolipin in relation to other mitochondrial phospholipids, Eur. J. Biochem. 199 (1991) 459.
[12] S. Nichols-Smith, S.-Y. Teh, T.L. Kuhl, Thermodynamic and mechanical properties of model mitochondrial membranes, Biochim. Biophys. Acta 1663 (2004) 82–88.
[13] A. Bruce, Skeletal muscle lipids: II. Changes in phospholipid composition in man from fetal to middle age, J. Lipid Res. 15 (1974) 103–108.
[14] M. Zhang, E. Mileykovskaya, W. Dowhan, Cardiolipin is required for supercomplex formation in the inner mitochondrial membrane, J. Biol. Chem. 277 (2002) 43553–43556.
[15] H. Schagger, Respiratory chain supercomplexes of mitochondria and bacteria, Biochim. Biophys. Acta 1555 (2002) 154–159.
[16] N.C. Robinson, Functional binding of cardiolipin to cytochrome oxidase, J. Bioenerg. Biomembranes 25 (1993) 153–163.

[17] K. Kagiyama, D.F. Pauly, H. Huges, B.Y. Yoon, M.L. Entman, J.B. McMillin-Wood, Protection by verapamil of mitochondria glutathione equilibrium and phospholipid changes during reperfusion of ischemic canine myocardium, Circ. Res. 61 (1987) 301–310.
[18] E.J. Lenefsky, T.J. Slabe, M.S. Stoll, P.E. Minkler, C.L. Hoppel, Myocardial ischemia selectively depletes cardiolipin in rabbit heart subsarcolemmal mitochondria, Am. J. Physiol.-Heart C 280 (2001) H2770–H2778.
[19] J.B. McMillin, G.E. Taffet, H. Taegtmeyer, E.K. Hudson, C.A. Tate, Mitochondrial metabolism and substrate competition in the aging Fisher rat heart, Cardiovasc. Res. 27 (1993) 2222–2228.
[20] S. Pepe, N. Tsuchiya, E.G. LaKatta, R.G. Hudson, PUFA and aging modulate mitochondrial membrane lipid composition and Ca^{++} activation of PDH, Am. J. Physiol.-Heart C 276 (1999) H149–H158.
[21] J.B. McMillin, W. Dowhan, Cardiolipin and apoptosis, Biochim. Biophys. Acta 1585 (2002) 97–107.
[22] N. Zamzami, G. Kroemer, Apoptosis: mitochondrial membrane permeabilization—The (w)hole story? Curr. Biol. 13 (2003) R71–R73.
[23] D.D. Newmeyer, S. Ferguson-Miller, Mitochondria: releasing power for life and unleashing the machineries of death, Cell 112 (2003) 481–490.
[24] F. Tokumasu, A.J. Jin, G.W. Feigenson, J.A. Dvorak, Atomic force microscopy of nanometric liposome adsorption and nanoscopic membrane domain formation, Ultramicroscopy 97 (2003) 217–227.
[25] S. Merino, Ò. Domènech, I. Díez, F. Sanz, M. Viñas, M.T. Montero, J. Hernández-Borrell, Effects of Ciprofloxacin on *Escherichia coli* lipid bilayers: an atomic force microscopy study, Langmuir 19 (2003) 6922–6927.
[26] P.E. Milhiet, M.C. Giocondi, O. Baghdadi, F. Ronzon, B. Roux, Ch. Le Grimellec, Spontaneous insertion and partitioning of alkaline phosphatase into model lipid rafts, EMBO Rep. 3 (2002) 485–490.
[27] J. Miñones Jr., P. Dynarowicz-Latka, O. Conde, J. Miñones, E. Iribarnegaray, M. Casas, Interactions of amphotericin B with saturated and unsaturated phosphatidylcholines at the air/water interface, Colloids Surf., B Biointerfaces 29 (2003) 205–215.
[28] D.B. Kell, On the functional proton current pathway of electron transport phosphorylation, Biochim. Biophys. Acta 549 (1979) 55–99.
[29] J. Jass, T. Tjärnhage, G. Puu, From liposomes to supported, planar bilayer structures on hydrophilic and hydrophobic surfaces: an atomic force microscopy study, Biophys. J. 79 (2000) 3159–3163.
[30] G. Cevc, D. Marsh, Phospholipid Bilayers. Physical Principles and Models, Wiley-Interscience, New York, 1987.
[31] D. Keller, N.B. Larsen, I.M. Møller, O.G. Mouritsen, Decoupled phase transitions and grain-boundary melting in supported phospholipids bilayers, Phys. Rev. Lett. 94 (2005) 1–4.
[32] P.R. Cullis, C.P. Tilcock, M.J. Hope, Lipid polymorphism, Membrane Fusion, Marcel Dekker, Inc., New York, 1991, pp. 35–64.
[33] I. Raviakine, A. Brisson, Formation of supported phospholipids bilayers from unilamellar vesicles investigated by atomic force microscopy, Langmuir 16 (2000) 1806–1815.
[34] H. Egawa, K. Furusawa, Liposome adhesion on mica surface studies by atomic force spectroscopy, Langmuir 15 (1999) 1660–1666.
[35] E. Mileykovskaya, W. Dowhan, R.L. Birke, D. Zheng, L. Lutterodt, Y.H. Haines, Cardiolipin binds nonyl acridine orange by aggregating the dye at exposed hydrophobic domains on bilayer surfaces, FEBS Lett. 507 (2001) 187–190.
[36] Ò. Domènech, S. Merino-Montero, M.T. Montero, J. Hernández-Borrell, Surface planar bilayers of phospholipids used in protein membrane reconstitution: an atomic force microscopy study, Colloids Surf., B Biointerfaces 47 (2006) 102–106.
[37] J. Schneider, Y.F. Dufrêne, W.R. Barger Jr., G.U. Lee, Atomic force microscope image contrast mechanism on supported bilayers, Biophys. J. 79 (2000) 1107–1118.
[38] J.K. Rainey, B.D. Skyes, Optimizing oriented planar-supported lipid samples for solid-state protein NMR, Biophys. J. 89 (2005) 2792–2805.
[39] C. Lei, U. Wollenberger, F.W. Cheller, Cytochrome c/Clay modified electrode, Electroanalysis 11 (1999) 274–276.
[40] E.J. Choi, E.K. Dimitriadis, Cytochrome c adsorption to supported, anionic lipid bilayers studied by atomic force microscopy, Biophys. J. 87 (2004) 3234–3241.
[41] H. Mueller, H.J. Butt, E. Bamberg, Adsorption of membrane-associated proteins to lipid bilayers studied with an atomic force microscope: myelin basic protein and cytochrome *c*, J. Phys. Chem., B 104 (2000) 4552–4559.
[42] D. Marsh, G.L. Powell, Properties of cardiolipin and functional implications for cytochrome oxidase activity, Bioelectrochem. Bioenerg. 20 (1988) 73–82.

Available online at www.sciencedirect.com
ScienceDirect
Biochimica et Biophysica Acta 1768 (2007) 100–106
BBA
www.elsevier.com/locate/bbamem

Supported planar bilayers from hexagonal phases

Òscar Domènech [a], Antoni Morros [c], Miquel E. Cabañas [d], M. Teresa Montero [b,e], Jordi Hernández-Borrell [b,e,*]

[a] Departament de Química-Física, Facultat de Química, Spain
[b] Departament de Fisicoquímica, Facultat de Farmàcia U.B. 08028, Spain
[c] Unitat de Biofísica, Departament de Bioquímica i Biología Molecular, Facultat de Medicina i, Spain
[d] Servei de Ressonància Magnética Nuclear (SeRMN), U.A.B., 08193-Bellaterra (Barcelona), Spain
[e] Centre de Referència en Bioenginyeria de Catalunya (CREBEC), Spain

Received 2 May 2006; received in revised form 2 June 2006; accepted 7 June 2006
Available online 14 June 2006

Abstract

In this work the presence of inverted hexagonal phases H_{II} of 1-palmitoy-2-oleoyl-*sn*-glycero-3-phosphoethanolamine (POPE) and cardiolipin (CL) (0.8:0.2, mol/mol) in the presence of Ca^{2+} were observed via ^{31}P-NMR spectroscopy. When suspensions of the same composition were extended onto mica, H_{II} phases transformed into structures which features are those of supported planar bilayers (SPBs). When characterized by atomic force microscopy (AFM), the SPBs revealed the existence of two laterally segregated domains (the interdomain height being ~1 nm). Cytochrome *c* (cyt *c*), which binds preferentially to acidic phospholipids like CL, was used to demonstrate the nature of the domains. We used 1-anilinonaphtalen-8-sulfonate (ANS) to demonstrate that in the presence of cyt *c*, the fluorescence of ANS decreased significantly in lamellar phases. Conversely, the ANS binding to H_{II} phases was negligible. When cyt *c* was injected into AFM fluid imaging cells, where SPBs of POPE:CL had previously formed poorly defined structures, protein aggregates (~100 nm diameter) were ostensibly observed only on the upper domains, which suggests not only that they are mainly formed by CL, but also provides evidence of bilayer formation from H_{II} phases. Furthermore, a model for the nanostructure of the SPBs is herein proposed.

Keywords: Liposome; Supported planar bilayers (SPBs); Hexagonal phase (H_{II}); ^{31}P-NMR; ANS fluorescence; AFM; Cytochrome *c* (cyt *c*)

1. Introduction

It is well known that phosphatidylethanolamines (PEs) and cardiolipin (CL), among other phospholipids, can adopt inverted hexagonal phases H_{II} in suspension under specific conditions [1]. However, the predominance of these kinds of phospholipids in the mitochondria or in the *Escherichia coli* cytoplasmic membrane does not result in hexagonal but in bilayer structures [2,3]. On the other hand, the formation of supported planar bilayers (SPBs) [4] from liposomes has emerged as an appropriate model to investigate the physicochemical properties of biomembranes by means of atomic force microscopy (AFM). SPBs represent an adequate model for investigating membrane properties such as phospholipid domains, protein insertion, and processes like cell adhesion or interactions of active molecules under biomimetical conditions [3,5–8]. SPBs are currently obtained by the so-called vesicle-fusion technique [9], which consists on the deposition of liposomes onto a convenient solid support and the latter's transformation into a planar bilayer after rupture and spreading [4,5,10,11]. In fact, an intriguing question is whether SPBs could be obtained from preparations of phospholipids in non-lamellar phases.

Of particular interest are the mixtures of PE and CL, due to their implications in many bioenergetic processes [12]. Although the occurrence of non-lamellar phases in vivo is doubtful, it is noteworthy that when cytochrome (cyt *c*), primarily associate with CL, it is released from the mitochondria at the onset of apoptosis [13]. Moreover, it has been demonstrated that the release mechanism depends on the presence of Ca^{2+} [14]. It is not known, however, how

* Corresponding author. Departament de Fisicoquímica, Facultat de Farmacia U.B. 08028, Spain.
E-mail address: jordihernandezborrell@ub.edu (J. Hernández-Borrell).

0005-2736/$ - see front matter © 2006 Elsevier B.V. All rights reserved.
doi:10.1016/j.bbamem.2006.06.012

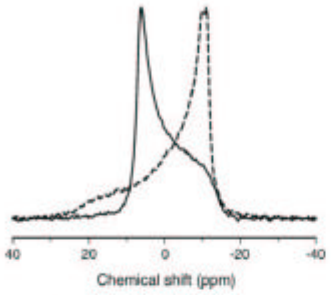

Fig. 1. Solid-state ^{31}P-NMR spectra at 25 °C corresponding to POPE:CL (0.8:0.2, mol/mol) dispersions in Ca^{2+} free 50 mM Tris–HCl, pH 7.40, 150 mM NaCl buffer (dashed line), and in 20 mM $CaCl_2$ added buffer (continuous line). Spectra were normalized to the same height. All chemical shift values are quoted in ppm with reference to external 85% phosphoric acid in H_2O as a reference (0 ppm), positive values referring to low-field shifts.

phospholipid phases might provide the adequate interfacial structure for cyt *c* binding under such conditions.

We have shown that SPBs can be formed from liposomes of 1-palmitoyl-2-oleoyl-*sn*-glycero-3-phosphoethanolamine (POPE) and CL (0.8:0.2) mol/mol [15]. On the other hand, it is worth noting that such liposomes are normally incubated in the presence of divalent cations when the suspensions are deposited onto mica. As discussed elsewhere [5,10], Ca^{2+} and Mg^{2+} ions appear to facilitate the extension and fusion of liposomes onto the negatively charge borne by the mica. Therefore, the existence of non-lamellar phases, albeit in two dimensions, should be considered.

In this regard, the main purposes of this study are to investigate whether: (i) SPBs of POPE:CL (0.8:0.2, mol/mol) could be effectively formed from H_{II} suspensions of the same composition; and (ii) if lamellar or H_{II}, phases may bind cyt *c*. By combining our AFM observations of SPBs and binding experiments in solution, using 1-anilinonaphtalene-8-sulfonate (ANS), we have investigated whether CL forms laterally segregated domains onto mica.

2. Materials and methods

2.1. Materials

1-palmitoyl-2-oleoyl-*sn*-glycero-3-phosphoethanolamine (POPE) and 99% pure cardiolipin (CL) were purchased from Avanti Polar Lipids (Alabaster, AL, USA) and used without further purification. 1-Anilinonaphtalene-8-sulfonate (ANS) was obtained from Molecular Probes (Eugene, OR). Horse heart

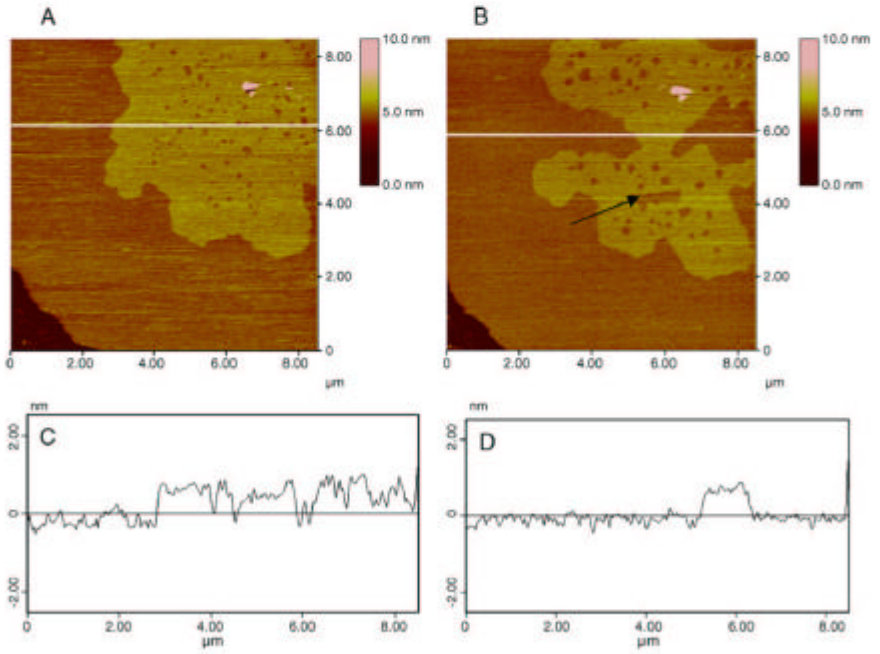

Fig. 2. (A) Topographic image of planar structures obtained by spreading POPE:CL (0.8:0.2, mol:mol) suspensions in 50 mM Tris–HCl, pH 7.40, 150 mM NaCl, 20 mM $CaCl_2$ after being washed with Ca^{2+} free buffer; (B) the same image scanned repeatedly by the AFM probe at a higher force (30 nN); (C and D) are the height profile analyses along the white lines shown in panels A and B, respectively.

cytochrome *c* was purchased from Sigma Chemical Co. (Madrid, Spain). Mica was obtained from Asheville-Schoonmaker Mica Co., VA, USA). Two different buffer solutions were used: (A) 50 mM Tris–HCl, pH 7.40, 150 mM NaCl and (B) 50 mM Tris–HCl, pH 7.40, 150 mM NaCl, 20 mM $CaCl_2$.

2.2. ^{31}P-nuclear magnetic resonance measurements

Chloroform/methanol (50:50, v/v) stock solutions of the desired mixture of POPE and CL were evaporated to dryness in a conical tube using a rotavapor. The resulting thin lipid film was then kept under high vacuum overnight to ensure the absence of organic solvent traces. Suspensions for ^{31}P-Nuclear Magnetic Resonance (^{31}P-NMR) spectroscopy were obtained by hydration in excess of either buffer A or B to a final concentration of 2.2 mM. The resulting suspension was then pelleted by ultracentrifugation at 115,000 × *g* for 1 h at 5 °C. The hydrated pellet was then resuspended in 300 μL of supernatant and placed in a conventional 5 mm NMR tube. A capillary tube containing ^2H_2O was added for field-frequency stabilization.

^{31}P-NMR spectra were recorded as detailed elsewhere [16] on a Bruker ARX-300 spectrometer (Bruker Española, S.A., Madrid), operating at 161.98 MHz using a 90° pulse sequence, with proton-decoupling conducted during signal sampling by means of a Waltz-16 composite pulse sequence [17,18]. The single pulse sequence was used instead of the phase-cycled Hahn echo pulse sequence [19] to obtain spectra with higher signal-to-noise ratios [20]. Each spectrum was the result of accumulating 4096 sampled scans using 2048 complex data points, with a 90° pulse of 16 μs (B_{eff}= 19.5 kHz), an interpulse delay of 2.1 s, and a spectral width of 50 kHz. An exponential multiplication resulting in a line broadening of 50 Hz was applied before Fourier transformation to improve the signal-to-noise ratio. Spectra were processed on a personal computer running the TopSpin v. 1.3 software (Bruker Biospin GmbH, Germany) on Debian GNU/Linux v. 3.1. All chemical shift values are quoted in parts per million (ppm) with reference to pure external 85% phosphoric acid in H_2O as a reference (0 ppm), positive values referring to low-field shifts.

2.3. Fluorescence measurements

As described elsewhere for fluorescence measurements [3] the lipids suspensions obtained either in buffer A or B (liposomes or H_{II} phases, respectively) were filtered through polycarbonate membranes (400 nm nominal diameter) using an Extruder device (Lipex Biomembranes Inc., BC) and diluted with appropriate buffer to a final concentration of 100 μM total phospholipids. Fluorescence measurements were carried out using an SLM-Aminco 8100 spectrofluorometer at 21 °C. Under continuous stirring ANS was added from a stock solution in ethanol (5 mM) to the cuvette to the desired final concentration (0–160 μM). The measurements were done using excitation and emission wavelengths of 380 and 480 nm, respectively. The excitation and emission slits

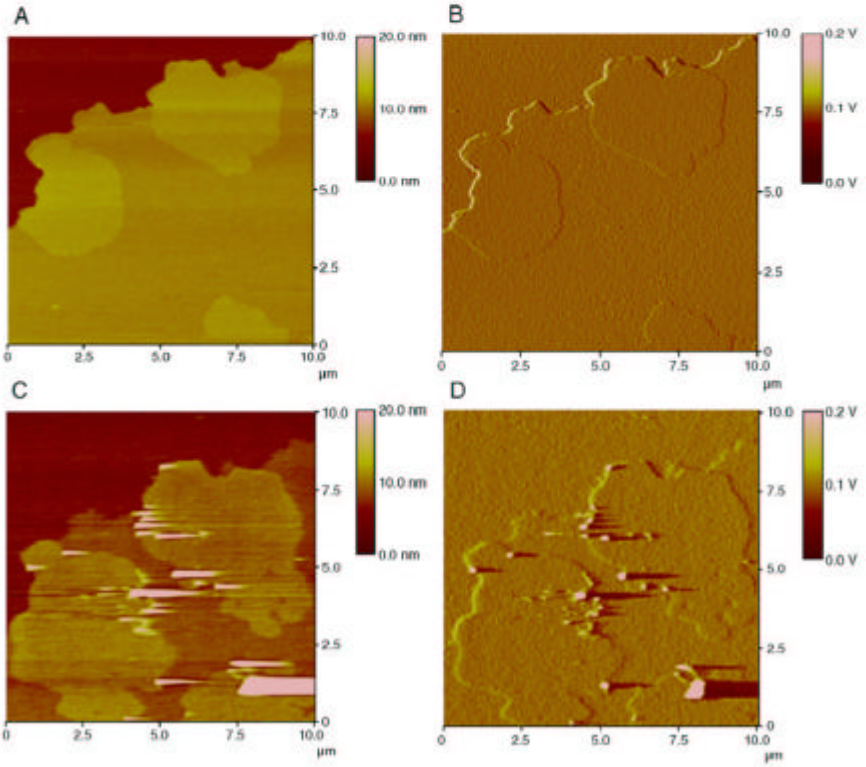

Fig. 3. (A) Topographic image of POPE:CL (0.8:0.2, mol:mol) SPBs at 24 °C; (B) deflection image of panel A; (C) topographic image of the SPB after the addition of cyt *c* (1 μM); (D) Deflection image of panel C.

were 8 and 8 nm and 4 and 4 nm, respectively. Cyt *c* was added to the cuvette to a final lipid-to-protein molar ratio of ~1 and incubated for 30 min at 24 °C.

2.4. Supported planar bilayers formation and AFM observations

The experimental procedures were adapted form previous works [3,7,15]. Briefly, 50 μL of the H_{II} phase suspensions (in buffer A) were pippeted onto ~0.5 cm^2 freshly cleaved mica sheet. After allowing the vesicles to adsorb at room temperature (24 °C) for 30 min the surface was gently washed with Ca^{2+} free buffer (buffer B) and the tip immediately immersed in the buffer. For in situ AFM measurements, cyt *c* was added into the fluid cell at a final concentration of 5 μM. All images were acquired in tapping mode with a Multimode Digital Instruments (Santa Barbara, CA) microscope controlled by a Nanoscope IV electronics fitted with a 15×15 μm scanner ("J"-scanner). Standard V-shaped Si_3N_4 tips, with a nominal force constant of 0.08 N m^{-1} (Olympus, Germany), were used. In order to minimize the forces exerted on the sample, the vibration amplitude of the tip was reduced as much as possible and amplitude setpoint was set as high as possible without losing contact with the surface of the sample. The scan rate was set to 1.5 Hz. Before every sample, the AFM liquid cell was washed with ethanol and ultra pure water (Milli Q reverse osmosis system), and allowed to dry in an N_2 stream. Mica discs (green mica) were cleaved with scotch and glued onto a Teflon disc by a water-insoluble epoxy. These Teflon discs were glued onto a steel disc and then mounted onto the piezoelectric scanner. All images were scanned under aqueous solution and processed with the Nanoscope IV software.

3. Results and discussion

In Fig. 1, the ^{31}P-NMR powder pattern spectra of the POPE:CL (0.8:0.2, mol/mol) systems at 25 °C in the buffer in the presence (continuous line) and absence (dashed line) of 20 mM $CaCl_2$ shows the typical features for the H_{II} and lamellar organizations, respectively. These results are in accordance with the fact that PEs, as well as CL, have a strong tendency to adopt H_{II} phases in the presence of Ca^{2+}. The existence of hexagonal phases of POPE:CL at 25 °C is in concordance with two facts: (i) POPE exhibits a typical bilayer-to-hexagonal phase transition between 66 and 74 °C, which in turn decreases in the presence of Ca^{2+} [21]; and (ii) CL adopts an H_{II} phase in the presence of Ca^{2+} [22]. Indeed, the POPE:CL system exhibits the coexistence of lamellar and H_{II} phases between 5 and 18 °C, H_{II} phase being predominant above 18 °C remaining so up to 70 °C in the presence of Ca^{2+} (^{31}P-NMR data not shown).

When POPE:CL lipid suspensions in Ca^{2+} containing buffer (i.e., in the H_{II} phase) (Fig. 1) were deposited onto mica, planar bilayer-like structures [4] with two domains were observed (Fig. 2A). The absence of distinctive geometrical facets as those reported for cubic and hexagonal phases of other compositions [23] indicate that the H_{II} phase of the POPE:CL system is not retained after adsorption onto the mica surface. Bilayer thickness can be inferred by measuring the step height between the top of the layer and the uncovered mica (red color in the lower-left corner). Thus, while the height of the lower domain, 4.64±0.16 nm (n=25), fell within the range expected for bilayer thickness [7] the upper domain appeared as an upper layer, measuring ~1.00±0.08 nm (n=50) above the lower domain. In addition, the thickness of the upper layer coincided with the depth of numerous defects (holes) observed. When this SPB was repeatedly scanned at a force of ~30 nN for 20 s (Fig. 2B), the upper layer became unstable and lipid molecules could be swept away. As can be observed by following the cross-sectional analysis along the white line drawn in Fig. 2C and D, this observation is consistent with the fact that the surface overlaying the lower domain decreased. Furthermore, the height of the upper domain was confirmed by measuring the depth of the small scratched area (indicated by the black arrow in Fig. 2B). As expected, the resulting measurement (~0.94±0.09 nm) coincided with the interdomain height reported above.

To investigate the nature of the upper domain, cyt *c* was injected into the AFM fluid imaging cell where the POPE:CL system was previously formed. Similar to Fig. 2, two domains can be easily distinguished by differences in the color scale of the topography image (Fig. 3A), as well as by the deflection images (Fig. 3B). When cyt *c* (positively charged at this pH) [24] was injected, small bright spots with a higher height emerged predominantly at the edges of the upper domain (Fig. 3C). Such behaviour has been observed for an alkaline phosphatase [25] which has been related to a decrease in the interfacial tension at the phase boundary. Besides, there is a lateral grow of the upper domain. This could be attributed either

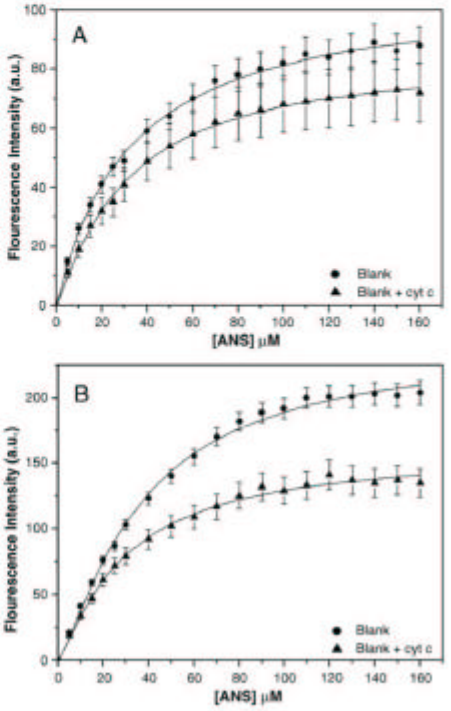

Fig. 4. Fluorescence intensity of ANS bound to POPE:CL (0.8:0.2, mol/mol) of the H_{II} phase (A) and liposomes (B) as a function of the free ANS concentration, in the absence (●) and presence of cyt *c* (▲). The total lipid concentration was 50 μM.

to a partial insertion of cyt *c* into the bilayer or to the thermal response of the phospholipids as a consequence of the continuous action of the laser. To assist with visualization, the corresponding deflection image (Fig. 3D) is presented. Here, poorly defined structures, presumably protein aggregates (~100 nm diameter), can be observed on the upper domain. In agreement with these observations, circular aggregates of cyt *c* have been observed on acid lipid bilayers, although of larger diameter (>400 nm) [26] than those observed here. However, the observation of single entities of cyt *c* appeared to depend on the balance between electrostatic and hydrophobic forces [27,28].

ANS is a fluorescent molecule extensively used for monitoring changes in the hydrophilic phosphate moiety of phospholipids [29,30]. Typically, the fluorescence intensity increases as the label is added to phospholipid suspensions until a plateau is reached at high probe concentrations [31]. These behaviours are illustrated by the Langmuir-like isotherms [16] obtained by labelling the POPE:CL systems with ANS in the presence (Fig. 4A) and absence (Fig. 4B) of Ca^{2+}. It is well known that cyt *c* associates electrostatically with acidic phospholipids at neutral pH [32]. On the other hand, at high CL contents (>20%) the protein becomes partially inserted into the bilayer [33]. Hence that ANS can be displaced from suspensions of POPE:CL in presence of cyt *c*. Consequently, the fluorescence of ANS decreased in both the H_{II} phase (Fig. 4A) and liposomes (Fig. 4B) as a result of the competition between cyt *c* and ANS for the same binding sites. Fluorescence intensity values for H_{II} phases in the presence of cyt *c* (Fig. 4A) revealed that cyt *c* binding was practically negligible because the values in the presence of protein fell within the same standard deviation values as obtained in its absence. In addition, the fluorescence intensities exhibited were higher for the lamellar than for the H_{II} phases. This behaviour is probably due to the fact that the anionic phospholipid-buffer interfaces are less exposed (negative curvature) compared with that of liposomes (positive curvature). However, the accessibility of cyt *c* for the polar head regions, which should diffuse through apolar regions to access the binding site, was clearly reduced in the case of the H_{II} phases. Although indirectly, this confirms the lamellar nature of the supported structures onto which cyt *c* binds (Fig. 3).

All of these findings led us to propose a model for interpreting those structures observed through the AFM (Fig. 5). Basically, POPE:CL is in a hexagonal phase when deposited onto the substrate (Fig. 5A). The presence of Ca^{2+} induces, in several intermediate steps similar to those depicted in Fig. 5B and C, the formation of planar structures in two levels or domains (Figs. 2 and 3). Although the composition of each domain is difficult to ascertain, we have previously reported [15] that there is a decrease only in the thickness of the lower domain but not in the upper domain by increasing the temperature. Therefore, it could be assumed that the lower domains are POPE-enriched bilayers. This is farther substantiated by two facts: (i) the height of these domains was consistent with the PE bilayers' height [11]; and (ii) the thermotropic gel-to-fluid phase transition was observed around

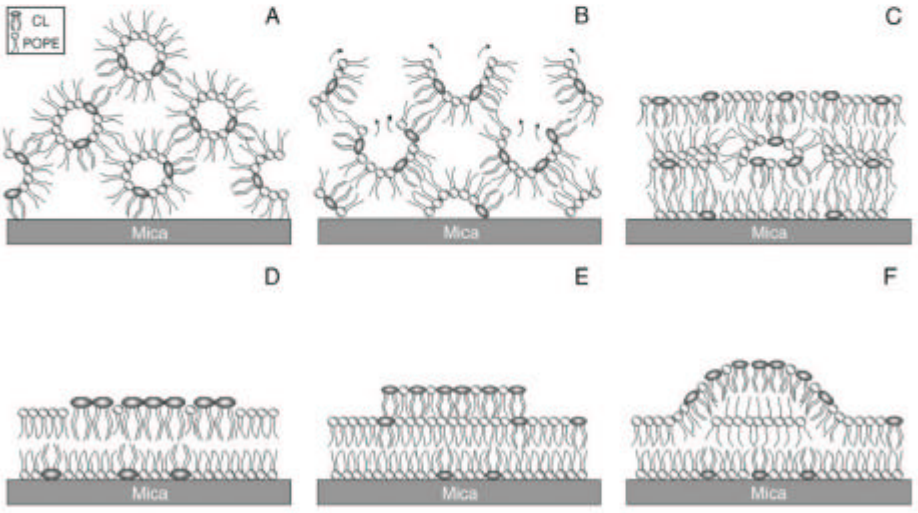

Fig. 5. Some of the events thought to occur during the formation of planar structures on mica: (A) POPE:CL (8:2, mol/mol) hexagonal (H_{II}) phase adsorption; (B) fusion onto mica; (C) H_{II} to lamellar phase transition showing an inverted micelle; (D) supported planar bilayer showing laterally segregated CL; (E) a hypothetical trilayer; and (F) a planar bilayer with the extended CL conformation.

24 °C [15]. Interpreting the upper domain that binds cyt *c* is a bit more difficult. As cyt *c* is anionic phospholipid-specific in nature, and taking into account the ability of Ca^{2+} to induce lateral phase separation of mixtures containing negatively charged phospholipids [10], it seems reasonable to assume that the upper domain should be mostly formed by CL (Fig. 5D). It is more difficult, however, to provide a reasonable explanation for the height of this domain, (within the range of the height of a phospholipid monolayer). Nevertheless, an overestimation of the height as a result of tip repulsion could not be excluded. Other potential scenarios to explain the occurrence of these domains include: (i) one possessing an upper CL-enriched monolayer adsorbed onto the bilayers (Fig. 5E); or (ii) one with CL molecules in "extended" conformation [34] resulting in the upper domains (Fig. 5F). Although possible, the existence of a monolayer with the acyl chain adsorbed on top of the polar head groups is unlikely based on the nature of the intermolecular forces that would be involved. On the other hand, an extended conformation would result as an intermediate step in the transformational process of H_{II} phases into bilayers when deposited onto mica. Thus, assuming that by the action of the tip, the molecules that are swept away (Fig. 2B) might be mainly of CL, the structural model shown in Fig. 2D could be the most likely. Other approaches and techniques will be undertaken for our group in the near future to demonstrate this hypothesis.

Acknowledgements

Ò.D. is the recipient of a "Recerca i Docència" fellowship from the University of Barcelona. This work has been supported by grants CTQ2005-07989 from the Ministerio de Ciencia y Tecnología (MCYT) and SGR2006-00664 and SGR2001-00197 from DURSI (Generalitat de Catalunya) Spain.

References

[1] J.M. Seddon, Structure of the inverted hexagonal (H_{II}) phase, and non-lamellar phase transitions of lipids, Biochim. Biophys. Acta 1031 (1990) 1–69.
[2] G.F. White, K.I. Racher, A. Lipski, F.R. Hallet, J.M. Wood, Physical properties of liposomes and proteoliposomes prepared from *Escherichia coli* polar lipids, Biochim. Biophys. Acta 1468 (2000) 175–186.
[3] S. Merino, Ò. Domènech, M. Vilfas, T. Montero, J. Hernández-Borrell, Effects of lactose permease on the phospholipid environment in which it is reconstituted: a fluorescence and atomic force microscopy study, Langmuir 21 (2005) 4642–4647.
[4] R.P. Richter, R. Bérat, A.R. Brisson, Formation of solid-supported lipid bilayers: an integrated view, Langmuir 22 (2006) 3497–3505.
[5] J. Jass, T. Tjärnhage, G. Puu, From liposomes to supported, planar bilayer structures on hydrophilic and hydrophobic surfaces: an atomic force microscopy study, Biophys. J. 79 (2000) 3159–3165.
[6] R.P. Richter, A.R. Brisson, Following the formation of supported lipid bilayers on mica: a study combining AFM, QCM-D, and ellipsometry, Biophys. J. 88 (2005) 3422–3433.
[7] Ò. Domènech, S. Merino-Montero, M.T. Montero, J. Hernández-Borrell, Surface planar bilayers of phospholipids used in protein membrane reconstitution: an atomic force microscopy study, Colloid Surf., B Biointerfaces 47 (2006) 102–106.
[8] Y.F. Dufrêne, G.U. Lee, Advances in the characterization of supported lipid films with the atomic force microscope, Biochim. Biophys. Acta 1509 (2000) 14–41.
[9] A.A. Brian, H.M. McConnell, Allogeneic stimulation of cytotoxic T cells by supported planar membranes, Proc. Natl. Acad. Sci. U.S.A. 81 (1984) 6159–6163.
[10] I. Raviskina, A. Brisson, Formation of supported phospholipids bilayers from unilamellar vesicles investigated by atomic force microscopy, Langmuir 16 (2000) 1806–1815.
[11] H. Egawa, K. Furusawa, Liposome adhesion on mica surface studied by atomic force microscopy, Langmuir 15 (1999) 1660–1666.
[12] E. Mileykovskaya, M. Zhang, W. Dowhan, Cardiolipin in energy transducing membranes, Biochemistry (Moscow) 70 (2005) 154–158.
[13] M. Ott, J.D. Robertson, V. Gogvadze, B. Zhivotovsky, S. Orrenius, Cytochrome c release from mitochondria proceeds by a two-step process, Proc. Natl. Acad. U.S.A. 99 (2002) 1259–1263.
[14] V. Gogvadze, J.D. Robertson, B. Zhivotovsky, S. Orrenius, Cytochrome c release occurs via Ca^{2+}-dependent and Ca^{2+}-independent mechanisms that are regulated by Bax, J. Biol. Chem. 276 (2001) 19066–19071.
[15] O. Domènech, F. Sanz, M.T. Montero, J. Hernández-Borrell, Thermodynamic and structural study of the main phospholipid components comprising the mitochondrial inner membrane, Biochim. Biophys. Acta 1758 (2006) 213–221.
[16] A. Grancelli, A. Morros, M.E. Cabañas, O. Domènech, S. Merino, J.L. Vázquez, M.T. Montero, M. Vilfas, J. Hernández-Borrell, Interaction of 6-fluoropsicolones with dipalmitoylphosphatidylcholine monolayers and liposomes, Langmuir 18 (2002) 9177–9182.
[17] J.A. Killian, C.H.J.P. Fabrie, W. Baart, S. Mansin, B. de Kruijff, Effects of temperature variation and phenethyl alcohol addition on acyl chain order and lipid organization in *Escherichia coli* derived membrane systems, A ^{2}H- and ^{31}P-NMR study, Biochim. Biophys. Acta 1105 (1992) 253–262.
[18] J.C. Gómez-Fernández, M.A. Llamas, F.J. Aranda, The interaction of coenzyme Q with phosphatidylethanolamine membranes, Eur. J. Biochem. 259 (1999) 739–746.
[19] M. Rance, R.A. Byrd, Obtaining high-fidelity spin-1/2 powder spectra in anisotropic media: Phase-cycled Hahn echo spectroscopy, J. Magn. Reson. 52 (1983) 221–240.
[20] R.N.A.H. Lewis, B.D Sykes, R.N. McElhaney, Thermotropic phase behavior of model membranes composed of phosphatidylcholines containing cis-monounsaturated acyl chain homologues of oleic acid: differential scanning calorimetric and ^{31}P NMR spectroscopic studies, Biochemistry 27 (1988) 880–887.
[21] R.M. Epand, R. Bottega, Determination of the phase behaviour of phosphatidylethanolamine admixed with other lipids and the effects of calcium chloride: implications for protein kinase C regulation, Biochim. Biophys. Acta 944 (1988) 144–154.
[22] B. de Kruijff, A.J. Verkley, C.J.A. Van Echteld, W.J. Gerritsen, C. Mombers, P.C. Noordam, J. de Gier, The occurrence of lipidic particles in lipid bilayers as seen by ^{31}PNMR and freeze-fracture electron-microscopy, Biochim. Biophys. Acta 555 (1979) 200–209.
[23] C. Neto, G. Aloisi, P. Baglioni, Imaging soft matter with the atomic force microscope: cubosomes and hexosomes, J. Phys. Chem. B 103 (1999) 3896–3899.
[24] C. Lei, F.W. Cheller, U. Wollenberger, Cytochrome c/Clay modified electrode, Electroanalysis 11 (1999) 274–276.
[25] P.E. Milhiet, V. Vié, M.C. Giocondi, Ch. Le Grimellec, AFM characterization of model rafts in supported bilayers, Single Mol. 2 (2002) 109–112.
[26] H. Mueller, H.J. Butt, E. Bamberg, Adsorption of membrane-associated proteins to lipid bilayers studied with an atomic force microscope: myelin basic protein and cytochrome *c*, J. Phys. Chem., B. 104 (2000) 4552–4559.
[27] P. Mustonen, J. Lehtonen, A. Koiv, P.K.J. Kinnunen, Effects of sphingosine on peripheral membrane interaction: comparison of adriamycin, cytochrome *c*, and phospholipase A_2, Biochemistry 32 (1993) 5373–5380.
[28] E.J. Choi, E.K. Dimitriadis, Cytochrome *c* adsorption to supported,

anionic lipid bilayers studied by atomic force microscopy, Biophys. J. 87 (2004) 3234–3241.
[29] J. Slavík, Anilinonaphtalene sulfonate as a probe of membrane composition and function, Biochim. Biophys. Acta 694 (1982) 1–25.
[30] J.Y.C. Ma, J.K.H. Ma, K.C. Weber, Fluorescence studies of the binding of amphiphilic amines with phospholipids, J. Lipid Res. 26 (1985) 735–743.
[31] J. Teissie, A. Baudras, A fluorescence study of the binding of cytochrome C to mixed-phospholipid microvesicles: evidence for a preferred orientation of the bound protein, Biochimie 59 (1977) 693–703.
[32] H. Görisch, D. Marsh, A. Rietveld, B. de Kruijff, Apocytochrome c binding to negatively charged lipid dispersions studied by spin-label electron spin resonance, Biochemistry 25 (1986) 2904–2910.
[33] Y.A. Domanov, J.G. Molotkovsky, G.P. Gorbenko, Coverage-dependent changes of cytochrome c transverse location in phospholipids membranes revealed by FRET, Biochim. Biophys. Acta 1714 (2005) 49–58.
[34] P.K.J. Kinnunen, Fusion of lipid bilayers: a model involving mechanistic connection to phase forming lipids, Chem. Phys. Lipids 63 (1992) 251–258.

Article submitted to Ultramicroscopy. Accepted 2007/01/26

Thermal response of domains in cardiolipin content bilayers

Òscar Domènech[†], Antoni Morros[‡], Miquel E. Cabañas[#],M. Teresa Montero[§,±], Fausto Sanz [±,†], Jordi Hernández-Borrell[§,±,*]

[†]Departament de Química-Física, Facultat de Química, [§]Departament de Fisicoquímica, Facultat de Farmacia U.B. 08028-Spain.[‡]Unitat de Biofísica, Departament de Bioquímica i Biología Molecular, Facultat de Medicina i [#]Servei de Ressonància Magnètica Nuclear (SeRMN), U.A.B., 08193-Bellaterra (Barcelona), Spain.

Abstract

In the study described here, supported planar bilayers (SPBs) of POPE:CL (0.8:0.2, mol:mol) were examined using atomic force microscopy (AFM). SPBs were formed from suspensions of POPE:CL (0.8:0.2, mol:mol) in inverted hexagonal (H_{II}) phases (buffer containing Ca^{2+}). Three laterally segregated domains which differ in height were observed at 24 °C. Based on the area accounted for each domain and the nominal composition of the mixture, we interpret that the higher domain is formed by CL, while the intermediate and lower domains are formed by POPE. The three domains respond to temperature increase with relative changes in their area. At 37 °C we observed that the increase in the area of the intermediate domain occurs at the expense of the lower domain. ^{31}P-NMR DSC were used in combination with AFM to characterize the phase behavior of the suspensions and to elucidate the nature of the structures observed.

Keywords: supported planar bilayers, . ^{31}P-NMR, DSC, AFM,

[±] Centre de Referència en Bioenginyeria de Catalunya (CREBEC)
* Corresponding author: jordihernandezborrell@ub.edu

1. Introduction

Among the main components of the mitochondrial inner membrane of eukaryotic and many bacterial cells, cardiolipin (CL), a doubly negatively-charged four-tailed phospholipid, is one of the most relevant constituents. The two-dimensional phospholipid matrix that constitutes the bilayer is formed by phosphatidylcholine (PC, 40 % in weight), phosphatidylethanolamine (PE, 40 %), and cardiolipin (CL, 20 %) [1].

It is believed that CL plays a crucial role in the transference of electrons from cytochrome c (cyt *c*) to specific transmembrane proteins involved in the energy transduction [2]. Related to that and based mainly on atomic force microscopy (AFM) observations, it has been demonstrated that there is a specific affinity of cyt *c* for CL [3, 4]. On the other hand, we studied in detail the mixing properties of 1-palmitoy-2-oleoyl-*sn*-glycero-3-phosphoethanolamine (POPE), and CL at the air water interface [5], reaching the conclusion, based on the values of the excess energy of mixing, that the POPE:CL (0.8:0.2, mol/mol) composition is the most stable. Notably, laterally segregated domains [6] were observed by means of atomic force microscopy (AFM) in supported planar bilayers (SPBs) [7] formed by deposition of lipid suspensions of the POPE:CL (0.8:0.2, mol/mol) composition onto a mica surface. In fact, the SPBs at 25 °C were obtained not from liposomes but from H_{II} phases [5, 8]. However, the mechanism of conversion of the H_{II} phases (suspensions) into lamellar phases (SPBs) onto mica remains unclear, and divalent cations such as Ca^{2+} and Mg^{2+} appear to be necessary to facilitate the extension onto the substrate. Several points arose from those experiments: (i) whether there is a response of the observed domains to changes in temperature; and (ii) whether a phase transition can be observed in these SPBs. In the present paper, we will address such points by combination of ^{31}P-NMR spectroscopy, differential scanning calorimetry (DSC) and AFM. While ^{31}P-Nuclear Magnetic Resonance (^{31}P-NMR) spectroscopy enable us to investigate the nature (H_{II} or lamellar phase) at different temperatures, DSC will enable us to obtain the enthalpy and temperature (T_m) of the transition of the phospholipid suspensions. The influence of the temperature on the domains will be assessed by AFM.

2. Materials and methods

1-palmitoyl-2-oleoyl-*sn*-glycero-3-phosphoethanolamine (POPE) and cardiolipin (CL), specified as 99% pure, were purchased from Avanti Polar Lipids (Alabaster, AL,

USA) and used without further purification. Chloroform/methanol (3:1, v/v) stock solutions of the desired phospholipids mixture were evaporated to dryness in a flask using a rotavapor. The resulting thin lipid film was then kept under high vacuum overnight to ensure the absence of organic solvent traces.

Suspensions for ^{31}P-Nuclear Magnetic Resonance (^{31}P-NMR) spectroscopy and DSC were obtained by hydration in excess of 50 mM Tris·HCl, 150 mM NaCl and with or without 20 mM $CaCl_2$, pH 7.40, to a final concentration of 2.5 mM. Samples for NMR where then pelleted by ultracentrifugation at 115,000*g* for 1 h at 5 °C. The hydrated pellet was then resuspended in 300 μL of supernatant and placed in a conventional 5 mm NMR tube. A capillary tube containing D_2O was added for field-frequency stabilization.

The ^{31}P-NMR spectra were recorded as detailed elsewhere [9] on a Bruker ARX-400 spectrometer (Bruker Española, S.A., Madrid) operating at 161.98 MHz using a 90° pulse sequence, with proton-decoupling during signal sampling by means of a Waltz-16 composite pulse sequence [10,11]. The single pulse sequence was used instead of the phase-cycled Hahn echo pulse sequence [12] to obtain spectra with higher signal-to-noise ratios [13]. Each spectrum was the result of accumulating 4096 scans sampled using 2048 complex data points, with a 90° pulse of 16 μs (B_{eff} = 19.5 kHz), an interpulse delay of 2.1 s, and spectral width of 50 kHz. An exponential multiplication resulting in a line broadening of 50 Hz was applied prior to Fourier transformation to improve the signal-to-noise ratio. The spectra were processed on a SGI Indigo workstation running the X-WINNMR v. 3.1 software. All chemical shift values are quoted in parts per million (ppm) with reference to external 85% phosphoric acid in H_2O (0 ppm), positive values referring to low-field shifts.

DSC analyses were performed using a MicroCal MC-2 calorimeter following procedures described elsewhere [14-16]. The obtained data were analyzed using the original calorimeter software. T_m was taken as the temperature of maximum excess specific heat (and measured to the nearest 0.5 °C). The calorimetry accuracy for T_m was ± 0.1 °C, ± 0.2 kcal mol^{-1}. Each sample was scanned in triplicate over the temperature range 4-40 °C at a scan rate of 0.47 °C min^{-1}. The base line was horizontal over the temperature range employed.

SPBs were made by vesicle fusion as previously described [5]. Briefly, lipids were dissolved in chloroform:methanol (3:1, v:v) and mixed to obtain the desired

composition in a conical tube. After mixing the lipids, the solvent was evaporated under a nitrogen stream to dryness. This lipid film was maintained under reduced pressure overnight and then hydrated in 50 mM Tris·HCl, 150 mM NaCl, 20 mM $CaCl_2$, pH 7.40 to a final concentration of 250 μM. To obtain large unilamellar vesicles (LUV) the hydrated lipids were extruded 10 times through two polycarbonate filters (400 nm pore size, Nucleopore, CA, USA) with an Extruder device obtained from Lipex Biomembranes (Vancouver, BC, Canada). In order to obtain supported bilayers, 50 μL of LUV suspension was pipetted on freshly cleaved mica (0.4 cm^2, from Asheville-Schoonmaker Mica Co., VA, USA) and incubated at room temperature for 20 min. After the incubation period, the samples were carefully rinsed with the same buffer without Ca^{2+} to remove the unadsorbed SUV. Mica supports were glued onto Teflon disks with a commercial epoxy and mounted on a steel disc.

Images were acquired with a commercial AFM (Nanoscope III, Digital Instruments, CA, USA) and Si_3N_4 cantilevers (Olympus, Tokyo, Japan) with a nominal spring constant of 0.08 $N{\cdot}m^{-1}$. The instrument was equipped with a "J" scanner (120 μm) with a Tapping® mode fluid cell. The cell was washed extensively with ethanol and water before each experiment to eliminate contaminants. The images were recorded in Tapping® mode under liquid environment. The set point was continuously adjusted during the imaging to minimize the force applied. The images were obtained in a zero scan angle. and the scan rate was adjusted between 1 and 1.8 Hz, according to the scan size. All images were processed using Digital Instrument software.

3. Results

3.1. Calcium influence in suspensions of POPE:CL (0.8:0.2, mol:mol)

^{31}P-NMR spectroscopy is an appropriate technique to unambiguously characterize lipid phases like lamellar or H_{II} to verify the existence of these phases in lipid systems. Figure 1 shows the ^{31}P-NMR powder pattern spectra of POPE:CL (0.8:0.2, mol:mol) systems at 15, 21 and 40 °C in the presence (continuous lines) and in the absence (dashed lines) of 20 mM $CaCl_2$. The samples in the absence of Ca^{2+} mainly showed the typical features of lamellar phase in the whole temperature range studied. In the presence of calcium however, the three spectra mainly showed the typical shape

corresponding to the H_{II} phase; at 15 °C a contribution of lamellar phase was observed which progressively disappeared when the temperature was increased.

In order to characterize the thermotropic behavior of this composition we show in Figure 2 the normalized DSC endotherms of POPE:CL (0.8:0.2, mol:mol) in the presence (continuous line) and in the absence (dashed line) of 20 mM Ca^{2+}. In the absence of calcium only a broad transition appeared in the temperature interval studied, with a T_m centered at 15.2 °C, attributable to the gel to liquid phase transition of the lamellar POPE:CL system. Nevertheless, in the presence of calcium a more complex endotherm appears consisting in a narrower peak with a pronounced tailing. The temperature of maximal excess specific heat (T_m) of the narrow peak occurred at 21.6 °C, similar to the T_m of the gel to liquid phase transition of pure POPE.

3.2. Topography of POPE:CL (0.8:0.2, mol:mol) microdomains

The SPBs obtained by extension on mica of the of H_{II} phases of POPE:CL (0.8:0.2, mol:mol) at room temperatures is shown in Figure 3. When the spreading process was stopped by washing with Ca^{2+}-free buffer, high surface coverage of the mica results (up to approximately 85% in Figure 3A). Some defects, holes, and red are visible in the images. At first sight, two laterally segregated domains, distinguishable by the difference in the color scale, are observed. The thickness of the underlying domain in Figure 3A (darker domain) was established in 4.64 ± 0.16 nm (n=25) by measuring the step height between the top of the layer and the uncovered mica. This value compares well with the depth of the observed holes. On the other hand, several small domains, the lighter patches seen in Figure A, were 1.00 ± 0.08 nm (n=25) taller than the underlying domain, and these small patches account for 20% of the total area covered by the SPB. Remarkably, a magnification of a small area of this SPB (see the inset in Figure 3A) reveals the existence of a third domain (black arrows in Figure 3B). This third domain is lower (~ 0.3 nm) than the second domain. Hence, we will use the terms upper domain (UD), intermediate domain (ID) and lower domain (LD) to differentiate between the three regions observed in the SPBs of POPE:CL (0.8:0.2, mol:mol).

The occurrence of three domains in a binary system suggests that, in addition to the lateral phase separation due to the differences in molecular structure, POPE and CL may simultaneously undergo time a thermal transition. Although we were working above the transition temperature of the mixture (see Figure 2), we investigated whether the SPB

responds to temperature changes. Thus, the images of SPBs at two temperatures studied are shown in Figures 4. At 24 °C, two domains (UD and ID) are observed (Figure 4A). However, a close inspection of the image revealed the existence of a small patch which constitute the third domain (LD). Notably, when the temperature was increased up to 37 °C (Figure 4B), the LD became unveiled and the three domains were clearly distinguishable. It appears that the LD was originated from the small patch observed in Figure 4A and at the expense of the ID. Besides, while the UD remains unaffected by repetitive scans of the area (Figure 4C), the LD expands, against the ID.

4. Discussion

POPE:CL (0.8:0.2, mol:mol), the most stable composition of this binary mixture according mixing properties studied in monolayers [5] was used in this study because of its biological significance [2].

^{31}P-NMR powder pattern spectra of the phospholipid suspensions used to prepare SPBs revealed that, at the temperatures of observation, the mixture is always in H_{II} phase. In agreement with works elsewhere released [5,8] the analysis of AFM images provided information to unambiguously establish that POPE:CL (0.8:0.2, mol:mol) suspensions in H_{II} phase, become oriented towards a lamellar structure when spread onto a mica surface. As has been shown for other phospholipid systems that include negatively charged species, the interaction between that species and the substrate depends on Ca^{2+} presence [17,18]. In our case Ca^{2+} should be considered as the main driving force for the transformation of H_{II} phases into SPBs. As described above in the methods section, after spreading the phospholipids in H_{II} phase, the process is usually stopped by washing with Ca^{2+}-free buffer [19]. Thus, while after washing the aqueous phase above the SPBs becomes free of the divalent cation, the aqueous space immediately below the inner leaflet facing the mica surface retains Ca^{2+}. On the other hand, pure POPE, like other PEs, could not free itself form SPBs spontaneously but mixed with CL. Therefore, it is likely to assume that CL adsorption onto negatively charged mica would be Ca^{2+}-mediated [20]. Similarly to a mechanism proposed elsewhere [21], the mobility of CL and, by extension, POPE, would become severely hindered by the presence of the cation. This will result in the lateral segregation in separated domains of POPE and CL that we observed by AFM. Besides, and based only on the nominal composition of our system and the estimated surface coverage, it can be

assumed that while the intermediate and lower domains are formed by POPE, the upper domain is formed by CL. This is in agreement with the observation that cyt *c* (positively charged at pH 7.40) adsorbs selectively onto upper domains [5,8].

Three domains were observed that respond to temperature increase with changes in their relative area and shapes. According to DSC data, the POPE:CL (0.8:0.2, mol:mol) suspensions used to prepare the SPBs will always be above T_m, either in presence (21.6 °C) or absence (15.2°C) of Ca^{2+}. Although differences (up to 2 °C) in the T_m values between liposomes and SPBs of the same composition have been reported [22, 23], it is unrealistic to assume that by increasing the temperature from 24 to 37 °C we would be observing the phase transition of the POPE:CL system in SPBs. The most dramatic change was the retraction of the intermediate domain, which is concomitant with the expansion of the lower domain. Assuming that both domains are formed by POPE, the step height difference between them (~0.3 nm) suggests that a thermal phase transition between two POPE phases is underway. However, since both phases are still present at 37 °C, above the T_m of the pure POPE, the phase change could not be attributed exclusively to the effect of the temperature. Alternatively, because the SPB is adsorbed onto mica in presence of Ca^{2+}, the existence of oriented hexagonal phases or other structures onto the substrate should be considered. However, other approaches should be used to prove this possibility [24]. Finally, it is worth mentioning that the monolayer of POPE exhibits a characteristic phase transition between two liquid condensed (LC) states at a surface pressure of 36.0 mN m^{-1}[5,25]. Therefore, it cannot be totally excluded that the thermal changes observed in the POPE bilayer domains of the SPBs could be related to changes in the equilibrium between these mesophases. Future studies are planned to address these points.

Acknowledgements

Ò.D. is a recipient of a 'Recerca i Docència' fellowship from the Universitat de Barcelona. This work was supported by grants CTQ2005-07989 from the Ministerio de Ciencia y Tecnologia and SGR00664, SGR2001-00197 from DURSI (Generalitat de Catalunya), Spain.

References

[1] S. Fleischer, G. Rouser, B. Fleischer, A. Casu, G. Kritchevsky, J. Lipid Res. 8 (1967) 170-180.

[2] T.H.Haines, N.A.Dencher, FEBS Lett. 528 (2002) 35-39.

[3] H.Mueller, H.J.Butt, E.Bamberg, J.Phys.Chem.B 104 (2000) 4552-4559.

[4] E.J. Choi, E.K.Dimitriadis, Cytocrome c adsorption to supported, anionic lipid bilayers studied by atomic force microscopy, Biophys.J. 87 (2004) 3234-3241.

[5] Ò. Domènech, F.Sanz, M.T. Montero, J. Hernández-Borrell, Biochim.Biophys.Acta 1758 (2006) 213-221.

[6] W.H.Binder, V.Barragan, F.M.Menger, Angew.Chem.Int. Ed. 42 (2003) 5802-5827.

[7] R.P.Richter, R.Bérat, A.R.Brisson, Langmuir 22 (2006) 3497-3505.

[8] Ò. Domènech, M.T. Montero, J. Hernández-Borrell, Biochim.Biophys.Acta (2006) (in press).

[9] A. Grancelli, A.Morros, M.E.Cabañas, O.Domènech, S.Merino, J.L.Vázquez, M.T.Montero, M.Viñas, J.Hernández-Borrell, Langmuir 18 (2002) 9177-9182.

[10] J.A.Killian, C.H.J.P. Fabrie, W.Baart, S.Morein, B. de Kruijff, Biochim. Biophys. Acta 1105 (1992) 253-262.

[11] J.C. Gómez-Fernández, M.A. Llamas, F.J. Aranda,membranas Eur. J. Biochem. 259 (1999) 739-746.

[12] M.Rance, R.A. Byrd, J. Magn. Reson. 52 (1983) 221-240.

[13] R.N.A.H. Lewis, B.D Sykes, R.N. McElhaney,. Biochemistry 27 (1988) 880-887.

[14] J. Villaverde, J. Cladera, A. Hartog, J. Berden, E. Padrós, and M Duñach, (1998), Biophys. J. 75 (1998) 1980-1988.

[15] J Villaverde, J. Cladera, E.Padrós, J.L. Rigaud and M. Duñach, Eur. J. Biochem. 244 (1997) 441-448.

[16] C. P. S. Tilcock, D. Fisher, Biochim.Biophys. Acta, **577** (1979) 53-61.

[17] I.Raviakinem A.Simon, A.R.Brisson, Langmuir 16 (2000) 1473-1474.

[18] F.F.Rosseti, M.Bally, R.Michel, M.Textor, I.Raviakine, Langmuir 21 (2005) 6443-6450.

[19] S. Merino, Ò. Domènech, I.Díez, F.Sanz, M. Viñas, M. T. Montero, J. Hernández-Borrell, Langmuir 19 (2003) 6922-6927.

[20] R.F.Richter, A.R.Brisson, Biophys.J., 88 (2005) 3422-3433.

[21] F.F.Rosseti, M.Textor, I.Raviakine, Langmuir 22 (2006) 3467-3473.

[22] J.Yang, J. Appleyard. J. Phys. Chem. B. 104 (2002) 8097-8100.

[23] Keller, D.; Larsen, N.B.; I.M. Møller, O.G. Mouritsen.Phys. Rev. Lett. 94 (2005) 025701/1-025701/4.

[24] J.K.Rainey, B.D.Sykes, Biophsy, J. 89 (2005) 2792-2805.

[25] D.K.Schwart, C.M.Knobler, J.Phys.Chem, 97 (1993) 8849-8851.

Figure Lengends

Figure 1

Solid-state ^{31}P-NMR spectra corresponding to POPE:CL (0.8:0.2, mol/mol) dispersions in Ca^{2+} free 50 mM Tris·HCl, pH 7.40, 150 mM NaCl buffer (dashed line), and in 20 mM $CaCl_2$ added buffer (continuous line), at 15°C, 21 °C and 49 °C. The spectra were normalized to the same height. All chemical shift values are quoted in ppm with reference to external 85% phosphoric acid in H_2O as a reference (0 ppm), positive values referring to low-field shifts.

Figure 2

Excess heat capacity measured as a function of temperature for POPE:CL (0.8:0.2, mol:mol) dispersions in Ca^{2+} free 50 mM Tris·HCl, pH 7.40, 150 mM NaCl buffer (dashed line), and in 20 mM $CaCl_2$ added buffer (continuous line).

Figure 3

Topographic image of supported planar bilayers (SPBs) obtained by spreading POPE:CL (0.8:0.2, mol:mol) suspensions in 50 mM Tris·HCl, pH 7.40, 150 mM NaCl, 20 mM $CaCl_2$ after being washed with Ca^{2+} free buffer (A). Zoom of the inset (B): upper domain (black star), intermediate domain (black arrows), lower domain (white asterisk), bare mica (white star). Images were obtained in Tapping® mode.

Figure 4

Topographic images at (A) 24 °C and (B) 37°C of a supported planar bilayer (SPBs) obtained by spreading POPE:CL (0.8:0.2, mol:mol) suspensions in 50 mM Tris·HCl, pH 7.40, 150 mM NaCl, 20 mM $CaCl_2$ after being washed with Ca^{2+} free buffer. (C) The SPB at 37°C after repetitive scanning. Upper domain (black star), intermediate domain (black arrows), lower domain (white asterisk), bare mica (white star). Images were obtained in Tapping® mode.

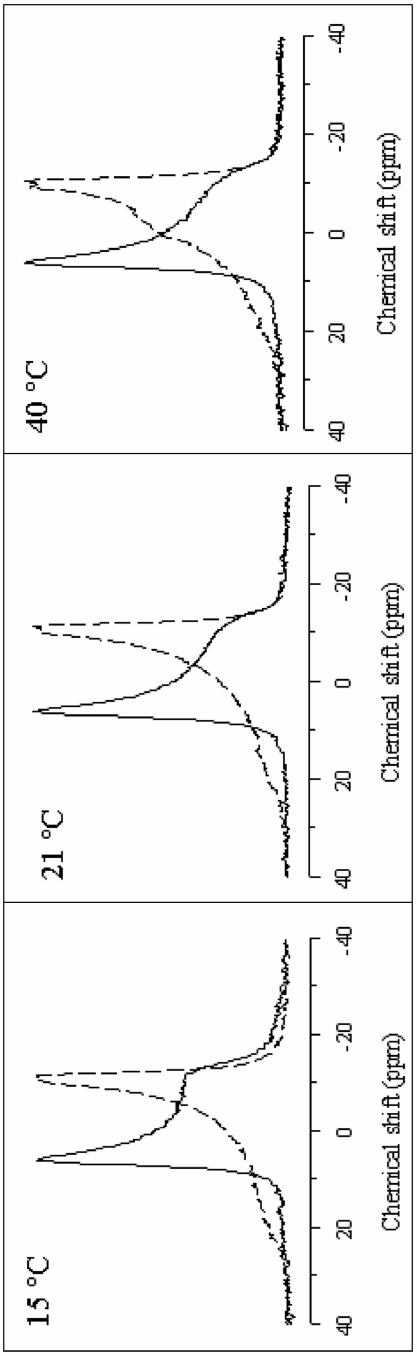

Figure 1

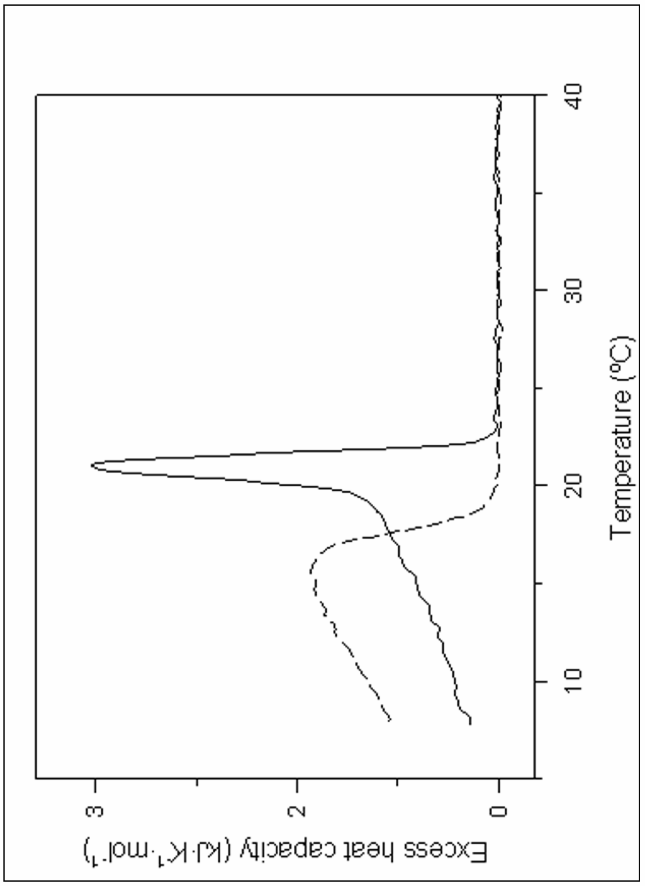
Excess heat capacity (kJ·K⁻¹·mol⁻¹)
0
2
3
10
20
30
40
Temperature (ºC)

Figure 2

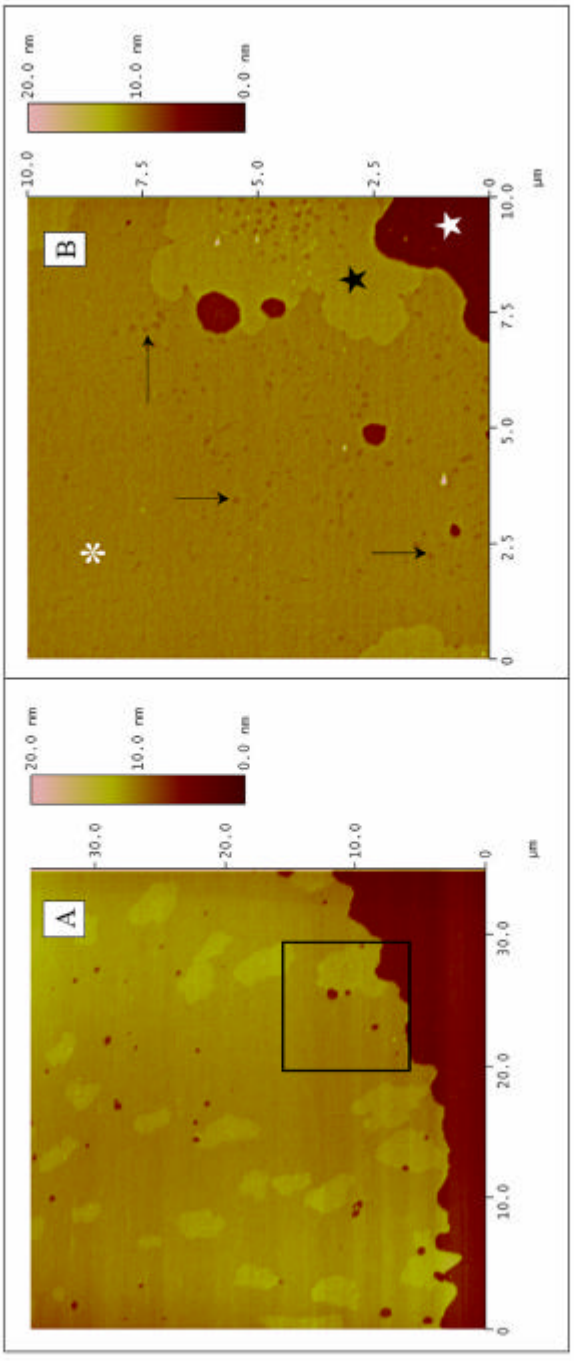

Figure 3

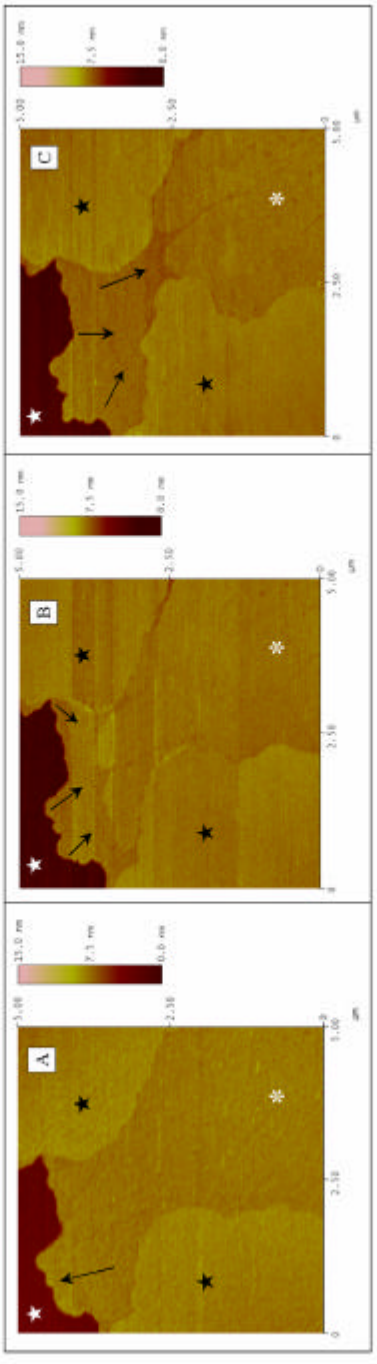

Figure 4

Article submitted to Biochimica et Biophysica Acta: Biomembranes.

Atomic force microcopy and force spectroscopy of Langmuir-Blodgett films formed by heteroacid phospholipids of biological interest

Sergi Garcia-Manyes[†,§,#] Òscar Domènech[§], Fausto Sanz[§],
M.Teresa Montero[‡] and Jordi Hernandez-Borrell[*,‡]

[§]Departament de Química Física and [‡] Departament de Fisicoquímica, Universitat de Barcelona, E-08028-Barcelona, Spain

Abstract

Langmuir-Blodgett (LB) films of pure 1-palmitoy-2-oleoyl-*sn*-glycero-3-phosphoethanolamine (POPE) and 1-palmitoy-2-oleoyl-*sn*-glycero-3-phosphocholine (POPC), as well as a mixed monolayer in which $\chi_{POPC} = 0.4$, were transferred onto mica and observed by atomic force microscopy (AFM). The force spectroscopy (FS) mode allowed us to characterize the nanomechanical properties of the LB monolayers extracted at different surface pressures. For pure POPC and pure POPE monolayers extracted at 30 mN m^{-1}, a small jump in the approaching force curve occurs only at very low force (POPC) or does not occur at all (POPE). However, for the mixed POPE:POPC monolayer the jump, or discontinuity in the force curve, occurs at higher forces (~ 800 pN). The nanostructure and nanomechanics of the POPE monolayer extracted at 36.5 mN m^{-1} were studied in detail, since the distinctive liquid condensed phase transition exhibited by this phospholipid was evident at this surface pressure.

Keywords: Atomic force Microscopy (AFM), Force spectroscopy (FS), Langmuir-Blodgett films (LB's).

[†] S.G.M. and Ò.D. contributed equally to this work.
[#] Present address: Biology Department,
Columbia University, New York, NY 10027, USA.
[*] Corresponding author: jordihernandezborrell@ub.edu

1. Introduction

The physicochemical properties of biological membranes are crucial to an understanding of membrane function, since their main role is to provide a barrier that divides electrolytic solutions into different compartments, guaranteeing at the same time membrane mechanical stability. Hence, understanding the relationship between the components of the membranes and their overall mechanical behavior has become an important issue, and has been the focus of great scientific effort in recent years.

Atomic force microscopy (AFM) is a powerful tool for understanding the mechanism of liposome fusion and deposition onto hydrophilic surfaces [1]. Moreover, it has provided a wealth of new information regarding bilayer topography [2-4], domain segregation [5, 6] bilayer phase transition [7, 8] etc. thanks to the ability to image surfaces with subnanometer resolution. In addition, AFM imaging has also been applied to study two-dimensional protein crystals [9, 10] and Langmuir-Blodgett (LB) films [11, 12]. On the other hand, the force spectroscopy (FS) mode has allowed researchers to gather additional information about the mechanics of different substrates using nanometric and subnanonewton resolution. In fact, FS has been applied to the understanding of nanomechanical properties of a vast number of well-defined molecular systems. These include indenting hard surfaces [13, 14] or cells [15] by an AFM tip, measuring the interactive forces arising between a chemically functionalized tip and a chemically derived surface (known as chemical force microscopy) [16], studying the solvation forces of liquids in the proximity of flat surfaces [17], measuring the entropic forces that play a role in the stretching simple polymers [18] or the unfolding polyproteins [19, 20]. Particularly in the case of lipid bilayers, FS has allowed scientists to experimentally measure the forces arising between phospholipid molecules, such as DLVO forces, hydration forces or steric forces [21]. Recent contributions have also dealt with membrane nanomechanics by measuring the elastic/plastic deformation of bilayers as the AFM tip applies a linearly increasing contact force on the membrane surface. These experiments have revealed a jump in the approaching force curve, interpreted as membrane breakthrough or membrane failure, as the AFM tip penetrates the membrane [22, 23]. The force at which this jump occurs is the maximum force that the membrane is able to withstand without breaking. Therefore, the elastic deformation region can be easily assessed from the force curves, measured as the reversible force regime before the 'jump' occurs. The jump indicates that the membrane has been

punctured, which implies the onset of bilayer plastic deformation. The quantitative measurement of the force at which the jump occurs is a direct measurement of bilayer nanomechanics, and this force can be regarded as a fingerprint of membrane composition, just as force is the fingerprint for an indented hard surface or an unfolded polyprotein. Most of the studies deling with the nanomechanical properties of the membranes have been conducted on supported planar bilayers (SPBs) [9] where the phospholipid molecules spontaneously assemble. Likewise, a direct measurement of the dependence of the lateral pressure (directly related to phospholipid packing within the network) and membrane (nano)mechanical stability is difficult to carry out when it comes to studying SPBs since it cannot be externally modified. In contrast, the use of Langmuir-Blodgett (LB) monolayers (where the lateral pressure is constant and externally controlled) would help to directly measure the effect of the applied lateral pressure on the nanomechanics of phospholipid monolayers. FS would also provide with structural information that is often difficult to obtain from AFM images: since most of such monolayers are intrinsically soft, contact-mode imaging of such monolayers may result in monolayer damaging while the AFM tip scans the surface. Imaging in tapping mode could reduce such interaction. However, if experiments are conducted in air, rather than in liquid environment, the snap-in force may be greater than the monolayer mechanical stability. In such cases, the soft AFM tip required to image soft layers would immediately make physical contact with the surface, thus penetrating the monolayer without guarding the electronic feedback signal against such force instability, with the overall result that no topographic information (e.g., the height of the monolayer) [24] could be obtained. Since the width of the jump in the force-distance curves mentioned above is intrinsically related to the monolayer depth, in this case FS allows the researchers to extract valuable structural and mechanical information that could not have been otherwise experimentally obtained.

Among subcellular organelles mitochondrial membranes are of particular interest. Phosphoethanolamine (PE) and phosphocholine (PC) are the major phospholipids present in significant amounts and that constitute the phospholipid matrix inner mitochondrial membranes. Both are zwitterionic phospholipids and influence the physicochemical properties of this membrane. On the other hand, among the zwitterionic phospholipids, PE is present in large amounts in membranes of eukaryotic and bacteria cells, where its presence is critical in such relevant processes as transmembrane protein assembly and solute transport. Such is the case of lactose

permease, for which the requirement of PE in functions in vivo has been clearly demonstrated [25]. In addition, PE appears to be related to the formation of phospholipid domains when lactose permease is reconstituted into proteoliposomes [10, 26].

Individual membranes are unique in composition. However, naturally occurring phospholipids include mixed acyl chains, one saturated (at the *sn*-1 position) and the other unsaturated (at the *sn*-2 position), linked to the glycerol backbone, normally in a fluid state under physiological conditions. Two synthetic phospholipids that accomplish these conditions are 1-palmitoy-2-oleoyl-*sn*-glycero-3-phosphoethanolamine (POPE) and 1-palmitoy-2-oleoyl-*sn*-glycero-3-phosphocoline (POPC). In a previous paper, we studied the mixing properties of POPE:POPC monolayers [27], our thermodynamic analysis revealing that the most stable monolayer was the one formed by POPE:POPC (0.6:0.4, mol/mol).

The aim of this paper is two-fold. On the one hand, we aim to get further insight into the topographic characterization of the POPC and POPE LB monolayers by means of AFM. On the other hand, we aim to gain information on the mechanical properties of such LBs using the FS mode through the force-distance curves. In particular, we are interested in studying nanomechanical stability of the monolayers, which is a straightforward reflection of their molecular organization and in the measurement of their thickness. Particular attention has been put into the LC-LC' [28] phase transition of POPE [27].

2. Materials and Methods

2.1 Preparation of Langmuir-Blodgett films

1-palmitoyl-2-oleoyl-*sn*-glycero-3-phosphoethanolamine (POPE), and 1-palmitoyl-2-oleoyl-*sn*-glycero-3-phosphocholine (POPC), specified as 99% pure, were purchased from Avanti Polar Lipids (Alabaster, AL, USA) and used without further purification. The subphase buffer for preparing the Langmuir-Blodgett films was a 50 mM Tris·HCl buffer (pH 7.40) containing 150 mM NaCl, prepared in Ultrapure water (Milli Q® reverse osmosis system, 18.3 MΩ·cm resistivity). Chloroform and methanol, HPLC grade, were purchased from SIGMA (St. Louis, MO, USA).

The lipids were dissolved in chloroform-methanol (3:1, v/v) to a final concentration of 1 mg·mL^{-1}. The preparation of the LBs for POPE, POPC and POPE:POPC (0.6:0.4, mol:mol) were performed in a 312 DMC Langmuir-Blodgett trough manufactured by NIMA Technology Ltd. (Coventry, England). The trough was placed onto a vibration-isolated table (Newport, Irvine, CA, USA) and enclosed in an environmental chamber. The subphase was filtered with a Kitasato system (450 nm pore diameter) before use. The resolution of surface pressure measurement was ± 0.1 mN·m^{-1}. In all experiments the temperature was controlled at 24.0 ± 0.2 °C by an external circulating water bath. Before each experiment, the trough was washed with chloroform and rinsed thoroughly with purified water. The cleanliness of the trough and subphase was ensured before each run by cycling the full range of the trough area and aspirating the air-water surface, while at the minimal surface area, to zero surface pressure.

The corresponding aliquots of lipid were spread, drop-by-drop, onto subphase solution with a Hamilton microsyringe. A period of 15 min was required to allow the solvent to evaporate before the experiment was started. The compression barrier speed, vis-à-vis the final surface pressure, was 5 cm^{2}·min^{-1}. LB films were transferred onto freshly cleaved mica, lifting the substrate, at a constant rate of 1 mm·min^{-1}. The transfer ratios were evaluated and proved near the unity, indicating that the mica was almost covered with the monolayer.

2.2 Atomic force microscopy imaging

AFM measurements were made at a constant temperature of 24 °C with a Nanoscope IV from Digital Instruments, Santa Barbara, CA, equipped with a 50 µm piezoelectric scanner. All the images were taken in air in contact mode with a silicon nitride cantilever and a nominal spring constant of 80 pN nm^{-1}. The applied force was kept as low as possible to minimize monolayer damaging. All the images were processed using Digital Instrument (Nanoscope 6.12r1) software.

2.3 Force Spectroscopy

FS was performed with a Molecular Force Probe1-D, (Asylum Research, Santa Barbara, CA). Force plots were acquired using V-shaped Si_3N_4 tips (OMCL TR400PSA,

Olympus) with a nominal spring constant of 80 pN nm^{-1}. Individual spring constants were calibrated using the equipartition theorem [29] after having correctly determined the photodetector optical sensitivity (V/nm) by measuring it at high voltages after several minutes of performing force plots to avoid hysteresis. Applied forces F are given by $F = k_c \times \Delta$, where Δ stands for the cantilever deflection. The surface deformation is given as penetration (δ), evaluated as $\delta = z - \Delta$, where z represents the piezo-scanner displacement. More than 300 force curves were acquired in at least 10 different spots of the same sample. The tip-sample approaching velocity was set for all force curves at 600-1000 nm s^{-1}.

3. Results and Discussion

Figure 1 displays the surface pressure-area isotherms of the pure POPE, POPC and POPE:POPC (0.6:0.4, mol:mol) at 24.0 ± 0.2 °C. The features of these isotherms were consistent with others in the literature [30]. The monolayer of pure POPC was always in the liquid expanded (LE) phase and showed a collapse surface pressure of 46 mN m^{-1}. In turn, the monolayer of POPE is in LE up to 36.0 mN m^{-1} where it exhibites the characteristic phase transition between two liquid condensed (LC) states, LC-LC′. The LC and LC' phases have been interpreted as two distinct tilted mesophases in long chain fatty acids [31] and have been also identified in phospholipids [27,32]. On the other hand, the collapse was observed at 50.7 mN m^{-1}. The mixed monolayer, with a $\chi_{POPC} = 0.4$, presents also the LC-LC′ phase transition, but now at a surface pressure of 44.7 mN·m^{-1} and a collapse surface pressure at 48.7 mN·m^{-1}.

The variation of compression modulus (C_s) values with π for the three monolayers are shown in the inset of Figure 1. As can be seen, below ~ 7 mN·m^{-1} the POPE monolayer always displays greater C_s values than the POPC and the mixed monolayer. This demonstrates that the pure POPE monolayer can have more compressibility at low surfaces pressures. From 7 to 25 mN·m^{-1}, the C_s values were always greater for the POPC than for the POPE monolayer. This fact should be attributed to the different size of the PE and PC headgroups [33, 34]. Furthermore, above 25 mN·m^{-1} the three monolayers showed similar mechanical compressibility as reflected by the C_s values. POPE monolayer showed a first-order transition at 36.0 mN·m^{-1} and a second order transition at 45.5 mN·m^{-1}. The first transition confirms the existence of LC and LC′

states, which simply reflect, as in other systems [35], a different molecular ordering. In fact, the LC and LC′ states have already been reported for OPPE, the structural enantiomer of POPE, and imaged by using the Brewster Angle Microscope (BAM) [32].

To perform a topographical characterization, POPC and POPE monolayers were transferred onto a mica substrate at a surface pressure of biological interest 30 mN m^{-1} [36] and imaged with AFM in contact mode. Figure 2 shows the AFM topographic images of pure POPC (Figure 2A) and POPE (Figure 2B) monolayers and the mixed monolayer with $\chi_{POPC} = 0.4$ (Figure 2C). It is important to point out that all monolayers remain in the LE phase at this surface pressure (see Figure 1). The AFM images provided continuous and smooth monolayers with average surface roughness, *Ra*= 0.10, 0.05 and 0.14 nm, respectively. These values are in close agreement with others elsewhere reported [37]. In turn, the LB image of the mixed monolayer (Figure 2C) provided visual evidence that POPE and POPC mix ideally at this molar fraction. This is in agreement with the behavior predicted from a thermodynamic study previously published [27].

The AFM images (Figure 2) reveal a continuous, homogeneous, and featureless LB formation. Since the monolayers are defect-free, other topographic characteristics such as monolayer height or monolayer (nano)mechanical properties are difficult to determine from the AFM images. Regarding the thickness, they can be inferred by scratching the surface and measuring the step height between the top of the monolayer and the uncovered mica. However, this has bee revealed inadequate method when dealing with phospholipids as POPE and POPC. Thus, we could not accomplish this method on the POPC monolayer because after scractching the layer, the phospholipid molecules tend to respread immediately fulling up the area uncovered (result not shown). Hence, the step height measurement can not be performed. Although, the molecular packing is more effective in the mixed monolayer than in the pure monolayers (Figure 1) similar behaviour was observed for the POPC:POPE mixture (results not shown). On the other hand, although we were able to scratch the POPE monolayer (Figure 3), the heights obtained ~ 0.48 nm, were below the values expected for a monolayer.

To obtain further information on mechanical properties, and particularly on the thickness of the monolayers under investigation, we have conducted FS experiments.

Interestingly, we observed that whereas for pure monolayers, a small jump in the approaching force curve occurs at very low forces for POPC (Figure 2A.1) and, or does not occur for POPE (Figure 2B.1) at all, for the mixed POPE:POPC monolayer the jump or discontinuity in the force curve, an unambiguous signature of its mechanical stability, occurs at higher forces (~ 800 pN). These results point out to the fact that there is a direct relationship between the compactness of the monolayer, reflected by the area/lipid values (Figure 1), and the mechanical stability of the monolayers.

It is worth mentioning here that the width of the jump observed in the force curves is interpreted as the height of the layer observed [24, 38]. As can be seen, the jump or breakthrough is clearly observed for POPC (Figure 2A.2) and POPC:POPE (Figure 2C.2). The width of the jump (~ 2 nm) correlates well with the height of phospholipid monolayers elsewhere published [39]. Remarkably, no jump or breakthough was observed in the POPE monolayer (Figure 2B.2) and for this reason height could not be established using FS. This result, however, was not totally unexpected because: (i) very low yield threshold values (~1.63 nN) have been reported for POPE bilayers [38]; and (ii) there are evidences of the extreme soft nature of other unsaturated PE monolayers [3, 21]. As a matter of fact in Figure 2A.1 one can observe that the jump occurs at a force value close to ~ 0 nN, which implies that POPC monolayer is punctured since the cantilever is in physical contact with the monolayer. Therefore, if lower values than the observed for POPC should be expected for POPE monolayers, it is not surprising that the jump not occurs in this case. These behaviors should be attributed to the chemical differences between PC and PE headgroups [33,34]. This observation suggests that when performing an AFM image in contact mode involving such soft monolayers, the tip may be partially indenting the surface. Besides, this interpretation is in agreement with force determinations carried out with DOPC [7] and DOPE [3,21,40], phospholipids with two double unsaturated acyl chains.

In conclussion, the thickness measurements obtained from AFM images for soft samples can, in general, be somewhat inaccurate due to the high probability the studied sample would be suffering damage as the scan is performed. This fact is particularly relevant in those cases in which the jump-to-contact force exceeds the mechanical stability of the monolayer. In such cases, once the tip is sufficiently close to the sample as to experience the snap-in (or jump-to-contact) force, it is physically in contact with the surface. Upon further extending the piezo, the cantilever starts exerting a pressure on the monolayer until it breaks, giving rise to the above-mentioned jump or

breakthrough. If the force required to break the monolayer is lower than the jump-to-contact force, then the yield threshold force occurs at 'negative forces', which implies that when performing AFM images in contact mode the surface may be damaged during the entire scan. It is therefore clear that FS, through force-extension curves, allows one to gather additional structural information, such as monolayer height, which cannot be obtained by contact mode AFM images.

As mentioned before, the very distinctive feature of POPE and OPPE isotherms is the so called LC-LC′ transition that occurs at ~36.5 mN m^{-1} [27, 32]. Figure 4 shows a contact mode AFM image of a POPE monolayer extracted at 36.5 mN m^{-1}, which corresponds to the plateau region shown in Figure 1. Unlike the featureless, homogeneous image shown in Figure 2B (extracted at 30 mN m^{-1}), the monolayer topography presents here a more complex structure, *Ra*= 0.16, in which two different regions can be observed. Clearly, the LB film transferred at 36.5 mN m^{-1} (Figure 4A) is not homogeneous and numerous domains, predominantly round in shape with diameters ranging from 500 ± 100 nm (n=10) to 87 ± 18 nm (n=30), are observed. A magnification of a small area of Figure 4A is shown in Figure 4B. At first sight, just judging the color scale, these domains would be interpreted as vacancies produced in the process of transference of the monolayer to the mica substrate. The depth of these structures was 0.80 ± 0.06 nm (n=30) and it is unlikely that such value may account for the thisckness a POPE monolayer. Indeed, values as low as ~1.8 nm have been reported for DOPE monolayers at 40 mN m^{-1} [39]. Since we are imaging the LB of POPE in the plateau region (Figure 1), where LC and LC' states coexist, it is an apealing possibility that in Figure 4 we would be observing some stage of the phase separation. This is, however, an unlikely because, the LC and LC' phases, represent two different tilted orientations of the POPE molecules and 0.8 nm would exceed the difference expected between both phases. At this point the topography images can not provide any information to discriminate between both phases. To definitively proof that the dark domains are the substrate, we have scratched the LB extracted at 36.5 mN m^{-1}. As evidenced in the profile analysis (Figure 5) the step height is 0.80 nm which coincides with the depth of the monolayer. Although the scratched square was not completely flat, *Ra*= 0.07 nm, it can be concluded that we are uncovering the mica during the scanning process. Therefore the domains observed in Figure 4 are real vacancies and not phospholipids phase. The occurrence of such defects is not occasional but repetitive. Hence that we suspect that during the LC-LC' transition, the molecules tilt changing the

interaction from the next-nearest neighbors to the nearest [31] resulting both, in the compaction of the monolayer and in the formation of free spaces that we observe as defects.

Finally, to evaluate whether the LC-LC' transition has any effect on the mechanical properties of the monolayer, the force curves performed on LBs of POPE extracted at 30 mN m^{-1} were compared to those obtained on a POPE LB monolayer extracted at 38 mN m^{-1} (Figure 6). Recalling the force plots on LB obtained at 30 mN m^{-1}, displayed in Figures 2B.1-2B.2, no breakthrough or jump in the force curve were observed, thus underscoring the low (or nonexistent) mechanical stability of the monolayer in its liquid phase. In contrast, the force curves obtained on the monolayer extracted at 38 mN m^{-1} exhibited a repetitive, clear jump in the approaching curve at a force value of ~ 2.2 nN, thus revealing a greater mechanical stability. Therefore, it seems clear that the sudden reduction in the area/molecule value (the plateau region in Figures 1 and 4) results in a more compact and packed molecular structure. This gives rise to an important increase in the force, which the monolayer is able to withstand before breaking. Importantly, the tip-distance curve derived from the piezo extension curve for the monolayer extracted at 38 mN m^{-1} enables us to established the monolayer width in ~ 2 nm. This value is greater than the difference obtained from the determination of depth in the domains in Figure 4. Again, FS demonstrates to be a useful tool to determine thickness of phospholipids monolayers. There are some variables, however, that have an effect on the membrane breakthrough force, such as the ionic strength of the measuring medium [37], the tip [41] and phospholipid chemistry, the tip as it increases in velocity [42], and temperature [43]. Future works in our laboratory will address these points.

Acknowledgements

S.G-M. would like to thank the Generalitat de Catalunya for financial support. Ò. D. is the recipient of a 'Recerca i Docència' fellowship from the University of Barcelona. This work was supported by Grant CTQ2005-07989 from the Ministerio de Ciencia y Tecnología (MCYT) and SGR00664 (Generalitat de Catalunya) of Spain.

References

[1] J. Jass, T. Tjärnhage, G. Puu, From liposomes to Supported Planar Bilayer Structures on Hydrophilic and Hydrophobic Surfaces: An Atomic Force microscopy Study, Biophys. J. 79 (2000) 3159-3163.

[2] T.C. Kaasgaard, J.H.Leidy, J.H. Ipsen, O.G.Mouritsen, K.Jorgensen. In situ atomic force microscope imaging of supported lipid bilayers, Single Mol. 2 (2001) 105-108.

[3] J.Schneider, Y.F. Dufrêne, W.R.Barger Jr., G.U.Lee, Atomic force microscope image contrast mechanism on supported bilayers, Biophys.J. 79 (2000) 1107-1118.

[4] J.Schneider, W. Barger, G.U. Lee, Nanometer scale surface properties of supported lipid bilayers measured with hydrophobic and hydrophilic atomic force microscope probes. Langmuir 19 (2003)1899-1907.

[5] Ò. Domènech, F.Sanz, M.T. Montero, J. Hernández-Borrell, Thermodynamic and structural study of the main phospholipids components comprissing the mitochondrial inner membrane, Biochim.Biophys.Acta 1758 (2006) 213-221.

[6] Ò. Domènech, M.T. Montero, Jordi Hernández-Borrell, Supported planar bilayers from hexagonal phases, Biochim.Biophys.Acta (in press).

[7] Z.V.Leonenko, E.Finot, H.Ma, T.E.Dahms, D.T. Cramb, Investigation of themperature-induced phase transitions in DOPC and DPPC phospholipids bilayers using temperature-controlled scanning force microscopy, Biophys. J. 86 (2004) 3783-3793.

[8] M.C.Giocondi, C.Le Grimellec, Temperature dependence of the surface topography in dimiristoylphosphatidylcholine/distearoylphosphatidylcholine multibilayers, Biophys.J., 86 (2004) 2218-2230.

[9] S. Merino, Ò. Domènech, I. Díez-Pérez, F. Sanz, M. T. Montero, J. Hernández-Borrell, Surface thermodynamic properties of monolayers versus reconstitution of a membrane protein in solid-supported bilayers, Colloid Surf. B-Biointerfaces 44 (2005) 93-98.

[10] S. Merino-Montero, Ò. Domènech, M. T. Montero, J. Hernández-Borrell, Preliminary atomic force microscopy study of two-dimensional crystals of lactose permease from *Escherichia coli,* Biophys.Chem. 118 (2005) 114-119.

[11] J.M.Solleti, M.Botreau, F.Sommer, W.L.Brunat, S.Kasas, T.M.Duc, M.R.Celio, Elaboration and characterization of phsopholipid Langmuir-Blodgett films, Langmuir 12 (1996) 5379- 5386

[12] S.Krol, M.Ross, M.Sieber, S.Kunneke, H.J.Galla, A. Janshoff, Formation of Three-Dimensional Protein-Lipid Aggregates in Monolayer Films Induced by Surfactant Protein B, Biophys J, 79(2000) 904-918.

[13] S.G. Corcoran, R.J. Colton, E.T. Lilleodden, W.W. Gerberich, Anomalous plastic deformation at surfaces: nanoindentation of gold single crystals, Phys.Rev. B. 66 (1997) 16057-16060.

[14] J.Fraxedas, S.Garcia-Manyes, P.Gorostiza, F.Sanz, Nanoindentation: toward the sensing of atomic interactions. Proc.Natl. Acad.Sci.U.S.A. 99 (2002) 5228-5232.

[15] S.Sen, S.Subramanian, D.E. Discher, Indentation and adhesive probing of a cell membrane with AFM: theoretical model and experiments, Biophys. J 89 (2005) 3203-3213.

[16] D.V. Vezenov, A.Noy, L.F. Rozsnyai, C.M.Lieber, Force titrations and ionization state sensitive imaging of functional groups in aqueous solutions by chemical force microscopy, J.Am.Chem.Soc 119 (1997) 2006-2015.

[17] S.J.O'Shea, M.E.Welland, Atomic force microscopy at solid-liquid interfaces, Langmuir 14 (1998) 4186-4197.

[18] T.Hugel, M.Rief, M. Seitz, H.E.Gaub, R.R.Netz, Highly Stretched Single Polymers: Atomic-Force-Microscope Experiments Versus *Ab-Initio* Theory Phys.Rev.Lett 94 (2005) 048301.

[19] M.Carrión-Vázquez, A.F.Oberhauser, S.B.Fowler, P.E. Marszalek, S.E. Broedel, J.Clarke, J.M.Fernández, Mechanical and chemical unfolding of a single protein: a comparison. Proc.Nalt.Acad.Sci.U.S.A. 96 (1999) 3694- 3699.

[20] H.Li, W.A.Linke, A.F.Oberhauser, M.Carrión-Vázquez, J.G.Kerkvliet, H.Lu, P.E. Marszalek, J.M.Fernández, Reverse engineering of the giant muscle protein titin, Nature 418 (2002) 998-1002.

[21] Y.F. Dufrêne, W.R.Barger, J.B.D.Greeen, G.U.Lee, Nanometer-scale surface properties of mixed phospholipid monolayers and bilayers, Langmuir 13 (1977) 4779-4784.

[22] I.Pera, R.Stark, M.Kappl, H.J.Butt, F.Benfenati, Using the atomic fore microscope to study the interaction between two solid supported lipid bilayers and the influence of synapsin, Biophys. J. 87 (2004) 2446-2455.

[23] H.J.Butt, V.Franz, Rupture of molecular thin films observed in atomic force microscopy. Theory. Phys.Rev. E. 66,0311601/1-0311601/9.

[24] E.J.Choi, E.K.Dimitriadis, Cytochrome c adsorption to supported, anionic lipid bilayers studied via atomic force microscopy, Biophys. J., 87 (2004) 3234-3241.

[25] Bogdanov,M., Dowhan, W. Phosphatidylethanolamine is required for *in vivo* function of the membrane-associated lactose permease of *Escherichia coli*, Biol. Chem. 270 (1995) 732-739.

[26] S. Merino, Ò. Domènech, M. Viñas, M. T. Montero, J. Hernández-Borrell, Effects of Lactose Permease on the Phospholipid Enviroment in Wich It Is Reconstituted: A Fluorescence and Atomic Force Microscopy Study, Langmuir 21 (2005) 4642-4647.

[27] Ò. Domènech, J. Torrent-Burgués, S. Merino, F. Sanz, M. T. Montero, J. Hernández-Borrell, Surface thermodynamics study of monolayers formed with heteroacid phospholipids of biological interest, Colloid Surf. B-Biointerfaces 41 (2005) 233-238.

[28] G.A.Overbeck, D.Möbius, A new phase in the generalized phase diagram of monolayer films of long-chain fatty acids, J.Phys.Chem., 97 (1993) 1999-8004.

[29] E.L.Florin, M.Rief, H.Lehmann, M.Ludwig, C.Dornmair, V.T.Moy, H.E.Gaub, Sensing specific molecular interactions with the atomic force microscope, Biosens.Biolectron. 10 (1995) 1344-1350.

[30] H.L.Brokman, K.R.Applegate, M.M.Momsen, W.C.King, J.A.Glomset, Packing and electrostatic behavior of *sn*-2-docosahexaenoyl and –arachidonoyl phosphoglycerides, Biophys.J., 85 (2003) 2384-2396.

[31] D.K.Schwart, C.M.Knobler, Direct observation of transitions between condensed Langmuir monolayer phases by polarized fluorescence microscopy, J.Phys.Chem, 97 (1993) 8849-8851.

[32] I.Rey-Gómez-Serranillos, J. Miñones (Jr.), P.Dynarowicz-Latka, J.Miñones, O.Conde, Surface behavior of oleoyl palmitoyl phosphatidyl ethanolamine (OPPE) and the characteristitcs of mixed OPPE-miltefosine monolayers, Langmuir 20 (2004) 11414-11421.

[33] D. Stigter, K.A.Dill, Lateral interaction among phsopjolipid head groups at the heptane/water interface, Langmuir 4 (1988) 200-209.

[34] M.Langmer, K.Kubica, The electrostatic of lipid surfaces, Chem.Phys.Lipids 101 (1999) 3-35.

[35] M.K.Durbin, A.Malik, R.Ghaskadvi, M.C.Shih, P.Zschack, P.Dutta, X-ray diffraction study of a recetly identified phase transition in fatty acid lang,uir monolayers, J.Phys.Chem., 98 (1994) 1753-1755.

[36] G. Cevc, D. Marsh, Phospholipid Bilayers. Physical Principles and Models, Wiley-Interscience, New York, 1987.

[37] P.E.Milhiet, C.Domec, M.C.Giocondi, N.Van Mau, F.Heitz, C.Le Grimellec, Domain formation in models of the renal brush border membrane outer leaflet, Biophys.J. 81 (2001) 547- 555.

[38] S.Garcia-Manyes, G.Oncins, F.Sanz, Effect of ion-binding and chemical phospholipids structure on the naomechanics of lipid bilayers studied by force spectroscopy, Biophys.J. 89 (2005) 1812-1826.

[39] J.M. Solleti, M.Botreau, F.Somer, T.M.Duc, M.R.Celio, Characterization of mixed miscible and nonmiscible phospholipid Langmuir-Blodgett films by atomic forece micrsocopy, J.Vac.Sci.Technol. 14 (1996) 1492-1497.

[40] Y.F. Dufrêne, T.Boland, J.Schneider, W.R.Barger., G.U.Lee, Characterization of the physical properties of model biomembranes at the nanometer scale with the atomic force microscope. Faraday Discuss.111 (1998) 79-94.

[41] R.P.Richter, A.Brisson, Characterization of lipid bilayers and protein assemblies supported on rough surfaces by atomic force microscopy, Langmuir 19 (2003) 1632-1640.

[42] V.Franz, S.Loi, H.Muller, E.Bamberg, H.H.Butt, Tip penetration through lipid bilayers in atomic force microscopy, Colloids and Surf. B: Biointerfaces 23 (2002) 191-200.

[43] Garcia-Manyes, S. G. Oncins, and F. Sanz. Effect of temperature on the nanomechanics of lipid bilayers studied by force spectroscopy. Biophys. J. 89(2005) 4261-4274.

Figure Legends

Figure 1. Surface-pressure area isotherms of pure and mixed monolayers at the air-water interface. (△) POPC, (□) POPE, (○) χ_{POPC} = 0.4. INSET. Compressibility modulus of the three monolayers. (△) POPC, (□) POPE, (○) χ_{POPC} = 0.4.

Figure 2. 2 μm^2 AFM contact mode images of POPC (A), POPE (B) and POPC:POPE (χ_{POPC} = 0.4) (C) monolayers extracted at 30 mN m^{-1}.
Force-piezoelectric extension curves on these POPC (A.1), POPE (B.1) and POPC:POPE (χ_{POPC} = 0.4) (C.1) monolayers. Inset: force vs. tip-sample approching curves derived from the previous force vs. piezoelectric extension curves for POPC (A.2), POPE (B.2) and POPC:POPE (χ_{POPC} = 0.4) (C.2), underscoring the low force contact region in which the jump or monolayer indentation can be observed.

Firgure 3. Example of determination of the thickness of a monolayers by using AFM contact mode. AFM topography image of a POPE monolayer transferred at 30 mN·m^{-1} (A). The monolayers thickness can be evaluated by scratching the surface. The height profile analysis (B) evidenced, however, that the AFM tip drift the phospolipid towards to the edges and that the mica is not totally flat due to the re-spreading of material over the substrate. The thickness of the monolayer obtained by measuring the step height between the monolayer and the substrate were 0.42 ± 0.07 nm clearly below the values expected for a monolayer.

Figure 4. π-A isotherm of the POPE monolayer with two AFM images: A) LB film at a π = 36.5 mN·m^{-1}. B) Amplification of image 3A.

Figure 5. Determination of the thickness of a monolayers of POPE transferred at 36.5 mN·m^{-1} by using AFM contact mode. (A). The monolayers thickness can be evaluated by scratching the surface. (B) The height profile analysisThe thickness of the monolayer obtained by measuring the step height between the monolayer and the substrate were 0.80± 0.07 nm.

Figure 6. (A) Surface-pressure area isotherms of pure POPE (extracted from Figure 1). Inset: zoom of the LC-LC' transition. (B, C). Force vs. piezo displacement curves on a POPE monolayer extracted at 30 mN m^{-1} and 38 mN m^{-1} (B, C, respectively). Insets: force vs. tip-sample approching curves derived from the previous force vs. piezoelectric extension curves, underscoring the low force contact region in which the jump or monolayer indentation can be observed.

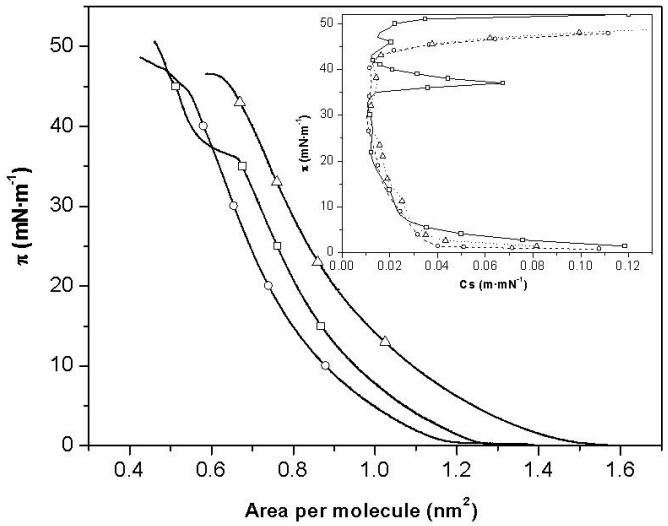

Figure 1

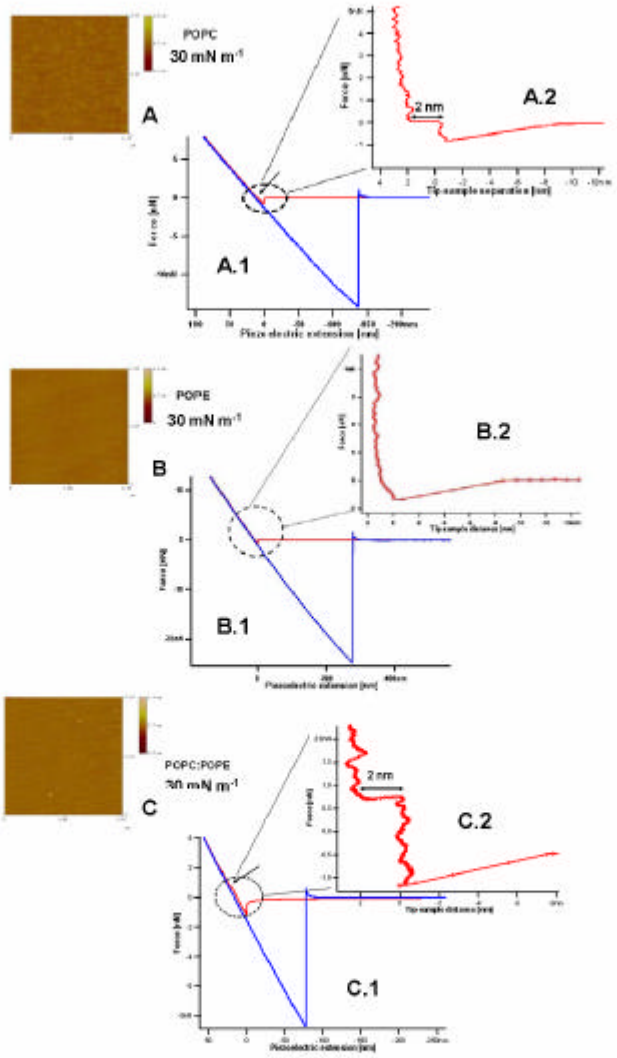
POPC
30 mN m-1
A
A.1
A.2
2 nm
POPE
30 mN m-1
B
B.1
B.2
POPC:POPE
30 mN m-1
C
C.1
C.2
2 nm

Figure 2

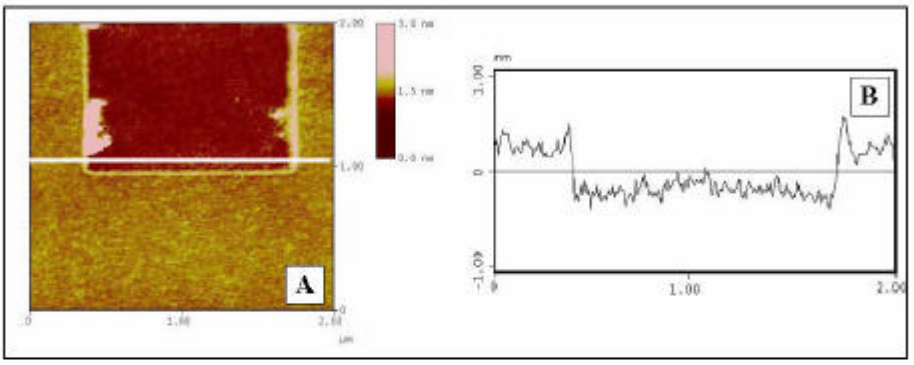

Figure 3

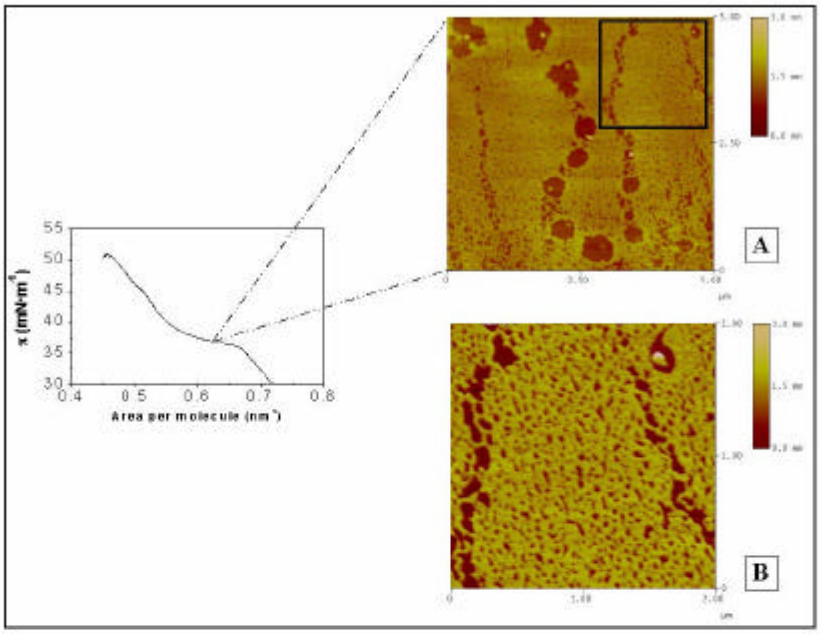

Figure 4

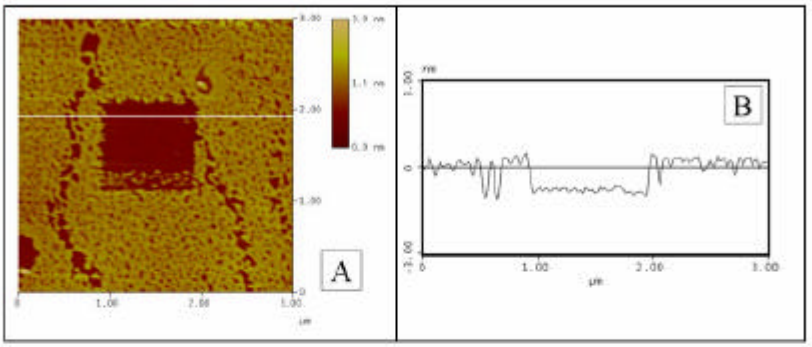

Figure 5

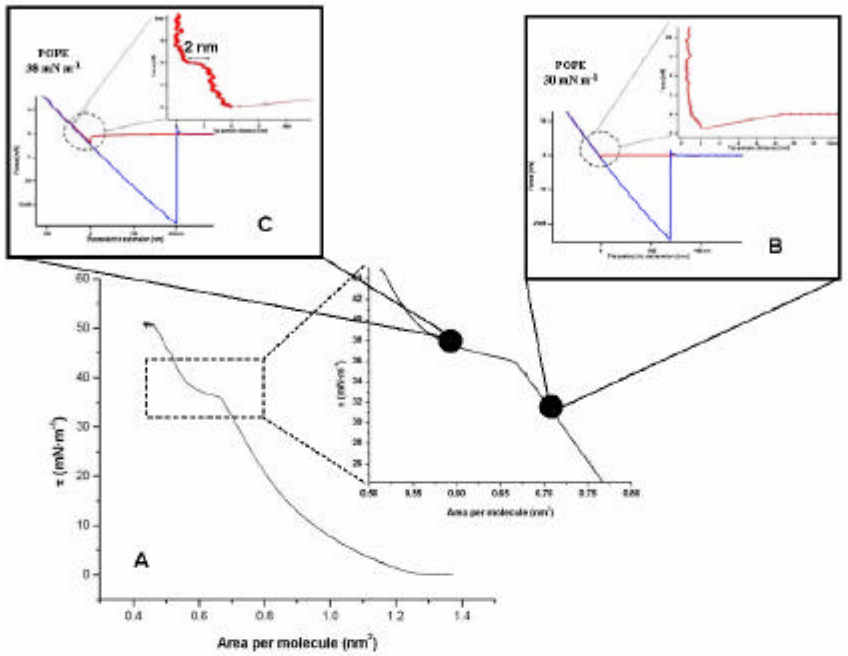

Figure 6

Article submitted to Langmuir.

Specific adsorption of cytochrome c on cardiolipin-glycerophospolipid monolayers and bilayers

Òscar Domènech[†], Lorena Redondo[§], M. Teresa Montero[§],
Jordi Hernández-Borrell[§,#]

[†]Departament de Química-Física, Facultat de Química
[§]Departament de Fisicoquímica, Facultat de Farmacia U.B. 08028- Spain.

Abstract

In this work we have studied the adsorption of cytochrome *c* (cyt *c*) on monolayers and liposomes formed with: (i) pure 1-palmitoyl-2-oleoyl-*sn*-glycero-3-phosphocholine (POPC), 1-palmitoyl-2-oleoyl-*sn*-glycero-3-phosphoethanolamine (POPE) or cardiolipin (CL); and (ii) the more thermodynamically stable binary mixtures POPE:CL (0.8:0.2, mol:mol) and POPC:CL (0.6:0.4, mol:mol). Surface constant pressure experiments have shown that the maximum and minimum interaction were undergone by the pure CL (anionic phospholipid) and the pure POPE (zwitterion) monolayers respectively. The observation by atomic force microscopy (AFM) of the images of Langmuir-Blodgett (LB) films extracted at 30 mN m^{-1} suggest that the different interaction of cyt *c* with the POPE:CL and the POPC:CL monolayers could be originated from lateral phase separation occurring in the POPE:CL mixture. The competence between 8-anilino-1-naphtalene sulfonate (ANS) and cyt *c* for the same binding sites in liposomes of identical nominal compositions that the monolayers was exploited to obtain binding parameters. In agreement with the monolayer experiments the largest binding was observed for the POPE:CL liposomes. All the observations strongly support the existence of a selective adsorption of cyt *c* on CL which is differently modulated by different neutral phospholipids (POPE and POPC).

1. Introduction

[#] Corresponding author: jordihernandezborrell@ub.edu

Cytochrome c (cyt *c*) is a peripheral membrane protein that is found associated with the inner membrane of mitochondria. It is an essential component of the mitochondrial respiratory chain that transfers electrons between the $CoQH_2$-cytochrome *c* reductase and the cytochrome *c* oxidase complexes. In part because cyt *c* is a soluble protein, it is often conceived as a shuttle for electrons. Far from this simple view, the mechanism by which cyt *c* diffuses between the reductant and the oxidant protein substrates may involve translational motion of cyt *c* in the aqueous intermembrane mitochondrial space or in the two-dimensional plane defined by the bilayer[1]. In this regard it has been early established using fluorescence of monolayers[2] and solid-state 31 P-NMR[3] that cyt *c* binds specifically to anionic phospholipids. More recently the nature of the phospholipid-cyt *c* interaction has been investigated by atomic force microscopy (AFM)[4] and combined with force spectroscopy (FS)[5]. The biological implications of such interaction appears to be related with the transport of electrons itself[6] as well as with the release of cyt *c* during process of apoptosis[7]. In both, relevant processes, the involvement of cardiolipin (CL) has been demonstrated. Actually we have evidenced the specific affinity of cy *c* for CL by using a combination of fluorescence measurements and AFM observations[8]. On the other hand major zwitterionic phospholipids that are present in significant amounts and that constitute the phospholipid matrix inner mitochondrial membranes i.e. phosphoethanolamine (PE) and phosphocholine (PC), could influence such interaction. In previous works we have studied the mixing properties of the binary systems: 1-palmitoy-2-oleoyl-*sn*-glycero-3-phosphoethanolamine (POPE), 1-palmitoy-2-oleoyl-*sn*-glycero-3-phosphocholine (POPC) and cardiolipin monolayers and supported planar bilayers (SPBs)[8,9]. Accordingly, the values of the Gibbs energy of mixing, the more stable monolayers assayed were: POPC:CL (0.6:0.4, mol:mol) and POPE:CL (0.8:0.2, mol:mol). Hence that those compositions were used to investigate the topographic characteristics of the SPBs through AFM. Thus, while POPC:POPE and POPC:CL yield homogeneous SPBs, lateral phase segregation of the POPE:CL system were observed[10]. In the present work we will

[1] Cramer,W.A.;Knaff,D.B. in *Energy transduction in biological membranas. A Texbook of Bioenergetics.* Springer-Verlag , N.Y. **1991**; p 164
[2] Teissie,J. *Biochemistry* **1981**, *20*, 1554-1560.
[3] Pinheiro,T.J.T.; Watts,A. *Biochemistry* **1994**, *33*, 2451-2458.
[4] Lei,C.;Wollenberger,U; Cheller,F.W. *Electroanalysis* **1999**, *11*, 274-276.
[5] Choi, E.J.;Dimitriadis,E.K. *Biophys.J.* **2004**, *87*, 3234-3241.
[6] Robinson, N.C. *J. Bioenerg. Biomem.* **1993**, 25, 153-163.
[7] McMillin,J.B.; Dowhan,W., *Biochim. Biophys. Acta* **2002,** *1582*, 97-107.
[8] Domènech,Ò; Sanz,F.; Montero,M.T.; Hernández-Borrell,J. *Biochim.Biophys.Acta* **2006**, *1758*, 213-221.
[9] Domènech,Ò.; Torrent-Burgués,J.; Merino,S.; Sanz,F.;Montero,M.T.; Hernández-Borrell,J. Colloid Surf. B-Biointerfaces **2005**, *41*, 233-238.
[10] Domènech,Ò.; Montero,M.T.; Hernández-Borrell,J. *Biochim.Biophys.Acta* **2006**, in press.

investigate the effects of cyt *c* on pure POPC, POPE and CL, and the more thermodynamically stable mixtures POPE:CL (0.8:0.2, mol:mol) and POPC:CL (0.6:0.4, mol:mol) at constant surface pressure. By combining our monolayer results with binding experiments in solution, using 8-anilino-1-naphtalene sulfonate (ANS)[11], we have investigated whether CL is essential for cyt c adsorption onto bilayers.

2. Materials and methods

2.1 Chemicals. 1-palmitoyl-2-oleoyl-*sn*-glycero-3-phosphocholine (POPC), 1-palmitoyl-2-oleoyl-*sn*-glycero-3-phosphoethanolamine (POPE), and cardiolipin (CL), specified as 99% pure, were purchased from Avanti Polar Lipids (Alabaster, AL, USA) and used without further purification. Horse heart cytochrome c (cyt c) was purchased from Sigma Chemical Co. (Madrid, Spain). 8-anilino-1-naphtalene sulfonate (ammonium salt; ANS) were purchased from Molecular Probes (Eugene, OR). The concentration of the spreading solutions of phospholipids were 1 mg mL^{-1} in chloroform-methanol (3:1, v/v). The buffer used was 50 mM Tris-HCl buffer (pH 7.40) containing 150 mM NaCl, prepared in Ultrapure water (Milli Q® reverse osmosis system, 18.3 MΩ·cm resistivity) and filtered with a Kitasato system (450 nm pore diameter) before use.

2.2 Preparation of lipid Monolayers: surface pressure-area isotherms and surface pressure constant experiments

The surface pressure (π) was measured with a resolution of ± 0.1 $mN \cdot m^{-1}$ using a 312 DMC Langmuir-Blodgett (LB) trough (NIMA Technology Ltd. Coventry, England). The working surface area of the through is 137 cm^2. The through was placed on a vibration-isolated table (Newport, Irvine, CA, USA) and enclosed in an environmental chamber. The temperature of the subphase was maintained at 24.0 ± 0.2 °C by using an external circulating water bath. Before each experiment, the trough was washed with chloroform and rinsed throughly with purified water. The cleanliness of the trough and subphase formed by the buffer was ensured before each run by cycling the full range of the trough area and aspirating the air-water surface, while at the minimal surface area, to zero surface pressure. Constant-surface pressure experiments were performed by spreading a desired lipid onto the subphase free of cyt c, and then compressing the lipid film to the desired surface pressure (π = 30 mN m^{-1}). Convenient

[11] Slavik, J. *Biochim.Biophys.Acta* **1982**, *694*, 1-25.

volumes of spreading solution of lipids were carefully deposited onto the subphase by using a microsyringe (Hamilton, Reno, NV). After 15 min to allow monolayer stabilization cyt *c* was injected beneath the monolayer to reach a final concentration of 2 μM (equivalent to a lipid to protein molar ratio (LPR) of 15. Thereafter the change of surface area per molecule (ΔA) with time (t) was measured. To obtain a quantitative interpretation of these experiments data were fitted to the following Langmuir-like equation

$$\Delta A = \Delta A_{max} \frac{(k_i t)^b}{1+(k_i t)^b} \quad (1)$$

where ΔA_{max} is the maximum increase of the area reached in steady-state conditions by the monolayer, k_i is a rate constant determined by the nature of the substances involved and the experimental conditions, and b is a parameter that is related with the cooperativity of the process. For compression isotherms the corresponding aliquot of lipid was spread onto the subphase solution. After a 15 min period the experiment was started. The compression barrier speed, calculated to the final surface pressure, was 5 $cm^2 \cdot min^{-1}$. Every π-A isotherm was repeated three times minimum, with the isotherms showing satisfactory reproducibility. LB films were transferred onto freshly cleaved mica, lifting the substrate at a constant rate of 1 $mm \cdot min^{-1}$. The transfer ratios were evaluated and were near the unity, indicating that the mica was almost covered with the monolayer.

2.3 Atomic Force Microscopy. Images were generated with a commercial AFM (Nanoscope III, Digital Instruments, CA, USA) and Si_3N_4 cantilevers (Olympus, Tokyo, Japan) with a nominal spring constant of 40 $N \cdot m^{-1}$. The instrument was equipped with a "J" scanner (120 μm) and the Tapping mode. Mica squares (0.4 cm^2, from Asheville-Schoonmaker Mica Co., VA, USA) were glued to a steal disc. Images were recorded in air at constant-force. The set point was continuously adjusted during the imaging to minimize the force applied. All the images were processed using Digital Instruments software.

2.4 Preparation of liposomes and binding experiments. Chloroform/methanol (3:1, v/v) stock solutions of desired lipid compositions were evaporated to dryness in a flask using a rotavapor. The resulting thin lipid film was then kept under reduced pressure overnight to ensure the absence of organic solvent traces. Multilamellar vesicles were obtained by hydration in buffer to a final concentration of 60 μM. Thereafter, suspensions were filtered through Nucleopore (Costar, Cambridge, MA) polycarbonate filters (200 nm nominal

diameter) using an Extruder (Lipex Biomembranes Inc., BC) device. Size and polydispersity of liposomes were monitored by quasi-elastic light-scattering (QLS) using an Autosizer IIc photon correlation spectrophotometer (Malvern Instruments, U.K.). A dominant peak was typically observed indicating the presence of ~ 200 nm sized-particles. Final lipid concentration was 50 μM assured by phosphorus quantification. The lipid-bound ANS shows intense fluorescence at 480 nm (excitation, 380 nm), while the non-bound ANS exhibits low fluorescence in aqueous solution. All measurements of ANS fluorescence were made in an SLM-Aminco 8100 spectrofluorometer provided with a jacketed cuvette holder. The temperature of the cuvette was kept constant at 24.0 ± 0.1 °C using an external circulating water bath (Haake, Germany). Stock solutions of ANS in ethanol were freshly prepared and protected from the light exposure. These experiments consisted in the incubation of cytochrome c to a final lipid to protein molar ratio of 15 (LPR ~ 1, w/w) for 30 min at 24 °C. Thereafter, the samples were titrated with the stock solutions of ANS. The adsorption data of ANS binding on bilayers were fitted to the following Freundlich-like isotherm[12]

$$[ANS]_B = C_{\max} \frac{(k[ANS]_\infty)^b}{1+(k[ANS]_\infty)^b} \qquad (2)$$

where k is the binding constant, C_{max} is the maximum concentration of ANS bound to liposomes, b is interpreted as the cooperativity of the binding process and B and ∞ subscripts refer to bound and free ANS concentration, respectively. The value of bound ANS can be calculated having into account that it is proportional to the fluorescence. Equation 2 can be used to calculate the variations in the electrostatic surface potential according to

$$\Delta\Psi = \frac{RT}{F} Ln\left(\frac{k_{cyt}}{k_0}\right) \qquad (3)$$

where T is the temperature, R the universal gas constant, F the Faraday constant and k_{cyt} and k_0 are the binding constants with and without the presence of cyt c, respectively.

[12] Montero,M.T.; Pijoan,M.; Merino-Montero,S.; Hernández-Borrell,J. *Langmuir* **2006**, *22*, 7574-7578.

3. Results and discussion

Firstly, we have carried out constant surface pressure measurements of monolayers at 30 mN m^{-1}, which is often assimilated to the surface pressure of the biological membranes[13]. Upon the injection of cyt *c* beneath the monolayers, the changes in the average area per molecule (ΔA) with time (t) were followed (Figure 1). As can be seen the maximum and minimum variations of ΔA were undergone by the pure CL (anionic phospholipid) and the pure POPE (zwitterion) monolayers respectively. For a better comparison the parameters obtained by fitting the experimental data of all the monolayers to the Eq. 1 are listed in Table 1. Here, for instance, it can be seen that ΔA_{max} for CL is ~ 9 fold ΔA_{max} for POPE. On the other hand, the k and b values for the pure CL monolayer were lower than for the other phospholipids. Besides, the ΔA_{max} values were slightly higher for pure POPC and mixed POPC:CL monolayers than for the pure POPE. It is worth noting that the ΔA_{max} reached by the POPE:CL mixture was significantly higher than the other monolayers with the only exception of the pure CL monolayer. Nevertheless, this not provides explanation on the different adsorption that we have observed between the two binary compositions studied in the present work. Indeed, the different behavior between POPC:CL (0.6:0.4, mol/mol) and POPE:CL (0.8:0.2, mol/mol) could not be a mere indication of the electrostatic nature of the cyt *c*–bilayer. In such a case, assuming that the main driving force of the interaction would be electrostatic, the POPC:CL monolayer, with a higher proportion of the anionic phospholipid, should result in a higher ΔA than the POPE:CL monolayer. However, that was not the case. These results point out to the fact that the nature of the interaction between cyt *c* and the phospholipid mixtures is not solely governed by electrostatic interactions[14]. Thus, while the interaction between cyt *c* and zwitterionic phospholipids (POPE and POPC) monolayers involves an hydrophobic contribution[15], the presence of anionic phospholipids[2] (in that work phosphatidilglycerol) has been probed to enhance the penetration of cyt *c*. Having into account that cyt *c* is positively charged at this pH[4], the increased penetration observed in CL presence may be attributed to the contribution of electrostatic interactions.

We know from a precedent work, where we studied the mixing properties of POPC:CL and POPE:CL monolayers[8], that the excess Gibbs energy of mixing (G^E) for both

[13] G. Cevc, D. Marsh, Phospholipid Bilayers. Physical Principles and Models, Wiley-Interscience, New York, **1987.**

[14] Kostrzewa,A.;Pali,T.;Froncisz,Marsh,D. *Biochemistry*, **2000**, *39*, 6066-6074.
[15] Quinn, P.J.; Dawson, R.M.C. *Biochem.J.* **1969**, 113, 791-804.

compositions are negatives and therefore the interactions between the molecules are mainly atractives. We concluded that in the range of molar fraction studied (χ_{CL}=0-1) the mixtures with either POPE or POPC mix ideally. In a recent work[16] based on the existence of two collapse pressures in the range χ_{CL} = 0.1-0.3, it was inferred that phase separation of the components occur and the thermodynamic analysis was supported by AFM observations. Therefore, looking for possible analogies, we have extended our work and investigated the surface pressure-area (π-A) isotherms of our systems for χ_{CL}<0.2. Thus, while POPC:CL monolayers were miscible in all proportions, even χ_{CL} <0.2 (data not shown), two well defined surface collapse pressures we have observed for the POPE:CL system at χ_{CL}<0.2 (Figure 2). This finding matches reasonably well with the behaviour of the DPPE:CL system[13]. According to the Gibbs-phase rule this would indicate that POPE and CL are not completely miscible at molecular level at the air water interface at χ_{CL}<0.2. To perform a topographical characterization of such monolayers, LBs of the systems under investigation were transferred onto a mica substrate at 30 mN m^{-1} and imaged with AFM in contact mode (Figure 3). As can be seen, POPC (Figure 3A) and POPC:CL (Figure 3D) (0.6:0.4, mol/mol) appeared as continuous and smooth with average surface roughness, *Ra* = 0.10, and 0.06 nm, respectively. On the other hand, the LBs of POPE (Figure 3B) and CL (Fig.3C) were not homogeneous. In the monolayer of POPE, *Ra* = 0.14, round structures of 75 ± 15 nm (n=50), randomly distributed and that amount for ~ 6.39 % of the total substrate area, appeared. The step height difference between the round structures and the upper layer region was ~1.16 nm. In the LB of CL (Figure 3C) structures with no particular shape are seen. The step height difference between these structures and the upper layer was ~ 0.90 nm. Both step height values were lower than expected for a monolayer, hence that we suspect that at this pressure, 30 mN m^{-1}, a overlayered structure has been transferred. Besides, the LB of the POPE:CL (0.8:0.2, mol/mol) monolayer yield also a non-homogeneous structure (Figure 3E). Interestingly, a magnification of two small areas of this LB (see the magnifications of the insets on the left side of Figure 3E) reveal the existence of two different regions, resembling the features of the pure POPE (Figure 3B) and CL (Figure 3C) respectively. Although non conclusive, this observation could indicate that a kind of lateral segregation occurs which matches with the formation of domains observed in supported planar bilayers (SPBs) of the same composition[8]. A note of caution should be added in making such comparison between

[16] Sennato,S.;Bordi,F.;Cametti,C.;Coluzza,C.;Desideri,A.;Rufini,S. *J.Phys.Chem.* **2005**, *109*,15950-15957.

LBs and SPBs because in Figure 3 we are showing the topographies of the acyl chains facing the air. Besides, as mentioned above the G^E values, -1.5 and -3.8 kJ mol^{-1}, for POPE:CL (0.8:0.2, mol/mol) and POPC:CL (0.6:0.4, mol/mol), respectively, indicate that the contribution of the repulsive interactions to the net G^E value are more important in the POPE:CL than in the POPC:CL system. Theoretically, it is likely to assume that this will result in a lateral segregation of the molecules.

In this regard an appealing possibility would be the selective adsorption of cyt *c* on enriched CL domains in monolayers. This would be the reason of the higher adsorption of cyt *c* on POPE:CL (0.8:0.2, mol/mol) system (Figure 1). Conversely, when CL is mixed with POPC, the electrostatic interaction is less favoured. Thus, the 3-4 molecules of CL necessaries for electron transport through cytochrome *c* oxidase[17] would be indicative of a stoichiometric requirement for the cyt *c*-CL binding. Remarkably, this requirement would be acomplished i.e. by the POPE:CL (0.8:0.2, mol/mol) system because of the lateral segregation but not for the POPC:CL (0.6:0.4, mol/mol) monolayer.

To further investigate the favoured interaction of cyt *c*, binding experiments on liposomes have been carried out. ANS is a fluorescent molecule that has probed to be useful for monitoring changes in the hydrophilic phosphate moiety of phospholipids caused by i.e. drugs[12,18] and cyt *c* itself[19]. Tipically, fluorescence intensities increase as ANS is added to liposomes until a plateau is reached at high probe concentrations (Figure 4 and 5). In presence of cyt *c* ANS is displaced as a result of the competition between the protein and the label for the same binding sites[9].Consequently, as a general behavior, in presence of cyt *c*, the fluorescence of ANS decreases.

The values obtained by fitting the isotherm (eq. 2) to the ANS binding data and the calculated surface potential values (eq. 3) are shown in Table 2. As can be seen the values reached at $t \rightarrow \infty$ (C_{max}) were always lower in presence of cyt *c*. In absence of protein, the greatest and lowerest values for C_{max} were for the POPC:CL (0.6:0.4, mol/mol) and, CL and POPE, bilayers respectively. In presence of cyt *c* the maximum displacement of ANS, that is the greatest binding of the protein, was shown by the POPE:CL (0.8:0.2, mol/mol) composition, which is in agreement with the largest adsorption observed for the POPE:CL monolayer (Figure 1). With the exception of CL, it can be said that he values *k* and *b* were higher in presence of cyt *c* in all cases. As can be seen by simple inspection of the binding

[17] Robinson, N.C. *J. Bioenerg. Biomem.* **1993**, *25*, 153-163.
[18] Vázquez,J.L.;Berlanga,M.;Merino,S.;Domènech,Ò.;Viñas,M.;Montero,M.T.;Hernandez-Borrell,J. *J.Photochem.Photobiol.* **2001**, *73*, 14-19.
[19] Teissie,J.; Baudras,A. *Biochimie* **1977**, *59*, 693-703.

curves, liposomes formed with pure phospholipids bound from very low amounts of cyt *c* for POPC (Figure 4A) to almost negligible amounts for POPE and CL (Figure 4B and 4C). On the other hand, the mixtures, either of POPC:CL (Figure 5A) or POPE:CL (Figure 5B), exhibited a largest binding. These behavior are in close agreement with the minimal adsorption of cyt *c* that we have observed onto POPC and POPE (Figure 1) and suggest, in agreement with results elsewhere reported[15], that cyt c would not penetrate into zwitterionic lipid monolayers.

The variations in the electrostatic surface potentials ($\Delta\Psi$) calculated according to eq. 3 are also shown in Table 2. According to the high standard deviations of the measurements only the $\Delta\Psi$ values for CL and POPE:CL are significant. The positive value for the POPE:CL and CL systems indicates that cyt *c* is able to screen, in some extension the negative charge bear by these liposomes. These behavior are in obvious agreement with the highest adsorption of cyt *c* on pure CL and POPE:CL monolayers (Figure 1). It is important to bear in mind that CL is a particular phospholipids that displays two different binding sites for cyt *c*[20,21]. Besides, recent surface force measurements[22] revealed that the absolute surface charge bear by CL liposomes can not be inferred simply assuming that the phospholipid is fully deprotonated at neutral pH. Possibly, changes in the structure of the bilayer in presence of the cyt *c*, involving the postulated CL extended conformation[23], could unveil the charge partially screened by the intramolecular hydrogen bond.

Indeed, the interaction of cyt *c* with acidic phospholipids, and particularly the level of penetration of the protein into the bilayer, seems to follow a subtle balance between electrostatic and hydrophobic interactions[24]. In addition, other factors that would influence the interaction are the orientation of the protein[25,26] and its possible partial unfolding at the surface of anionic phospholipids[3,27]. Whichever the exact mechanism involved, taking into account the whole body of results presented in this paper, the POPE:CL system, with the nominal mole fraction of CL found in the inner mitochondrial membrane, provide additional evidences[8,10] of the selective adsorption of cyt *c* on CL domains.

---

[20] Rytömaa,M. ;Kinnunen, P.K.J. *J.Biol.Chem.* **1994**, *269*, 1770-1774.
[21] Gorbenko,G.P.; Molotovsky,J.G.;Kinnunen,P.K.J. *Biophys.J.* **2006**, *90*, 4093-4103.
[22] Nichols-Simth,S. ;Kuhl,T. *Coll.and Surfaces B: Biointerfaces* **2005**, *41*, 121-127.
[23] Kinnunen,P.K.J. *Chem.Phys.Lipids* **1996**, *81*, 151-166.
[24] Bernad,S.;Oellerich,S.;Soulimane,T.;Noinville,S.;Baron,M.H.; Patermostre,M.;Lecomte,S. *Biophys, J.* **2004**, *86*,3863-3872.
[25] Gorbenko,G.;Domanov,Y. Biophys.Chem. **2003**, *103*,239-249.
[26] Domanov,Y.A.;Molotkovsky,J.G.;Gorbenko,G.P. *Biochim.Biophys.Acta* **2005**, *1716*,49-58.
[27] Spooner,P.J.R.;Watts,A. *Biochemistry*, **1991**,*30*, 3871-3879.

Acknowledgements

This work has been supported by grants CTQ2005-07989 from the Ministerio de Ciencia y Tecnología (MCYT) and SGR00664 from DURSI (Generalitat de Catalunya) Spain.

Figure Legends

Figure1. Increase of the surface area A as as function of time of monolayers of CL (■), POPE (●), POPC (○), POPE:CL (0.8:0.2, mol/mol) (□), and POPC:CL (0.6:0.4, mol/mol) (▲).

Figure 2. Surface pressure versus area per molecule isotherms of (■) POPE, (●) POPE:CL (0.95:0.05, mol/mol), (□) POPE:CL (0.90:0.10, mol/mol) and (○)POPE:CL (0.80:0.20, mol/mol).

Figure 3. AFM Tapping mode images of POPC (A), POPE (B), CL (C) POPC:CL (0.6:0.4, mol/mol) (D), and POPE:CL (0.8:0.2, mol/mol) (E) monolayers extracted at 30 mN m^{-1}. Amplification of image (F).

Figure 4. Concentration of ANS bound for liposomes formed with POPC (A), POPE (B), CL (C) as a function of the free ANS concentration, in the absence (■) and in presence (□) of cyt *c* 2 μM. The total lipid concentration was 50 μM. Values are the average of 3 independent experiments.

Figure 5. Concentration of ANS bound for liposomes formed with POPC:CL (0.6:0.4, mol/mol) and (D) POPE:CL (0.8:0.2, mol/mol) as a function of the free ANS concentration, in the absence (■) and in presence (□) of cyt *c* 2 μM. The total lipid concentration was 50 μM. Values are the average of 3 independent experiments.

Table Legends

Table 1.
Parameters obtained from constant-surface pressure experiments. ΔA_{max} is the maximum increase of the area reached in steady-state conditions by the monolayer, k_i is the rate constant and *b* is the cooperativity of the process.

Table 2. Parameters obtained from ANS binding data on. C_{max} is the fluorescence intensity (related with the maximum concentration bound), *b* is the cooperativity, *k* is the binding constant, $\Delta\psi$ is the variation in the surface potential of liposomes.

	POPC	POPE	CL	POPC:CL (0.6:0.4, mol/mol)	POPE:CL (0.8:0.2, mol/mol)
ΔA_{max} (Å^2 molecule^{-1})	2.9 ± 0.2	1.49 ± 0.13	12.9 ± 0.5	2.23 ± 0.09	6.4 ± 0.3
k (x 10^{-2}) s^{-1}	2.8 ± 0.5	2.5 ± 0.5	1.7 ± 0.2	2.5 ± 0.2	2.9 ± 0.4
b	0.91 ± 0.13	1.2 ± 0.3	0.67 ± 0.03	1.00 ± 0.09	0.91 ± 0.11

Table 1

13

	POPC		POPE		CL		POPC:CL (0.6:0.4, mol/mol)		POPE:CL (0.8:0.2, mol/mol)	
		+ cyt c		+ cyt c		+ cyt c		+ cyt c		+ cyt c
C_{max} (μM)	5.05	3.44	2.5	3.0	2.92	0.47	7.4	4.43	6.4	2.38
b	0.97	1.50	1.02	1.53	1.3	1.1	1.22	1.49	1.21	1.40
k (μM^{-1}) x 10^{-2}	3.29	8.2	2.5	2.6	3.4	5.9	3.06	3.7	2.3	5.0
$\Delta\psi$ (mV)	-	+ 2.40 ± 1.50	-	+3.40 ± 1.80	-	+ 13.4 ± 1.5	-	+ 0.20 ± 1.30	-	+ 8.40 ± 1.20

Tabel 2

14

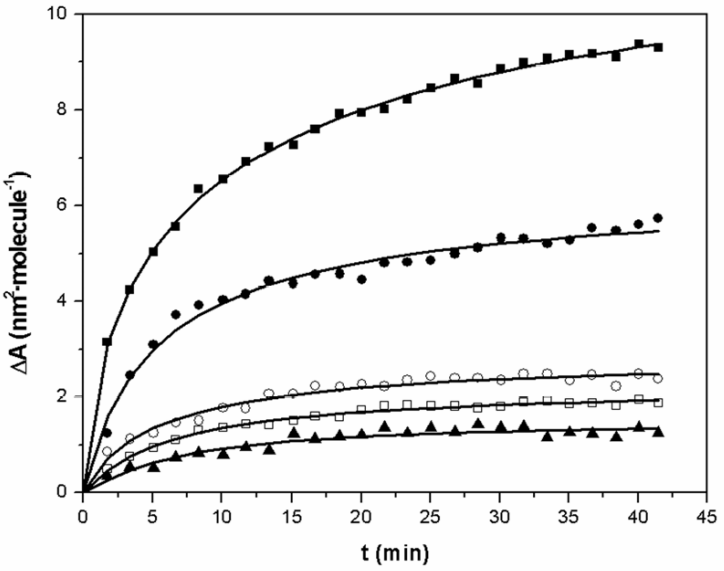

Figure 1

15

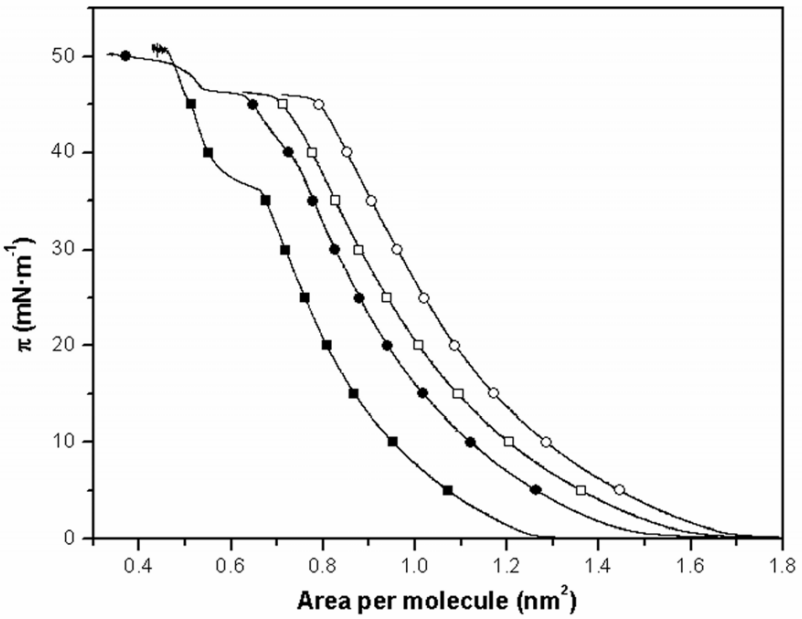
50
40
30
20
10
0
π (mN·m-1)
0.4
0.6
0.8
1.0
1.2
1.4
1.6
1.8
Area per molecule (nm2)

Figure 2

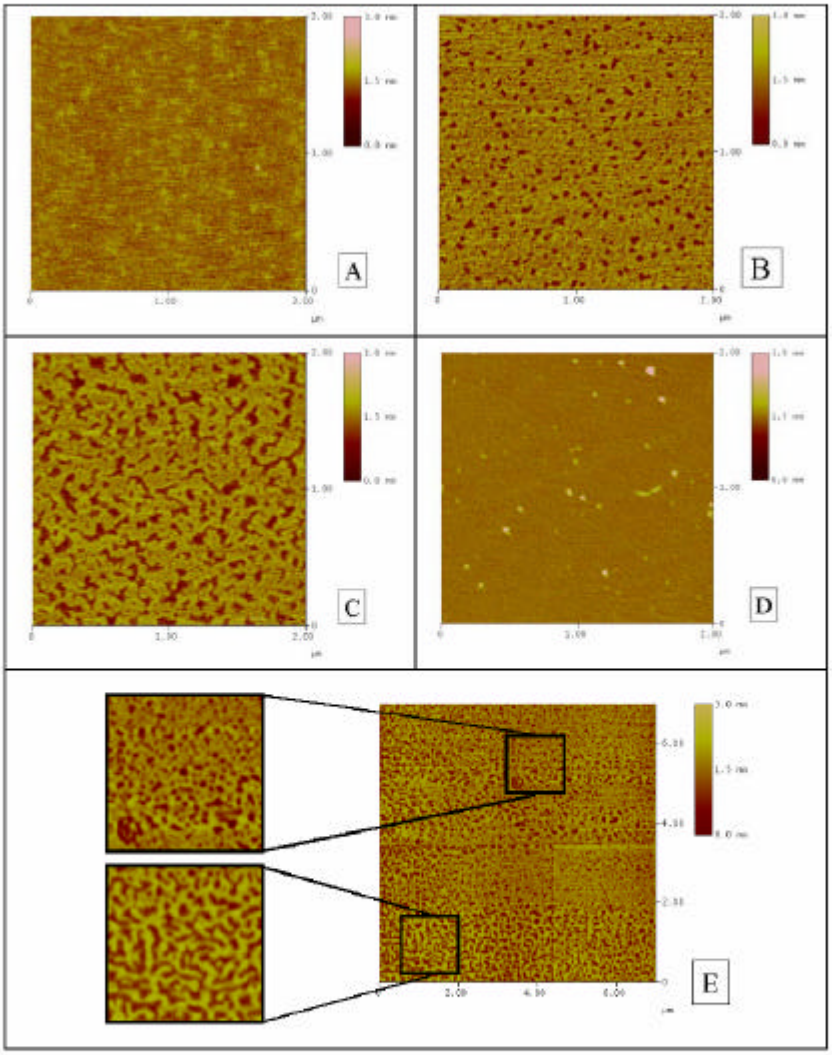

Figure 3

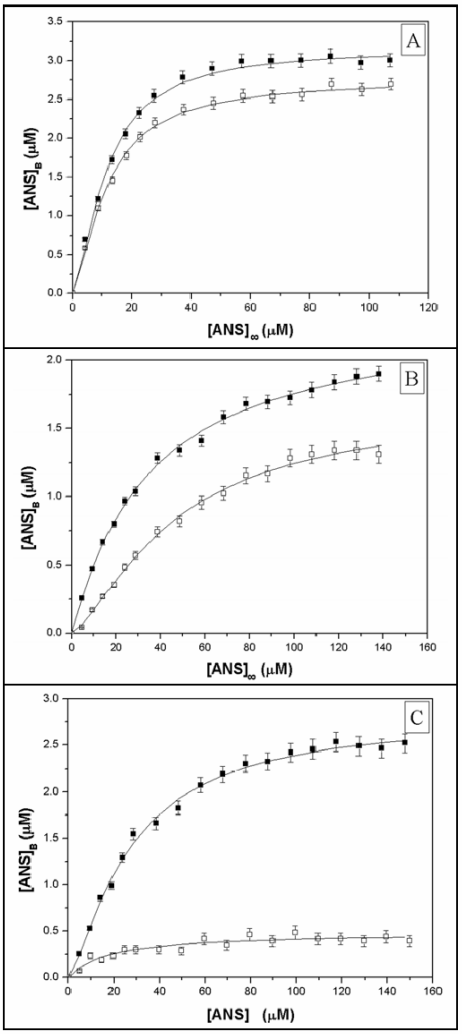

Figure 4

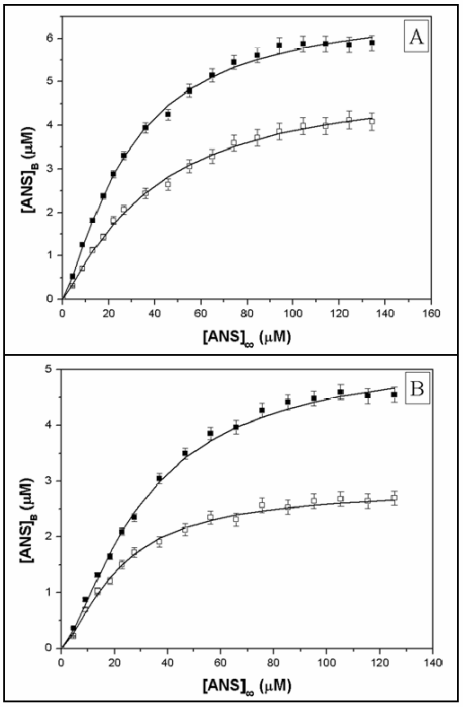

Figure 5